DYNAMIC MONTE CARLO SIMULATION OF ATOM TRANSFER RADICAL COPOLYMERIZATION

BY

MASIHULLAH JABARULLA KHAN

A Thesis Presented to the
DEANSHIP OF GRADUATE STUDIES

KING FAHD UNIVERSITY OF PETROLEUM & MINERALS

DHAHRAN, SAUDI ARABIA

In Partial Fulfillment of the
Requirements for the Degree of

MASTER OF SCIENCE

In

CHEMICAL ENGINEERING

MAY 2009

DHAHRAN 31261, SAUDI ARABIA

DEANSHIP OF GRADUATE STUDIES

This thesis, written by **MASIHULLAH JABARULLA KHAN** under the supervision of his thesis advisor and approved by his thesis committee, has been presented to and accepted by the Dean of Graduate Studies, in partial fulfillment of the requirements for the degree of **MASTER OF SCIENCE IN CHEMICAL ENGINEERING**

Thesis Committee

Dr. Mamdouh Al-Harthi
(Committee Chairman)

Prof. Ibnelwaleed Ali Hussein
(Member)

Dr. Abdulhadi Al-Juhani
(Member)

A. Al Amer

Prof. Adnan M. Jarallah Al-Amer
(Department Chairman)

Dr. Salam A. Zummo
(Dean of Graduate Studies)

14/6/09
Date

To

My Beloved Parents

for their

Innumerable prayers, encouragement and motivation.

ACKNOWLEDGMENTS

All praise and thanks are due to Almighty Allah, Most Gracious and Most Merciful, for the immense beneficence which has resulted in the accomplishment of this research. May peace and blessings be upon prophet Muhammad (PBUH), his family and his companions.

I would like to acknowledge KFUPM for the support extended towards my research through its remarkable facilities and for providing me with the opportunity to pursue graduate studies.

All parents are a gift to their children and my parents have always been there for me in my good and difficult times. They have supported me in everything that I have attempted, and their continual encouragement helped me complete this task. My family has always been a pillar of support for me, especially my mother and sister. Their continuous encouragement and motivation lifted my confidence whenever I encountered problems. Words fall short in conveying my gratitude towards them. A prayer is the simplest way I can repay them - May Allah (S.W.T.) give them good health and give me ample opportunity to be of service to them throughout my life.

I acknowledge with enormous gratitude the inspiration, encouragement, valuable time and guidance bestowed by my Thesis Committee Chairman, Dr. Mamdouh Al-Harthi. I am deeply endowed to him for being so patient and considerate to me throughout the duration of the research.

I am also greatly indebted to my thesis committee members, Dr. Ibnelwaleed Ali Hussein and Dr. Abdulhadi Al-Juhani, for their valuable comments which have increased the value of my research.

Special thanks are due to all my colleagues in the department and in the University who were always there to help me in my work.

TABLE OF CONTENTS

LIST OF TABLES

LIST OF FIGURES

THESIS ABSTRACT (English)

NAME: MASIHULLAH J.KHAN

TITLE: DYNAMIC MONTE CARLO SIMULATION OF ATOM TRANSFER RADICAL COPOLYMERIZATION

MAJOR: CHEMICAL ENGINEERING

DATE: May 2009

In this thesis, mathematical modeling of Atom Transfer Radical Copolymerization (ATRcP) was done in batch and semi batch reactors. In addition we modeled the diffusion effects on ATRcP. The formation of Gradient polymers, a new genre of copolymers, was also studied. Continuous reactors were also simulated for this novel polymerization process.

The model was used to predict monomer conversion, average molecular weight, polydispersity index, and copolymer composition as a function of polymerization time and/or conversion. The model was also used to predict the distribution of molecular weight, chemical composition, and comonomer sequence length at any polymerization time or comonomer conversion. The simulations were helpful in predicting comonomer composition drift and in designing products with specific chemical composition distributions and comonomer sequence lengths

Dynamic Monte Carlo simulation was used in mathematical modeling and analysis. The Gillespie's algorithm was used for dynamic Monte Carlo simulation. Here, a control volume is chosen and then the experimental rates of reactions were transformed into stochastic rates. The probability of a reaction taking place was calculated to model the elementary reaction taking place within the reactor.

THESIS ABSTRACT (Arabic)

ملخص الرسالة

الاسم: مسيح الله جبر الله خان

عنوان الرسالة: تحليل مرشح طول موجة يتحوي على ثقوب هوائية

الدرجة: الماجستير في الهندسة الكيميائية
تاريخ التخرج: 5-2008م

في هذه الاطروحه تم إنشاء نموذج رياضي لعملية البلمره المعروفة بالنقل الذري الراديكالي لعدد من المفاعلات وكذلك تم إنشاء نموذج رياضي لتشكيل جديد من اللدائن يعرف بالمتدرج ودراسة تأثير الانتشار الجزيئي على خواص المنتج النهائي.

يتمكن النموذج الرياضي من دراسة خواص كثيرة للبوليمر المنتج مثل أطوال الجزيئات وأوزانها الذرية وتركيباتها الكيميائية بالإضافة إلى كمية المواد المنتجة خلال فترة التفاعل وغيرها من المواصفات المهمة التي ستساعد على الفهم العميق لهده العملية.

النموذج مبني على طرق مونت كارلو للمحاكاة وتستخدم طريقة غليسبي الشهيرة في التحليل والنمذجة وكذلك يتم استخدام معاملات تفاعلات مستخدمة ومستخرجة من تجارب معملية مثبته في أوراق علمية منشورة في عدد من المجلات العلمية

درجة الماجستير في العلوم

جامعة الملك فهد للبترول والمعادن

الظهران، المملكة العربية السعودية

CHAPTER 1

INTRODUCTION

1.1 Research Background

Polymers, either synthetic or natural, are present in every aspect of our daily lives. Many modern functional materials, pharmaceutical equipments, electronic devices, automobile parts, etc., have polymeric components. Polymers are replacing traditional materials because of their low cost and special applications. Our lives have been thoroughly changed with the advent of mobile phones, computers, refrigerators, electrical domestic appliances, television, etc. and all of these appliances have parts made of synthetic polymeric materials to a large extent. Polymeric materials are also everywhere in our homes: floor carpeting, glue, pipes, paint, wallpaper, foils, electric insulation and moldings are examples of components based on synthetic polymers. The development of new polymers, and the modification and enhancement of the old ones, are goals of many researchers in both industry and academia.

Polymers can be synthesized via several different methods, such as free radical polymerization, anionic and cationic polymerization, ring-opening polymerization, and coordination polymerization. Of these techniques, free radical polymerization is the most widely used industrially. This technique is much simpler than the others and it is applicable to a wide variety of monomers. However, free radical polymerization offers

poor control over the molecular weight and polydispersity index of the resulting polymer. In addition, it is impossible to make polymers with complex and well defined macromolecular architectures, such as block copolymers, with conventional free radical polymerization.

Living free radical polymerization techniques (LFRP) are promising solutions for the limitations of conventional free radical polymerization. Although LFRP processes generally have low rates of polymerization, they can make polymers that are well defined with respect to:

1. Topology: linear, star-shaped, and comb-shaped chains.

2. Terminal functionalities.

3. Comonomer composition and intramolecular distribution: statistical, periodic, block, graft, and gradient copolymers.

4. Molecular weight: predetermined by the ratio of monomer concentration to initiator, having a polydispersity index close to one.

1.2 Free Radical Polymerization

Free-radical polymerization (FRP) is one type of chain growth polymerization technique, and it is a very useful method for large scale production of a variety of polymers. Most of the vinyl polymers can be produced industrially by free-radical polymerization. Compared to other polymerization techniques, free radical polymerization is much less sensitive to impurities. It is not sensitive to water and

sometimes it is carried out in aqueous media. There are three basic steps of FRP namely initiation, propagation and termination. The reaction mechanism and the corresponding rate equations are given in Table 1.1.

Initiation	$I \rightarrow 2R\bullet$ $R\bullet + M \rightarrow P_1$
Propagation	$Pn + M \rightarrow P_{n+1}$
Termination	$Pn + Pm \rightarrow$ Polymer

Table 1.1: Basic steps of free-radical polymerization

Copolymerization

Copolymerization is the best way to produce a polymer with properties that are intermediate between the properties of the respective homopolymers. It is an important process from a commercial point of view because it can produce new polymers with completely different properties. An unlimited number of polymeric structures with a wide range of properties and applications can be synthesized via copolymerization of a few different types of comonomers.

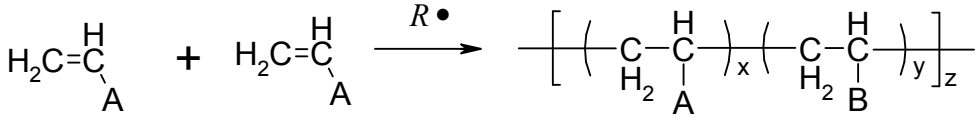

Figure 1.1 General copolymerization reaction scheme.

One way to categorize copolymers is based on their architecture. Figure 2.2 shows how copolymers are classified as statistical, alternating, block, and graft. In statistical or random copolymers, the placement of the comonomers in the chain is random. In alternating copolymers, comonomer molecules alternate in the chain. If long sequences of one comonomer are followed by long sequences of the other comonomer, the resultant copolymer is called a block copolymer. Block copolymers can be diblock, triblock or multiblock depending on the number of comonomer types used during polymerization. Graft copolymers are branched polymers where the backbone is made of one copolymer type and the branches are made of another copolymer type.

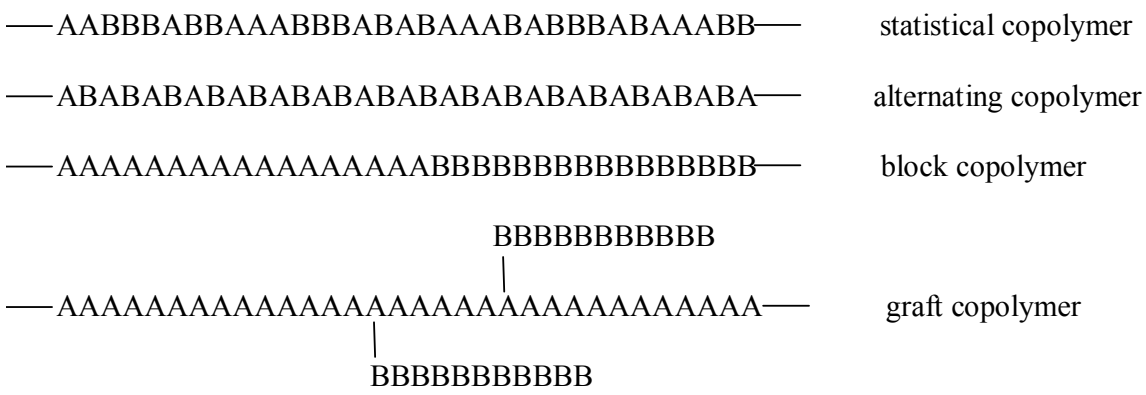

Figure 1.2 Types of copolymer topologies.

1.3 Living Free Radical Polymerization

The control of macromolecular structure can lead to the development of new polymer products with improved and/or new materials properties. Of all polymerization techniques, living polymerization offers the best control over macromolecular structure. During living polymerization, polymer chains grow without permanent chain termination

or transfer reactions. The absence (or reduction) of termination reactions leads to polymers with narrow molecular weight distributions (MWD) if initiation reactions are fast. The width of the MWD is commonly measured as the ratio of the weight average molecular weight to the number average molecular weight (M_w/M_n) and called polydispersity index (PDI). In living polymerization, PDI approaches one ($1 < PDI < 1.2$). In addition, living polymerization also provides end-group control and thus enables the synthesis of polymers with various chain end functionalities. Finally, block copolymers can be made with living polymerization by sequentially polymerizing comonomer of different types in the same reactor [1].

Living ionic (anionic or cationic) polymerization has perfect control over molecular architecture because chain ends having a similar electrostatic charge repel each other. This repulsion between the chain ends prevents them from combining in termination reactions. However, living ionic polymerization techniques have some disadvantages. The growing carbonium ion is extremely reactive toward traces of oxygen, water, or carbon dioxide. Therefore, the polymerization system should be totally devoid of these impurities. Even when the concentration of these impurities is at levels of parts per million, they can markedly affect the polymerization. Therefore, these systems require great care in purification and drying of solvent and monomers and in handling the initiator solution. The polymerization temperature is another disadvantage for living ionic polymerizations: High reaction temperatures are not suitable and the optimum temperature range is very low, varying from -20 ^{o}C to -78 ^{o}C. [2] Instead of living ionic polymerization, living free radical polymerization (LFRP) was found to be more suitable to produce living/controlled polymers [1].

The concept of LFRP is based on the reduction of termination reactions by decreasing radical concentration. The approach to reduce the radical concentration and to protect the polymer chains from termination reactions is based on a reversible activation/deactivation process. Figure 2.3 illustrates this concept. In LFRP, while a polymer radical ($R\bullet$) propagates monomers (M), it can also be deactivated, forming a dormant chain (D).

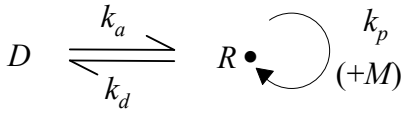

Figure 1.2 General LFRP mechanism.

Nitroxide mediated polymerization (NMP) is one of the earliest methods of LFRP. Figure 1.4 shows the general mechanism of NMP, where X represents the nitroxide group, D is the dormant species, $R\bullet$ is the polymer radical, k_a is the dissociation constant, and k_d is the coupling constant. At low temperatures, the dormant chain is stable and therefore the nitroxide group behaves as an inhibitor. However, at elevated temperatures, the dormant chain may undergo hemolytic cleavage (dissociate), leading to polymer radicals and nitroxide groups. The polymer radical can grow, terminate or couple with the nitroxide group again to form the dormant species. As we will discuss later in more detail, this equilibrium between active and dormant species leads to the production of polymer chains with controlled molecular weight and narrow MWDs.

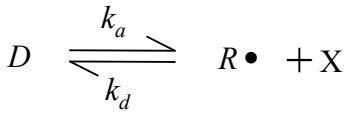

Figure 1.3 General NMP mechanism. *D*: dormant species; $R\bullet$: propagating radical; *X*: the nitroxide group.

Reversible addition-fragmentation chain transfer (RAFT) and atom transfer radical polymerization (ATRP) can be applied to a wider range of temperatures and monomer types than NMP. Since ATRP is the main focus of this thesis, the following section will describe it in more detail.

1.4 Atom Transfer Radical Polymerization

Since 1995 (the year of the independent discoveries of ATRP by Matyjaszeweski's group[3] and Sawamoto's group[4]) the technical literature on this process has been growing very rapidly. Several reviews, books, and book chapters summarize hundreds of papers that appeared in the literature on ATRP of a large variety of monomers.[5-9] ATRP can synthesize various polymers with controlled molecular weight and narrow MWD. It can be carried out in a wide range of polymerization temperatures and is not very sensitive to the presence of oxygen and other inhibitors. [10]

Figure 1.5 shows the general mechanism of ATRP. In addition to the monomer, the ATRP system consists of an initiator that has an easily transferable halide atom (RX) and a catalyst. The catalyst (or activator) is a lower oxidation state metal halide (MtnX)

with a suitable ligand (L). Polymerization starts when the halide atom transfers from the initiator to the catalyst to form a free radical $R\bullet$ and a higher oxidation state metal halide Mtn+1-X (deactivator). This step is called activation or forward reaction. The deactivation step or backward reaction pushes the reaction to form dormant species (RX) rather than the radical's $R\bullet$.The reaction of monomer molecules (M) in the propagation step is similar to conventional free radical polymerization.

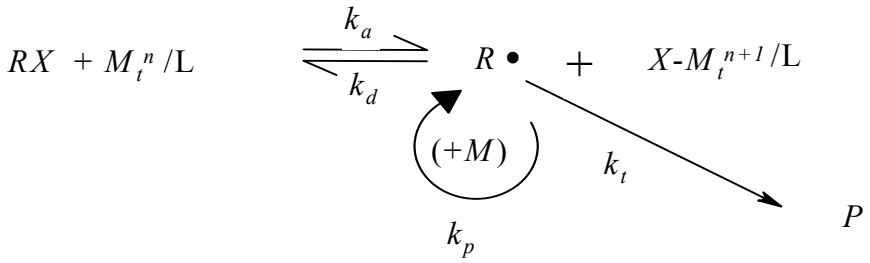

Figure 1.5 ATRP Mechanism. RX: dormant species (alkyl halide); M_t^n/L : activator (metal complex); R• : propagating radical;$X\text{-}M_t^{n+1}/L$: deactivator; M: monomer; P: dead chain.

Termination reactions may occur in ATRP, especially in the beginning of the polymerization. Transfer reactions may also occur in ATRP. Fast initiation and rapid reversible deactivation will lead to better control and narrow MWD. The equilibrium constant is the ratio between the activation constant and the deactivation constant (Keq=ka/kd). If the equilibrium constant is too small, ATRP will not occur or it will occur very slowly. Additionally, as the equilibrium constant increases, the concentration of radicals increases.

Compared to conventional free radical polymerization, the new and the key component in ATRP is the catalyst. Suitable ligands should complex with a metal halide to form the ATRP catalyst. The metal halide should have at least two oxidation states and should have good affinity toward halogen atoms. ATRP systems using Cu,[11] Rh,[12] Ni,[13] Pd,[14] and Fe,[15] transition metals in conjunction with suitable ligands such as substituted and unsubstituted bipyridines, and amines[16] have been used as catalysts.

1.5 Copolymerization via ATRP

Shortly after its discovery, it was found out that most of the vinyl monomers could be copolymerized through ATRP. While conventional free radical polymerization produces copolymers with broader chemical composition distribution because of the termination reactions, the living nature of ATRP leads to the production of copolymers with narrow chemical composition distribution. In fact, ATRP (and other living polymerizations) can make copolymers with backbone compositions varying from random to gradient by varying the composition of the comonomer during the polymerization.[17] While the synthesis of block copolymers is difficult in conventional free radical polymerization, LFRP techniques are ideally suited for the synthesis of block copolymers.

Various block copolymers have been synthesized by ATRP using the macroinitiator method. In this method, the first monomer type is polymerized with an initiator having the proper end carbon halide, yielding polymer chains with end carbon

halide bonds (macroinitiators) that can be used to initiate the polymerization of the second monomer type to produce AB block copolymers.

Bifunctional initiators can also be used to prepare ABA triblock copolymers. They can polymerize the first monomer type to produce chains that have two functional end groups (difunctional macroinitiators). The produced macroinitiator can be used to polymerize the second monomer type to form ABA triblock copolymers. Figure 1.6 illustrates this idea.

$$XRX + [A] \rightarrow XAAAAARAAAAAX$$
$$XAAAAARAAAAAX + [B] \rightarrow XBBBBAAAAARAAAAABBBBBX$$

Figure 1.6 Illustration of triblock copolymer. XRX: bifunctional initiator; [A]: monomer A; [B]: monomer B

Star polymers can also be prepared via ATRP. The use of multifunctional initiators to synthesize star polymers was introduced by Matyjaszewski et al. in 1995. Figure 1.7 shows an example of an initiator that can be used to form star polymers.[18]

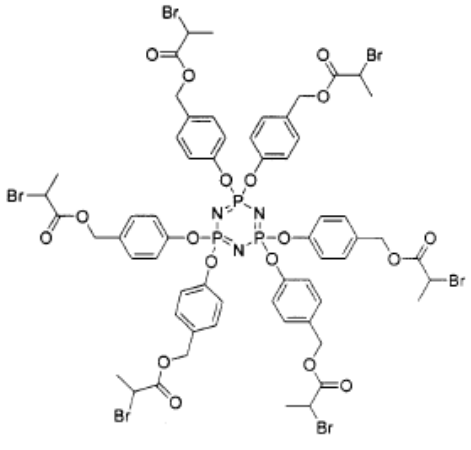

Figure 1.7 ATRP initiator for synthesizing star polymers.

1.6 Gradient Copolymers

The constantly advancing technologies of the world demand newer, higher performance and more specialized materials. One solution to this problem, which has recently been receiving attention, is the preparation and use of gradient materials.[19,20] These gradient materials blend the properties of two or more materials in a continuous manner from one area of the material to another.

Two methods of making gradient materials have been studied.[20] The first is the construction of macroscopic gradient materials, in which several homopolymers are prepared sequentially on a surface of other material. The various homopolymers and copolymers diffuse within the gradient material, leading to a continuous and systematic macroscopic change in the composition of the material. In this way the polymers synthesized are chemically homogeneous, but the bulk material is heterogeneous in composition. Materials of this type have been reported from several sources, and they have demonstrated numerous interesting properties properties,[20,21] leading to their use in such applications as highbandwidth optical fibers.[21]

The second method of producing gradient materials relies on the gradient copolymers or molecular gradients and will be one of the primary focus of the proposed work. Gradient copolymers are copolymers in which the instantaneous composition varies continuously along the chain contour. [19, 22] This is in contrast to block copolymers, in which the instantaneous composition changes discontinuously along the chain. As shown in Figure 1.8, composition along the chain varies in different ways for block, gradient and random copolymers. The composition does not vary in a block

copolymer until after the crossover point between blocks. A random copolymer shows no continuous change in composition. Gradient copolymers have a continuous change in composition from one end of the chain to the other. In order to achieve this continuous change in instantaneous composition, all chains must be initiated simultaneously, and must survive until the end of the polymerization. Therefore, a living (ionic) or controlled/living radical polymerization technique must be employed, as the significant presence of chain-breaking reactions would lead to heterogeneity in both composition and molecular weight.

In addition to these mechanistic requirements, synthesizing well-defined gradient copolymers also requires facile cross-propagation. This is very hard to fulfill in ionic copolymerization since reactivities for monomers in ionic systems do not favor cross-propagation. [23] In contrast, free radical polymerization abounds with examples of monomers that easily cross-propagate. [24] Therefore, for synthesizing a well-defined gradient copolymer, Atom transfer radical Copolymerization offers a very attractive and powerful option.

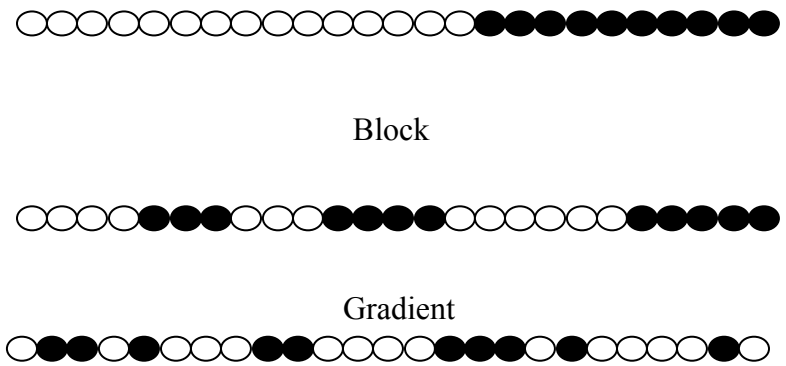

Figure 1.8 Schematic representation of the composition in block, gradient and statistical copolymers, in which the open circles denote monomer 1 and the closed circles denote monomer 2.

1.7 Literature Review

The literature review starts from the inception of controlled/living radical polymerization in 1969 to the recent advances made in the fields of ATRP, NMP and RAFT. Section 1.7.1 will concentrate on controlled/living radical polymerization. Section 1.7.2 will enumerate the work done on modeling of NMP. Section 1.7.3 and 1.7.4 will list the work done modeling on RAFT and ATRP respectively. The literature review will involve both homopolymerization and copolymerization. The use of different modeling techniques pertaining to our objectives will be the focus. In addition, every chapter breifly reiterates the literature review pertaining to subject matter in brief.

1.7.1 Controlled / Living Radical Polymerization

Borsig et al in 1969 first reported the concept of controlling radical polymerization. The group used bulky diaryl and triaryl ester groups on methacrylate monomers, and they observed an increase in the molecular weight with conversion. The formation of block copolymers was inferred. [25] The process still suffered from low initiation efficiencies and the PDI was relatively high. Also the relationship between molecular weight and conversion was not linear.

In 1982, the term living radical polymerization was coined by Otsu et al., during their work on the iniferter mechanism. [26] The group stated the organic disulfide initiator with chain transfer and termination as initiator - transfer agent - terminator (iniferter). They used tetraethylthiuram disulfide in the thermal / photo polymerization of styrene and MMA and obtained functionalized polymers having initiator fragments and chain terminators. Another work by Otsu et al. [27] utilized the S-alkyl dithiocarbomate group

which undergoes reversible photodissociation to a reactive alkyl radical and an inert dithiocarbomate group. The use of dithiocarbomates hindered the living nature of the chain end, due to decomposition of dithiocarbomates, but there were readily utilized for making block and graft copolymers.

The concept of using transition metal compounds for the formation of persistent radicals to produce polymers in a controlled manner was also investigated. Lee et al in 1978 polymerized methyl methacrylate (MMA) initiated by benzoyl peroxide (BPO) in the presence of chromium (III) acetate. [28] The group reported the increase in molecular weight with conversion and the formation of block copolymers. Mandare et al. [29] and Arvanitopoulus et al. [30] also used transition metal compounds for the formation of persistant radicals to polymerize acrylates in a controlled manner. High molecular weight polyacrylates with very lower polydispersities were prepared.

In 1985, Rizzardo et al. [31] introduced the concept of stable free radical polymerization using persistent nitroxyl radicals. The authors reported that the rate limiting step for the formation of well defined polymers was affiliated to the degenerative transfer of alkoxyamine between polymer chains. George et al. [32] who gave a more precise understanding to the process in their first publication. They reported the polymerization of styrene with a free radical initiator (Benzoyl peroxide) and a stable free radical (TEMPO). They produced polystyrene with a polydispersity of 1.26. They inferred that the polydispersity remains constant over the entire course of the reaction, suggesting that the reaction is proceeds via a type of living chain mechanism. The incremental increase in molecular weights also suggested that the reaction proceeds thru a type of living radical polymerization. They attributed the control of polymerization to the

homolytic cleavage of polymer chain and TEMPO adduct. This led to the concept of Nitroxide mediated polymerization (NMP).

Another approach to produce controlled polymers is based on the degenerative transfer reactions. In this process, the control is achieved by thermodynamically neutral exchange of a group between the growing radicals, present at very low concentrations, and a dormant species, present at much higher concentrations. If the exchange reactions are very fast relative to propagation reaction, the resulting polymers have low polydispersity. Various alkyl iodides were used as transfer agents. Rizzardo et al., [32] used thiocarbonylthio compounds as transfer agents, and they became the pioneers in establishing the process called reversible addition fragmentation transfer (RAFT).

The challenge to produce controlled polymers resulted in the process called atom transfer radical polymerization in 1995. A review of these three prominent processes namely, NMP, RAFT and ATRP will be dealt in the following sections.

1.7.2 Nitroxide Mediated Polymerization (NMP)

Rizzardo et al and George et al were the pioneers in establishing the process of NMP as explained in the previous section. In 1996, the first work on modeling NMP was initiated by George et al. [33] They modeled NMP using a kinetic approach developed to calculate the effect of exchange between a dormant and an active species in group transfer polymerization. A general solution for the molecular weight distribution as a function of conversion was derived. They only considered the rate constants for propagation, the trapping of the growing chains by nitroxide radical, and the release of the growing chain. They obtained a very good fit between modeling and experimental

results. The group concluded that the polydispersity in the bulk living free radical polymerization mediated by nitroxide is controlled by the exchange rate between the growing and dormant chains. At high conversion, where the rate of polymerization is high, there can be some irreversible chain termination and some autopolymerization.

Fukuda et al. [34] in 1997 investigated the mechanism and kinetics of nitroxide-mediated polymerization on the basis of a set of experimental data collected for the polymerization of styrene at high temperature in the presence of a polystyrene adduct with 2,2,6,6-tetramethylpiperidinyl-1-oxy (PS-TEMPO) or its unimer model (BS-TEMP). They included thermal initiation, bialkyl termination, the decomposition of the active chain end, and the stationary state with respect to the radical concentration. The model was developed by using the method of moments to quantify polydispersity, average molecular weight and other properties. A better fit was obtained against the experimental data for polymerization of styrene. Similarly the Monte Carlo method was applied to model NMP by He et al. [35] in 1997. They predicted the kinetics and chain length distribution obtained in LFRP by using a hybrid monte carlo algorithm. They modeled two classes of living radical polymerizations, one which was initiated by alkoxyamines and the other by nitroxide radical, 2,2,6,6-tetramethyl-1-piperidinyloxy, mediated radical polymerization. They studied the effects of experimental variables, such as the concentration ratio of stable free radicals to initiators, initiation rate constants, etc., on the kinetics and molecular weight distributions. A comparison between simulated and analytical results was made. They concluded that by taking thermal initiation into consideration, the algorithm reproduces the experimental results very well.

In 1999, Matyjaszewski and Shipp[36] made a comprehensive model for ATRP, NMP and RAFT. Their work was different from his predecessor's as they made a comparison between the three polymerization processes. They compared the rates, molecular weight and functionality between the three polymerization processes. The factors leading to deviation from the living behavior were also clearly discussed. This was one of the papers which concentrated on the three methods in unison.

He et al. continued their work on using Monte Carlo simulations to better understand the process of NMP. In 2000, He et al. [37] extended their previous work by studying four rate enhancing cases of NMP by Monte Carlo method. They continued studying the use of Monte Carlo simulations to better understand the process of NMP. They studied the kinetics and molecular weight distribution of the polymers. They inferred that the equilibrium between growing and dormant chains shifted in favor of the growing chains for all the four cases. They also studied the optimization of rate-enhancement in living free-radical polymerization. In the early 21th century, living radical polymerization became a major area of research due to its potential applications as custom made and high performance polymers. A few concentrated on persistent radical effect in the NMP [38] while the focus here pertains to the interest of the thesis. Two areas are of utmost importance, namely:

1. Modeling of NMP in various reactors and thereby predicting their microstructural properties.

2. Diffusion Studies in NMP

Lima and co-workers [39] in 2002 developed a detailed kinetic model for the nitroxide mediated polymerization of styrene. They considered all the prominent reactions, many of which were neglected in the previous efforts on modeling. The reaction mechanism included the following reactions: chemical initiation, reversible nitroxyl ether decomposition, monomer dimerization, thermal initiation, propagation, reversible monomeric and polymeric alkoxyamine formation (production of dormant species), alkoxyamine decomposition, rate enhancement, transfer to monomer and dimer, as well as conventional termination. The qualitative simulations and the detailed mechanistic discusssions presented by these researchers provided a deeper insight into some aspects of the NMP process.

Schulte et al. [40] extended the work on nitroxide mediated polymerization of styrene by varying the concentration of alkoxyamine. The group studied the effect of the variation of the alkoxyamine concentration on the conversion and polydispersity. Four different alkoxyamine were studied, and modeling nonlinear dynamics were discussed by the group.

In 2006, Guillaneuf et al[41] used the commercial software PREDICI to analyze the validity of kinetic rate constants used for the NMP of MMA using the new crowded SG1-based alkoxyamine. They concluded that kinetic rate constants currently in use were incorrect, and the strong penultimate effect drastically increased the equilibrium constant, preventing a well-controlled polymerization. Guillaneuf et al[42] synthesized polystyrene by using NMP and modeled this process using PREDICI. They used the modeling studies to investigate the synthesis of high molar masses living polystyrene. Polystyrene with

number average molecular weight of up to 200,000 g.mol^{-1} was obtained with a living fraction close to 60%.

Batch reactors were primarily used in all the modeling cases explained above. Modeling NMP of styrene in a CSTR was discussed by Lemoine-Nava et al. [43] in the year 2005. The group investigated the non-linear behavior of the styrene nitroxide-mediated radical polymerization (NMRP) taking place in a continuous stirred tank reactor (CSTR). The cooling water flow rate, feed stream temp., cooling water feed temp., monomer feed stream concentration and residence times were chosen as the bifurcation parameters. Their group provided a broad picture of using NMP for the large scale production of this class of polymers. Whereas Lemoine-Nava et al. modeled NMP in a CSTR exclusively, Zhang and Ray [44] utilized a CSTR to model living radical polymerization by using the method of moments in 2001. They analyzed ATRP and NMP in various reactors such as batch, semibatch and CSTR's. They validated their results against experimental data for nitroxide-mediated styrene polymerization and atom transfer radical copolymerization of styrene and n-butyl acrylate. The group gave a theoretical differences obtained while using different reactors. They concluded that semibatch reactors were best suited for making polymers with controlled architecture.

The idea of utilizing semibatch reactors to produce polymers with controlled architecture interested many researchers working in the field of living polymerization. Cunningham et al. [45] utilized a semibatch reactor to model NMP. The group developed a mechanistic model for high-temp. (138°) styrene semibatch polymerization. The group incorporated the gel effect associated with the termination reaction to model NMP. They concluded that implementation of a gel effect correlation to represent the change in the

diffusion-controlled termination rate coefficient with conversion improves the fit to the thermally initiated system, but is not required to represent the production of low molecular weight material by conventionally initiated FRP or NMP. The low initiator efficiency found in NMP is well explained by a reaction network involving combination of free nitroxide with methyl radicals formed from initiator decomposition.

The work utilizing batch, semibatch reactors in the field of NMP has been discussed in the above sections. The emphasis was also on such modeling techniques as method of moments and Monte Carlo simulation. The drawback of the method of moments to predict the chain length distribution facilitated the use of other methods in order to predict the entire microstructural properties. Monte Carlo methods were one of the better techniques for predicting the chain length distribution as explained before. The years 2007 and 2008 saw the development of another technique called probability generating function and the utilization of tubular reactors in living radical polymerization. Asteasuain et al.[46] developed a tool for designing "living" free radical polymerization processes in tubular reactors, in order to achieve tailor-made MWDs. They developed a model for nitroxide-mediated controlled free radical polymerization. Their objective of predicting the MWDs was achieved accurately and efficiently by means of the probability generating function (pgf) transformation. They also obtained a good fit against the experimentally available data. They showed the potential of the resulting model for optimization activities involving the complete MWD. In 2008 the same group published another paper to model NMP while giving more emphasis on optimization of the process in a tubular reactor. [47] These were the modeling efforts done in the field of NMP.

In order to complete the literature review, it is imperative that we include the effect of diffusion in NMP. Most of the authors either avoid the effect of diffusion or they considered only the bimolecular termination to model NMP. Lima et al. [48] qualitatively modeled the effect of diffusion controlled reactions in NMP. The group developed a kinetic model for the nitroxide-mediated radical polymerization of styrene by considering diffusion-controlled effects on the bimolecular radical termination, monomer propagation, dormant polymer activation, and polymer radical deactivation reactions. Free-volume theory was used to study the effect of diffusion. They concluded that diffusion controlled-termination enhances the living behavior of the system, whereas diffusion controlled -propagation, diffusion controlled -activation and deactivation worsens it. Lima et al also [49] simulated the polymerization of styrene by using monomolecular and bimolecular initiators. They studied the effect of using different reaction temperatures. They simulated the polymerization rate, molecular weight, development and evolution of the concentration of species participating in the reaction mechanism. These are the contributions in the field of modeling NMP until the present time.

1.7.3 Reversible Addition Fragmentation Chain Transfer

Shipp and Matyjaszewski [36] simulated NMP, RAFT and ATRP of styrene in 1999. The results have been previously discussed under NMP; hence to avoid repetition, the discussion has been omitted in this category. He et al. [50] modeled NMP by using the Monte Carlo method and they continued using Monte Carlo simulation to model RAFT polymerization also. The group studied the kinetics and chain length distribution of polymers obtained by reversible addn.-fragmentation chain transfer (RAFT) process. The

results predicted that the molecular weight of the polymers simulated increased linearly with monomer conversion, and they obtained a polydispersity lower than 1.1. They validated their model against the experimental results reported for styrene and Methyl methacrylate. The model was in agreement with the experimental results reported in the literature.

Zhang and Ray [51] in 2001 developed a comprehensive model combining living RAFT polymerization chemistry with a tank reactor model to analyze process development and design issues. Experimental data from Methyl methacrylate solution polymerization in a batch reactor were compared with the model to establish the reversible reaction rate constants in the presence of the RAFT chain transfer agent, cumyl dithiobenzoate or 2-cyanoprop-2-yl 1-pyrrolecarbodithioate, with AIBN initiator. Examples of a batch reactor, a single continuous stirred tank, a series of continuous stirred tank reactors and a semibatch reactor

In 2002, Davis et al. [52] used the commercial software PREDICI to model RAFT polymerization. They simulated conversion vs. time plots and full molecular weight distributions by using the PREDICI program. They studied the conditions leading to inhibition and rate retardation that act as a guide to optimum living polymerization behavior. They demonstrated that the inhibition period of considerable length is induced either by slow fragmentation of the intermediate RAFT radicals appearing in the pre-equilibrium or by slow re-initiation of the leaving group radical of the initial RAFT agent. It was demonstrated that the size of the rate coefficient controlling the addition reaction of propagating radicals to polyRAFT agent, k_{β}, was mainly responsible for optimizing the control of the polymerization.

Barner-Kowollik et al[53] also modeled RAFT process using the commercial program package PREDICI. They studied the cumyl dithiobenzoate-mediated bulk polymerization of styrene at 60 °C as a case study. They used the experimentally obtained molecular weight distribution for obtaining the rate coefficients by modeling the time-dependent evolution of experimental molecular weight.

Barner-Kowollik et al[54] simulated the RAFT polymerization using the mechanism suggested by CSIRO group since several mechanisms were reported for RAFT. They simulated the conversion and the molecular weight distribution by using PREDICI. They concluded that the size of the rate coefficient controlling the addition reaction of propagating radicals to polyRAFT agent was mainly responsible for optimizing the control of the polymerization.

Wulkow et al[55] in 2004 modeled the RAFT polymerization by using PREDICI. Two major concerns were addressed by Wulkow et al. One was the debate about the nature of the RAFT mechanism and the other was the validity of PREDICI software to model it. They used the PREDICI software to deduce the rate constants using experimental results. They also explained the mathematical procedure incorporated in PREDICI for modeling.

Lima et al[56] compared the reaction mechanism of RAFT by using PREDICI and a self developed program in FORTRAN. They studied all the reactions related to RAFT polymerization. They studied three different major mechanisms expressed in the literature for their modeling study. A comparison of the models for the different reaction mechanisms was clearly presented. The validity of PREDICI to model RAFT

polymerization was analyzed, and they concluded that PREDICI does have the ability to model RAFT. They concluded that the ambiguous values of the rate constants were the problem more than the PREDICI software.

Lima et al[57] simulated the RAFT polymerization in super critical carbon dioxide. This was the first attempt to model RAFT polymerization in super critical carbon dioxide by using PREDICI. The simulations brought out the kinetic and physical properties for the polymerization of methyl methacrylate by using AIBN. The temperature and pressure was 65°C and 200 bar.

Wang et al. published a series of papers on the modeling aspects for RAFT polymerization. Their first paper depicted a mathematical model for the RAFT scheme which was able to predict the various polymer microstructural properties. [58] They used the method of moments as the modeling technique. The model could predict the monomer conversion, number average molecular weight and polydispersity. It also provided detailed information about the development of various types of chain species during polymerization, including propagating radical chains, adduct radical chains, dormant chains, and three types of dead chains.

Wang et al. [59] derived the development of monomer conversion, as well as propagating radical, adduct radical, dormant chain, and dead chain concentrations in reverse addition-fragmentation transfer polymerization (RAFT). The relations for the profiles of propagating radical concentration and conversion versus time were derived, and the analytical equations were verified against numerical solutions of the mass-

balance differential equations. Their derivation involved the steady-state hypothesis for radical and RAFT agent concentrations.

Prescott in 2003 studied the influence of chain length dependent termination in RAFT polymerization[61]. He inferred that higher transfer constant for RTAs and short dormant chains exhibit significantly shorter radical lifetimes and produces lesser conversion than systems without RTA, while longer dormant chains lead to an extension of radical lifetimes and an increase in the number of radicals. He suggested several experimental techniques which included the use of oligomeric adducts to the RTA, which seemed to offer solution to the known problems of RTA systems in bulk, solution and particularly emulsion polymerization.

Yong et al[62] in 2006 modeled the reaction of dithioester and alkoxyamine to better understand the RAFT polymerization. The kinetics of the model reaction was analyzed and compared with that of pure alkoxyamine homolysis with a Monte Carlo simulation. They inferred that a higher concentration of persistent radicals are formed while for a fast RAFT mechanism the concentration is closely similar to that of pure alkoxyamine. They showed that the Monte Carlo simulation can measure the individual rate constant of the RAFT process, such as the rate const. of addition with a large excess of alkoxyamine.

In 2007, Tobita[63] developed a mathematical model using the Monte Carlo method in a dispersed medium assuming ideal miniemulsion. They studied the effect of particle size on the molecular weight distribution and polymerization rate in NMP and RAFT polymerization. They concluded that rate enhancement by reducing the particle

size were found only for the systems with fast fragmentation of adduct radicals in RAFT system.

Drache et al. [64] implemented a kinetic model for the RAFT scheme with the Monte Carlo method. This was a purely simulated work by the group. The group extended their work to corroborate experimental and simulated results by using Monte Carlo. [65] This work clearly showed the excellent agreement between the experimental and simulated results. They developed a model for reversible addition fragmentation chain transfer polymerization. The conversion, molecular weight and concentration of the RAFT species were obtained by FTIR spectroscopy, size exclusion chromatography and ESR spectroscopy respectively for the bulk polymerization of Methyl methacrylate. The obtained kinetic data served as a parameter set for Monte Carlo modeling of RAFT. Their experimental and simulated data were compared and showed excellent agreement.

Modeling Diffusion controlled reactions in RAFT polymerization were studied by David et al. [66] They conducted experimental analysis coupled with modeling to understand the phenomenon of diffusion controlled reactions in RAFT polymerization. The group used the free volume theory to model diffusion limitations of both termination and RAFT exchange reactions. Model predictions were compared to experimental results of methyl methacrylate polymerization with cumyl dithiobenzoate as a RAFT agent.

Research on modeling RAFT polymerization by Konkolewicz et al., in 2008 [67] presented the argument that, even though many mathematical models were developed which corroborated with experimental data, still there was a compromise in some of the factors. They dealt with commonly used models and their disadvantages in dealing on a

realistic scale. They developed a kinetic scheme which assumed that the equilibrium constant is large (consistent with the slow fragmentation model) and that only very short radicals may terminate with the intermediate formed during in the RAFT process. They concluded that their model was consistent with all experimental data observed to date and fitted the available quantum calculations. That concludes the review on RAFT polymerization.

1.7.4 Atom Transfer Radical Polymerization

The pioneer in the ATRP process was Krzysztof Matyjaszewski in 1999. Matyjaszewski and Shipp [68] developed a kinetic model for atom transfer radical polymerization of styrene. They used the commercial software package PREDICI to simulate the model. ATRP was subjected to the Persistent Radical effect (PRE). They studied the effect of PRE by taking into consideration the diffusion controlled termination reaction. They concluded that the effect of PRE was not visible, since the polymerization goes to high conversion and hence a higher viscosity which conceals the effect of PRE. They also concluded that the thermal initiation does not a play a role in ATRP.

Zhu modeled ATRP using the method of moments. [69] He simulated properties such as monomer conversion, average molecular weight and PDI. His model accounted for the effects of side reactions, bimolecular termination and chain transfer.

Matyjaszewski et al. in 2000 studied the concept of gradient copolymers as it offered a huge potential for manufacturing custom made polymers.[70] Their specific focus was to use atom transfer radical copolymerization to synthesize gradient copolymers with various composition profiles. They simulated atom transfer radical

polymerization in both batch and semi-batch conditions to produce gradient copolymers. The physical properties of gradient copolymers, and possible future work in the field of gradient copolymers were discussed.

Matyjaszewski and Lutz in 2002 modeled the evolution of chain-end functionality of polymers synthesized by ATRP. [71] They compared various kinetic models and established the effect of specific side reactions involved in ATRP. They concluded that the slow elimination of hydrobromic acid from the polymer end-groups, as well as the thermal self-initiation of the monomer, may affect the chain-end functionality. Although the polymerization possesses several characters of a living process (i.e. linear increase of molecular weight vs. conversion, low PDI), the final polymer showed limited functionality. Zhang and Ray have significantly contributed to the field of living polymerization with the perspective of using different reactors for large scale production. In 2002, they developed a tubular reactor model for living polymerization. [72] They tried to develop a tool which could be utilized for manufacturing tailor-made polymers. They validated their model at the plug flow reactor limit using batch experimental data for both TEMPO-mediated styrene polymerization and atom transfer radical copolymerization of styrene and n-butyl acrylate. This is one of the first works in modeling atom transfer radical copolymerization to make tailor-made products. They studied the effects of residence time distribution and the effect of Peclet number on reactor operation and polymer properties. They concluded that, by using an interstage feed of the more reactive monomer, polymers with a uniform copolymer composition and a narrow MWD could be prepared with tubular reactors.

Al-Harthi et al. carried out a series of experimental and simulation works in the field of atom transfer homo and co-polymerization. They used the Monte Carlo simulation predominantly due to its ability to predict the chain length distribution. The group also compared the performance of method of moments and Monte Carlo simulation. Al-Harthi et al. suggested a model for ATRP homo polymerization using the Monte Carlo method based on the Gillespie algorithm. [73] They modeled the ATRP of styrene and validated their model against their experimental results. Both the method of moments and Monte Carlo were used for modeling for comparing their accuracy. Conversion, PDI, Number average molecular weight and MWD were well represented and gave a very good fit against the experimental results. They concluded that Monte Carlo simulation can predict all the features of ATRP, including the linear increase of the molecular weight with conversion and the production of polymers with narrow MWD. The Monte Carlo simulation was compared with the method of moments and found to be more versatile than the latter because it can predict the complete MWD of the polymer.

The same group in 2006 studied the effect of using bifunctional initiators on ATRP.[74] They used the method of moments to predict monomer conversion, average molecular weights and PDI as a function of polymerization time in batch reactors. The main objective of the work was to quantify how polymerization conditions affect monomer conversion and polymer properties by examining the effect of several rate constants such as activation, deactivation, propagation and chain termination, and of catalyst and initiator concentration, on polymerization kinetics and polymer properties. They concluded that the bifunctional initiators produced a higher molecular weight

polymer at the same conditions while the equilibrium constant was a key factor in controlling the living nature of ATRP.

Al-Harthi et al. studied the diffusion effects on ATRP while using bifunctional initiators.[75] They used the method of moments for modeling ATRP while incorporating the free volume theory to study the phenomena of diffusion controlled reactions. A quantitative approach to understand the effect of diffusion on bimolecular termination, activation, deactivation and propagation reactions was investigated. They validated their model against the solution polymerization of styrene, solution polymerization of MMA and bulk polymerization of butyl acrylate. They concluded that the diffusion effects enhanced the livingness of the polymerization.

Al Harthi et al, having used the method of moments to study the effect of bifunctional initiators, moved ahead to incorporate the Monte Carlo method for modeling the same effect.[76] Their primary reason was to understand the chain length distribution which was not available in their previous simulation and to optimize the process of using Monte Carlo. Their work was to compare the method of moments and Monte Carlo results for PDI, conversion and number average molecular weight. They obtained excellent agreement between the two methods. They also simulated the performance of mono functional and bifunctional initiators by using Monte Carlo simulation. They optimized the performance of their algorithm in terms of the size of control volume. These studies led them to a faster algorithm.

Al Harthi et al. further illustrated the use of bifunctional initiators by experimental and modeling the ATRP of styrene.[77] Bulk ATRP of styrene was carried out at 110 °C

using benzal bromide as bifunctional initiator and 1-bromoethyl benzene as monofunctional initiator. CuBr/2,2'-bipyridyl was used as the ATRP catalyst. They used the polymerization kinetic data obtained for styrene by using a mono and bifunctional initiator, and they compared it with a mathematical model based on the method of moments and another one using Monte Carlo simulation. They showed that both the models could predict the conversion, PDI and number average molecular weight very well, and in addition the Monte Carlo simulation was able to predict the MWD accurately. Their stance that a bifunctional initiator produced a high molecular weight polymer was experimentally proven. Later they extended their study to atom transfer radical copolymerization of styrene-acrylonitrile copolymers by bifunctional initiators. [78] This experimental analysis investigated a simultaneous and sequential addition of the comonomers. The monofunctional initiators produced a higher molecular weight polymer on simultaneous addition, while the bifunctional initiators performed better on sequential addition. This led the researchers to provide a kinetic model for atom transfer radical copolymerization by the method of moments.[79] That generic model could predict conversion, copolymer composition, average molecular weight and PDI. They assessed the model's reliability by comparing it with experimental data from the literature (copolymerization of styrene and n-butyl acrylate) and from their lab (copolymerization of styrene and acrylonitrile). The concluded that the model proved that the copolymer composition in the ATRcP is independent of the ATRP parameters.

Al Harthi et al. modeled an interesting concept of using a graft copolymers made with ATRP and metallocene catalysts. [80] Monte Carlo simulation was used to describe the microstructure of polymers made with a combination of coordination polymerization

and ATRP. ATRP was used in the first step to produce monodisperse macromonomers that were subsequently copolymerized with ethylene by using a coordination catalyst in semi-batch mode. The chain length distribution and the grafting density were the most important microstructural details predicted in this study. Al-Harthi et al. used a batch reactor predominantly in all their work detailed in this discussion.

Millar et al[81] in 2007 developed a novel parallelized approach for Monte Carlo simulation in order to simulate the entire molecular weight distribution. They developed an algorithm utilizing advanced compiler technology coupled with parallel processing in order to reduce the simulation time while utilizing higher control volume. This parallel Monte Carlo method is in line with the latest developments in the h-p Galerkin method-based PREDICI software in terms of computation speed and the details provided. They also concluded that the parallel Monte Carlo method can be fused with the h-p Galerkin methods.

Zhu et al. were in parallel with Al Harthi et al. in the field of ATRP. They also published a series of papers on modeling and experimental results in this field. They used only used the method of moments to study ATRP in batch and semibatch while also providing a quantitative approach to diffusion effects in ATRP. Zhu et al. in 2007 modeled ATRcP in a semibatch reactor. [82] Their idea was for the production of gradient copolymers with control. Design of the composition vs. chain length profile to develop polymer materials with tailor-made properties was studied. They used three different reactivity ratios (representative not experimental) to study the control achieved in a semibatch reactor for tailor made polymers. Zhu in 2008 extended his study to achieve gradient copolymers of MMA and tertiary butyl methacrylate (tBMA) by using a

semibatch reactor. [83] Zhu et al. used the method of moments to model ATRcP in a semibatch reactor by using the terminal model. They established the equilibrium constants in the ATRP of MMA and tBMA by the data correlation. Zhu et al also produced two studies on the effect of diffusion on ATRP. In 2002 they made a qualitative analysis of diffusion controlled reactions in ATRP initiated by a monofunctional initiator.[84] They considered the equilibrium reactions, propagation, termination and transfer reactions. They concluded on a similar note as Al-Harthi et al who later in 2006 modeled diffusion by using bifunctional initiators (as previously mentioned). They concluded that the overall effect of diffusion-controlled phenomena in ATRP is to enhance the livingness of the system. They used the experimental data from the literature for styrene, methyl methacrylate, and methyl acrylate ATRP homopolymerizations to validate the kinetic model. In 2008, Zhu et al. modeled the diffusion controlled ATRP which were introduced to cross linking. [85]

Cunningham et al contributed further to the polymer reaction engineering aspects. The group in 2007 studied the batch and semibatch polymerization of styrene experimentally while a mathematical model was also developed. [86] They used a heterogeneous catalyst ATRP catalyst system which provided excellent molecular weight control. There experimental and modeling results were in agreement and provided insight into the polymer reaction engineering aspects in this field.

Najafi et al[87] in 2009 applied the Monte Carlo method to study the effect of chain length dependent bimolecular termination on ATRP. They inferred that the bimolecular termination rate constant fell sharply during the course of polymerization when they applied the chain length dependency. A linear relationship is obtained for the

molecular weight and conversion. They also inferred that the concentration of the catalyst in lower valence state increases and reaches steady state at higher conversion. They predicted that the amount of ligand used was also smaller when chain length dependant termination rate constants are used.

ATRP is versatile in producing tailor- made products with low PDI. Researchers are also analyzing various catalyst and optimization procedures to reduce the cost of manufacturing. With ATRP becoming an extensive topic of research, this thesis is of value to the field as it provides more insight into ATRP especially ATRcP.

1.8 References

[1] M. Kamigaito, T. Ando, M. Sawamoto, Chem Rev **2001**, 101, 3689.

[2] K. Davis, K. Matyjaszewski, Statistical, gradient, block and graft copolymers by controlled/living radical polymerization, **2002**.

[3] T. Davis, K. Matyjaszewski, Handbook of radical polymerization, 2002, pp 523.

[4] X. Zhang, K. Matyjaszewski, Macromolecules **1999**, 32, 1763.

[5] S. Forster, T. Plantenberg Angew. Chem., Int. Ed. **2002**, 41,688.

[6] Z. Gao, S. K. Varshney, S. Wong, A. Eisenberg Macromolecules**1994**, 27, 7923.

[7] M. Nakano, H. Matsuoka, H. Yamaoka, A. Poppe, D. Richter Macromolecules **1999**, 32, 697.

[8] L. Zhang, A. Eisenberg, Science **1995**, 268, 1728.

[9] R. Xu, M. A. Winnik, G. Riess, B. Chu, M. D. Croucher Macromolecules **1992**, 25, 644.

[10] Y. Nakayama, M. Miyamura, Y. Hirano, K. Goto, T. Matsuda Biomaterials **1999**, 20, 963

[11] S. H. Y. Cheo, P. Wang, K. L. Tan, C. C. Ho, E. T. Kang J. Mater. Sci.: Mater. Med. **2001**, 12, 377.

[12] S. Belfer, R. Fainshtain, Y. Purinson, J. Gilron, M. Nystrom, M. Manttari J. Membr. Sci. **2004**, 239, 55.

[13] Y. Liu, J. Y. Lee, E. T. Kang, P. Wang, K. L. Tan. React. Funct. Polym. **2001**, 47, 201.

[14] B. Reining, H. Keul, H. Hocker, polymer, **2002**, 43, 7145.

[15] M. Mukkaram, A. Harald, D. Stover, Macromolecules, **2004**, 37, 5219.

[16] L. Zhongyu, L. Pengpeng, H. Julina, Journal of Polymer Science, Part A: Polymer Chemistry, **2006**, 44, 4361

[17]A. Napoli, N. Tirelli, G. Kilcher, A. Hubbell, Macromolecules, **2001**, 34, 8913.

[18] J. Katja, C. Xianyi, K. Jorgen, B. Walther, Macromolecules, **1998** ,*31*, 538.

[19] T. Pakula, K. Matyjaszewski, Macromol. Theory Simul. **1996**, *5*, 987.

[20] M. Kryszewski, Polym. Adv. Technol. **1997**, 8, 244.

[21] Y. Koike, Polymer **1991**, *32*, 1737.

[22] D. Greszta, K. Matyjaszewski, Polym. Prepr. (Am. Chem. Soc.,Polym. Div.) **1996**, *37*, 569.

[23] S.M. Carbanions, Living Polymers and Electron Transfer Process. Interscience: New York, **1968**

[24] G. Moad, D.H. Solomon, The Chemistry of Free Radical Polymerization. Elsevier: New York, **1995**

[25] E.Borsig, M.Lazar, M.Caplan, S.Florian, Angew Macromol. Chem.**1969**, *9*, 89

[26] T.Otsu, M.Yoshida Makromol.Chem.Rapid.Communication, **1982**, *3*, 127

[27] T.Otsu, A.Kuriyama, Polymer Journal, **1988**, *17*, 97

[28] M. Lee, Y. Minoura Chemical society, Faradays transaction, **1978**, *74*, 1726

[29] D. Mandare, S.Gaynor, K.Matyaszewski, Polymer Preparation (American Chemical Societry. Division of Polymer Chemistry), **1994**, *35*, 700

[30] L.D. Arvanitopoulos , M.P. Greul, H.J. Harwood, Polymer Preparation (Americal Chemical Society. Division of Polymer Chemistry), **1994**, *35*, 549

[31] D.H. Solomon, E. Rizzardo, P. Cacioli, US Patent 4,581,529, 1985

[32] M.K. Georges, R.P.N. Veregin, P.M. Kazmaier, G.K. Hamer, Macromolecules **1993**, *26*, 2987

[33] R.P. N.Veregin, P.G.Odell, Michalak, M.Lora, M.K.Georges, Macromolecules **1996**, *29*, 3346

[34] T. Fukuda, Y. Tsujii, T. Miyamoto,Book of Abstracts, 213th ACS National Meeting, San Francisco, April 13-17, **1997**

[35] J. He, H. Zhang, J. Chen, Y. Yang, Macromolecules **1997**, *30*, 8010

[36] D.A. Shipp, K. Matyjaszewski, Polymer Preprints (American Chemical Society, Division of Polymer Chemistry) **1999**, *40*, 450

[37] J. He, L. Li, Y.Yang, Macromolecular Theory and Simulations **2000**, *9*, 463

[38] J.F. Lutz, P. Lacroix-Desmazes, B. Boutevin, Macromolecular Rapid Communications **2001**, *22*, 189

[39] J. Bonilla, E. Saldivar, A. Flores-Tlacuahuac, E. Vivaldo-Lima, R. Pfaendner, F. Tiscareno-Lechuga, Polymer Reaction Engineering 2002, 10, 227

[40] T. Schulte, C.A. Knoop, A. Studer, Journal of Polymer Science, Part A: Polymer Chemistry **2004**, *42*, 3342

[41] Y. Guillaneuf, D. Gigmes, R. A. Marque, P.Tordo, D.Berlin, Macromolecular Chemistry and Physics **2006,** *207*, 1278

[42] Y. Guillaneuf, P. Dufils, L.Benoit, G.Olivier, D.Marque, R.A.Sylvian, D.Bertin, P.Tordo

[43] R. Lemoine-Nava, A. Flores-Tlacuahuac, E. Saldivar-Guerra, Chemical Engineering Science **2005**, *61*, 370

[44] M. Zhang, W.H. Ray, Journal of Applied Polymer Science **2002**, *86*, 1630

[45] Y. Fu, M.F. Cunningham, R.A. Hutchinson, Macromolecular Reaction Engineering 2007, 1, 243

[46] M. Asteasuain, M. Soares, M.K. Lenzi, M.F.Cunningham, C. Sarmoria, J.C. Pinto, A. Brandolin, Macromolecular Reaction Engineering **2007**, *1*, 622

[47] M. Asteasuain, M. Soares, M.K. Lenzi, R.A. Hutchinson, M.F. Cunningham, A. Brandolin, J.C. Pinto, C. Sarmoria, Macromolecular Reaction Engineering **2008**, *2*, 414

[48] M. Roa-Luna, A. Nabifar, N.T. McManus, E. Vivaldo-Lima, L.M. Lona,

A. Penlidis, Journal of Applied Polymer Science **2008**, *109*, 3665

[49] J. Belincanta-Ximenes, V.R.P. Mesa,.; M.F. Lona, E. Vivaldo-Lima, N. McManus, A. Penlidis, Macromolecular Theory and Simulations **2007**, 16, 194

[50] L. Li, J.P.He, Y. Yang, Gaodeng Xuexiao Huaxue Xuebao **2000**, *21*, 1146

[51] M. Zhang, W.H. Ray, Industrial & Engineering Chemistry Research **2001**, *40*, 4336

[52] P. Vana, T.P. Davis, C. Barner-Kowollik, Macromolecular Theory and Simulations **2002**, *11*, 823

[53] C. Barner-Kowollik, J.F. Quinn, D. Morsley, T. Davis, Journal of Polymer Science, Part A: Polymer Chemistry **2001**, *39*, 1353

[54] C.Barner-Kowollik, T.P. Davis, P. Vana, Macromolecular Theory and Simulations **2002**, 823

[55] C.Barner-Kowollik, T.P. Davis, M. Busch, M. Wulkow J Polym Sci Part A: Polym Chem **2004**, *42,*1441

[56] J. Pallares, J. Gabriel; F. Citlalli, E.Vivaldo Lima L.M. F. Lona, A. Penlidis Journal of Macromolecular Science, **2006,** *43*,1293

[57] J. Gabriel, M. Luz Castellanos-Cárdenas P.R. García-Morán, E. Vivaldo-Lima, G. Luna-Bárcenas, A. Penlidis

[58] R.A. Wang, S. Zhu, Journal of Polymer Science, Part A: Polymer Chemistry **2003**, *41*, 1553

[59] R.A. Wang, S. Zhu,Macromolecular Theory and Simulations **2003**, *12*, 663

[60] S.Prescott, Macromolecules **2003**, *36*, 9608

[61] Y. Ao, J. He, X. Han, Y. Liu, X. Wang, D. Fan, J. Xu, Y. Yang, Journal of Polymer Science, Part A: Polymer Chemistry **2006**, *45*, 374

[62] H. Tobita, F. Yanase, From Macromolecular Theory and Simulations **2007**, *16*, 476

[64] M. Drache, K. Drees, G. Schmidt-Naake, DECHEMA Monographien **2004**, *138*, 479

[65] M. Drache, P. Vana, G. Schmidt-Naake, World Congress of Chemical Engineering, July 10-14, **2005**, *84560/1*

[66] A.D. Peklak, A. Butte, G. Storti, M. Morbidelli, Journal of Polymer Science, Part A: Polymer Chemistry **2006**, *44*, 1071

[67] D. Konkolewicz, B.S. Hawkett, A. Gray-Weale, S. Perrier, Macromolecules **2008**, *41*, 6400

[68] D.A. Shipp, K. Matyjaszewski, Macromolecules **1999**, *32*, 2948

[69] S. Zhu, Macromolecular Theory and Simulations **1999**, *8*, 29

[70] K. Matyjaszewski, M.J. Ziegler, S.V. Arehart, D.Greszta , T. Pakula Journal of Physical Organic Chemistry **2000**, *13*. 775

[71] J.F. Lutz, K. Matyjaszewski, Macromolecular Chemistry and Physics **2002**, **203**, 1385

[72] M. Zhang, W.H. Ray, Journal of Applied Polymer Science **2002**, *86*, 1047

[73] M. Al-Harthi, J. Soares, L. Simon, Macromolecular Material Science **2006,** *291*, 993

[74] M. Al-Harthi, J. Soares, L. Simon, Macromolecular Theory and Simulation **2006,** *15*, 198

[75] M. Al-Harthi, J. Soares, L. Simon, Macromolecular Chemical Physics. **2006**, *207*, 469

[76] M. Al-Harthi, J. Soares, L. Simon, Macromolecular Reaction Engineering **2007**, 1, 95

[77] M. Al-Harthi, L. Cheng, J. Soares, L. Simon, Journal of Polymer Science, Part A: Polymer Chemistry **2007**, *45*, 2212

[78] M. Al-Harthi, A. Sardashti, J. Soares, L. Simon, Polymer, **2007**, *48*, 1954

[79] M. Al-Harthi, J. Soares, L. Simon, Macromolecular Reaction Engineering **2007**, *1*, 468

[80] M. Al-Harthi, J. Soares, L. Simon, Macromolecular Symposia, **2006**, *243*, 83.

[81] H. Chaffey-Millar, D. Stewart, M.T. Chakravarty, G. Keller, C.Barner-Kowollik, Macromolecular Theory and Simulations **2007**, *16*, 575

[82] S. Zhu, R. Wang,Y. Luo, B. Li, *AIChe J*. **2007**, *53*, 174

[83] Y. Zhao, Y. Luo, C. Ye, B. Li, S. Zhu, Journal of Polymer Science, Part A: Polymer Chemistry **2008**, *47*, 69

[84] O.Delgadillo-Velazquez, E. Vivaldo-Lima, I.A. Quintero-Ortega, S Zhu AICHE journal **2002,** *11*, 2597

[86] Q. Yu, Z. Qin, J. Li, S. Zhu, Polymer Engineering and Science **2008**, *48*, 1254

[87] Y. Fu, M.F Cunningham, R.A. Hutchinson, Macromolecular Reaction Engineering. **2007**, *1*, 425

CHAPTER 2

METHODOLOGY

Monte Carlo simulation is a method that solves a probabilistic model of physical and chemical process through the use of a random number generator. The observations generated are then analyzed by statistical methods, such as means, modes, variances and distributions, to produce useful information concerning the probabilistic model that underlies the simulated random experiment. Ulam in 1946 named this approach in honor of a relative who was a gamble. Metropolis also made important contributions to the development of such methods. In this chapter, section 2.1 gives a general Monte Carlo procedure. Section 2.2 provides a detailed description of how the Monte Carlo approach was transformed to the language of MATLAB (i.e. coding and programming) to achieve our objectives.

2.1 General Monte Carlo Procedure

The dynamic Monte Carlo approach used in this thesis is based on the method proposed by Gillespie. Suppose we consider the following basic kinetic scheme:

Initiation $$PR + M \xrightarrow{k_i} R_1 \bullet \quad (2.1)$$

Propagation: $$R_r \bullet + M \xrightarrow{k_p} R_{r+1} \bullet \quad (2.2)$$

Termination by Combination: $$R_r \bullet + R_m \bullet \xrightarrow{k_{tc}} P_{r+m} \quad (2.3)$$

where M is the monomer, PR is the propagating radical during initiation, Rr ● is polymer radical. P_r and P_m are the dead polymer chains. k_p is the propagation rate constant, k_{tc} is the rate constant of termination by combination, k_i is the initiation rate constant, and the subscripts r and m indicate the number of monomer molecules in the chain.

First the deterministic, or experimental, rate constant (k^{exp}) should be changed to stochastic, or Monte Carlo, rate constants (k^{MC}) according to the following equations

$$k^{MC} = k^{\exp} \text{ for first order reactions} \quad (2.4)$$

$$k^{MC} = \frac{k^{\exp}}{VN} \text{ for bimolecular reactions between different species} \quad (2.5)$$

$$k^{MC} = \frac{2k^{\exp}}{VN} \text{ for bimolecular reactions between similar species} \quad (2.6)$$

Secondly all concentrations should be transformed to number of molecules in the control (simulation) volume V; in our example we have only monomer concentration, consequently:

$$X_m = [M]\, NV \quad (2.7)$$

where N is the Avagadro's number

Then calculate the reaction rate for every reaction according to the equations:

Rate of initiation:

$$\mathrm{Ri} = k_i^{MC} X_{pr}\ X_m \tag{2.8}$$

Rate of propagation:

$$R_p = k_p^{MC}\ X_r\ X_m \tag{2.9}$$

Rate of termination by combination:

$$R_{tc} = \frac{k_{tc}^{MC} X_r (X_r - 1)}{4} \tag{2.10}$$

where X_r and X_m are the number of polymer radicals and monomer molecules respectively.

The total reaction rate (R_{sum}) is then calculated as the summation of the individual reaction rates.

Then the probability of any reaction (P_v) taking place at a given time is calculated by the following equation:

$$P_v = \frac{R_v}{R_{sum}} \tag{2.13}$$

Then the following relation is used to determine which reaction type will take place at a given polymerization time:

$$\sum_{v=1}^{\mu-1} P_v < r_1 < \sum_{v=1}^{\mu} P_v \tag{2.14}$$

where μ is the number of the selected reaction type and r_1 is a random number uniformly distributed between [0, 1]. Another random number is generated to determine the time interval (τ) between two consecutive reactions. The time step is related to the inverse of total stochastic rates and the natural logarithmic of r_2 according to the equation:

$$\tau = \frac{1}{\sum_{v=1}^{N} R_v} \ln\left(\frac{1}{r_2}\right) \tag{2.15}$$

The algorithm for a general Monte Carlo simulation comprises of the following steps:

1. Input the deterministic reaction rate constant, k_1^{exp}, k_2^{exp}, k_3^{exp} ,…k_μ^{exp}, simulation volume,V, Avagadro's number, N, reactant concentration (mol/Volume)

2. Set time to zero and conversion to zero , *t=0 and x=0*

3. Calculate the stochastic rate constants, k_1^{MC}, k_2^{MC}, ……. k_μ^{MC} using equation 2.5, 2.6 or 2.7

4. Calculate and store the rates of reaction R_1, R_2 ….. R_μ for the selected reaction mechanism

5. Calculate and store the sum of the rates of reaction, R_{sum} according to the following equation: $R_{sum} = \sum_{\mu=1}^{M} R_\mu$ where R_μ is the rate of the μ^{th} reaction and M is the number of reactions.

6. Get two random numbers, r_1 and r_2, uniformly generated between 0 and 1, and calculate μ and τ according equations 2.14 and 2.15.

7. Select which reaction will occur according to equation 2.14

8. Update the number of molecules of each type in the reactor

9. Update the simulation time, t , by $t = t + \tau$, and calculate the conversion, x

10. Return to step 4 until we obtain the desired polymerization time $t = t_{final}$ or final conversion $x = x_{final}$

The sequence of the steps could be altered or changed depending on convenience, flexibility and programming skills of the programmer.

2.2 Detailed Monte Carlo Procedure and MATLAB programming:

We consider the following mechanism for ATRcP under consideration in this thesis.

Initiation steps:

$$I + C \xrightarrow{k_a} PR + CX \tag{2.16}$$

$$PR + CX \xrightarrow{k_d} I + C \tag{2.17}$$

$$PR + M_A \xrightarrow{k_{iAA}} R_{1,A} \tag{2.18}$$

$$PR + M_B \xrightarrow{k_{iBB}} R_{1,B} \tag{2.19}$$

Equilibrium and propagation steps:

$$D_{r,A} + C \xrightarrow{k_{a,A}} R_{r,A}\bullet + CX \tag{2.20}$$

$$D_{r,B} + C \xrightarrow{k_{a,B}} R_{r,B}\bullet + CX \tag{2.21}$$

$$R_{r,A}\bullet + M_A \xrightarrow{k_{p,AA}} R_{r+1,A}\bullet \tag{2.22}$$

$$R_{r,B}\bullet + M_B \xrightarrow{k_{p,BB}} R_{r+1,B}\bullet \tag{2.23}$$

$$R_{r,A}\bullet + M_B \xrightarrow{k_{p,AB}} R_{r+1,B}\bullet \tag{2.24}$$

$$R_{r,B}\bullet + M_A \xrightarrow{k_{p,BA}} R_{r+1,A}\bullet \tag{2.25}$$

$$R_{r,A}\bullet + CX \xrightarrow{k_{d,A}} D_{r,A} + C \tag{2.26}$$

$$R_{r,B}\bullet + CX \xrightarrow{k_{d,B}} D_{r,B} + C \tag{2.27}$$

Transfer to monomer steps:

$$R_{r,A}\bullet + M_A \xrightarrow{k_{tr,AA}} P_r + R\bullet \tag{2.28}$$

$$R_{r,A}\bullet + M_B \xrightarrow{k_{tr,AB}} P_r + R\bullet \tag{2.29}$$

$$R_{r,B}\bullet + M_B \xrightarrow{k_{tr,BB}} P_r + R\bullet \tag{2.30}$$

$$R_{r,B}\bullet + M_A \xrightarrow{k_{tr,BA}} P_r + R\bullet \tag{2.31}$$

Termination by combination:

$$R_{r,A}\bullet + R_{m,A}\bullet \xrightarrow{k_{tc,AA}} P_{r+m} \tag{2.32}$$

$$R_{r,A}\bullet + R_{m,B}\bullet \xrightarrow{k_{tc,AB}} P_{r+m} \quad (2.33)$$

$$R_{r,B}\bullet + R_{m,B}\bullet \xrightarrow{k_{tc,BB}} P_{r+m} \quad (2.34)$$

Termination by disproportionation:

$$R_{r,A}\bullet + R_{m,A}\bullet \xrightarrow{k_{td,AA}} P_r + P_m \quad (2.35)$$

$$R_{r,A}\bullet + R_{m,B}\bullet \xrightarrow{k_{td,AB}} P_r + P_m \quad (2.36)$$

$$R_{r,B}\bullet + R_{m,B}\bullet \xrightarrow{k_{td,BB}} P_r + P_m \quad (2.37)$$

In Equations 2.16 to 2.37, I is the initiator, C and CX are the catalyst in its low and high valence states, M_A and M_B are the comonomers, $R_{r,A}\bullet$ and $R_{r,B}\bullet$ are polymer radicals terminated in monomer A and B, P_r is a dead polymer chain, D_r is a dormant polymer chain, k_i is the initiation rate constant, k_a is the activation rate constant, k_d is the deactivation rate constant, k_p is the propagation rate constant, k_{tc} is the rate constant of termination by combination, k_{td} is the rate constant of termination by disproportionation, k_{tr} is the transfer rate constant, and the subscripts r and m indicate the number of monomer molecules in the chain. The subscript A denotes that the chain ends with monomer A and the subscript B has an equivalent meaning.

The following assumptions and hypothesis are made in this mechanism:

1. All reactions are irreversible
2. All reactions are elementary
3. Rate Constants are chain length independent

4. Initiator and catalyst efficiencies are constant

5. Thermal initiation does not occur

Even though a general Monte Carlo mechanism has been given before, a detailed description of how Monte Carlo simulation was done in this thesis will be interesting and will help the reader understand more about this process.

Step 1:

As stated before, we input the following constants:

- Temperature
- Concentration of Monomer A (*CMA*) and Monomer B (*CMB*)
- Avogadro's Number (*N*)
- Experimental Rate Constants (k_1^{exp}, k_2^{exp}, k_3^{exp} ,...k_μ^{exp})
- Reactivity ratios r_1 and r_2

Step 2:

During polymerization in ATRcP, five different species are formed within the reactor, namely:

- Dormant chain with end group corresponding to monomer A ($D_{r,A}$)
- Dormant chain with end group corresponding to monomer B ($D_{r,B}$)
- Growing Polymer Radicals with end group corresponding to monomer A ($R_{r,A}$)

- Growing Polymer Radicals with end group corresponding to monomer B ($R_{r,B}$)
- Dead Polymer chains (P)

MATLAB relies heavily on the creation of matrices in order to transform physical processes and to simulate such processes. A normal matrix represented by [ ] needs to have an equal number of rows when constructing a column matrix.

Example: $A = \begin{bmatrix} 1 & 0 & 0 & 1 \\ 1 & 1 & 1 & 1 \\ 1 & 0 & 1 & 1 \end{bmatrix}$ is the correct representation for a normal matrix

However in the case of polymerization, we have thousands of unequal polymer chains. Hence to represent such a scenario, a special type of matrix called cell matrix represented by { } is utilized in our case.

Example: $B = \left\{ \begin{bmatrix} 1 \\ 0 \\ 0 \\ 0 \\ 1 \end{bmatrix} \begin{bmatrix} 1 \\ 0 \\ 0 \end{bmatrix} \begin{bmatrix} 1 \\ 0 \\ 0 \\ 0 \\ 1 \\ 0 \\ 1 \\ 1 \end{bmatrix} \begin{bmatrix} 1 \\ 0 \end{bmatrix} \right\}$ is a special matrix type consisting of collection of independent matrices.

Such a matrix allows us to know the following vital information:

1. Total number of chains, corresponding to 4 in example B
2. Chain length of independent chains - corresponding to (5,3,8,2) from example B

3. Sequence Length Distribution

   Consider chain 3 (the longest chain). The program can access each element within the chain. If we assign 1 for monomer A and 0 for monomer B, the program scans for the sequence and gives us the following diads.

   [10]-AB, [00]-BB, [01]-BA,[01]-BA. Thus by assigning 0 and 1 for monomer A and B, we can easily know the diads and triads since we are able to access every element in every chain.

4. Molecular Weight Distribution (MWD)

   Chain lengths are obtained from individual chains. From the chain length, the molecular weight could be obtained by knowing the physical properties of the monomers. Since individual chain lengths and their corresponding molecular weights are obtained, the MWD can be generated by Monte Carlo simulation.

5. The type of end group in the chain (monomer A ended or monomer B)

Thus we allocate four cell matrices to $D_{r,A}$, $D_{r,B}$, $R_{r,A}$ and $R_{r,B}$ to the following cell matrices Da, Db, Ra and Rb respectively. The dead polymer chains are denoted by a normal matrix P. The dead polymers chains are classified as a normal matrix since only addition of terminated chains is involved without any further operations on them.

Step 3:

The number of monomer molecules, catalyst and initiator are calculated by using the following relationship.

$$X_A = [M_A] N V$$

$$X_B = [M_B] N V$$

$$X_i = [I] N V$$

$$X_C = [C] N V$$

The objective is to eliminate the volume in the concentration and to find the number of molecules of monomer, catalyst and initiator.

The experimental rates are also converted into stochastic rates by equations 2.5, 2.6 and 2.7.

Step 4:

The rate of the reaction is calculated and explained by the following examples.

Example 1: Initiation

Consider the following initiation reaction (equation 2.16)

$I + C \xrightarrow{k_a} PR + CX$,

The rate of the reaction would be calculated as

R (1) = $k_{a1}^{MC} X_C X_i$

where k_{a1}^{MC} is the stochastic rate constant of activation for monomer A.

Example 2: Equilibrium

Consider the following equilibrium reaction (equation 2.20)

$$D_{r,A} + C \xrightarrow{k_{a,A}} R_{r,A} \bullet + CX$$

The rate of the reaction would be calculated as

R (5) = $k_{a1}^{MC} X_{da} X_C$

Thus all the rate of reaction are calculated as a product of their respected stochastic rate and number of molecules of either dormant chains, catalyst, monomers or growing polymer radical chains

Step 5

The next step is to calculate the total rate and probability of each reaction. Summation of all the rates gives us the total rate of reaction. The probability of a particular reaction to take place is calculated from equation 2.13.

Example 3:

Probability of Activation Reaction = Rate of Activation reaction / Total Rate of Reactions (R_{sum})

while the probability of the specific reaction type is obtained by generating a random number uniformly distributed between 0 and 1. By using the random number and the probability of individual reactions, a suitable reaction is chosen. This is illustrated with an example below:

Example 4:

A random number is generated in MATLAB by the command rand (r_1 = rand) results in an output of 0.25 (Case 1). Consider that individual probabilities of three reactions are P1 =0.1, P2=0.25, P3=0.65. The program would choose the reaction having the probability of 0.25 (P2 in this case which refers R (2) for the reaction type). Consider another case where we again generate a random number and we get an output of 0.5 (Case 2). In this case the program will pick a value which is above P2 namely P3. Thus the program chooses which reaction type to take place at every loop.

Case 1:

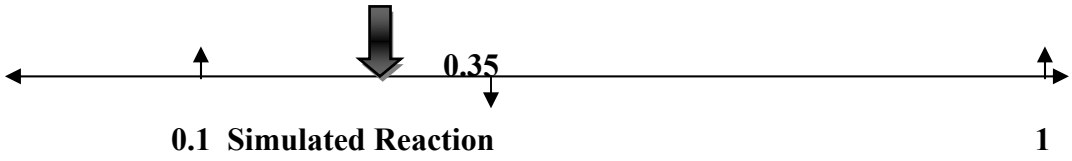

Case 2:

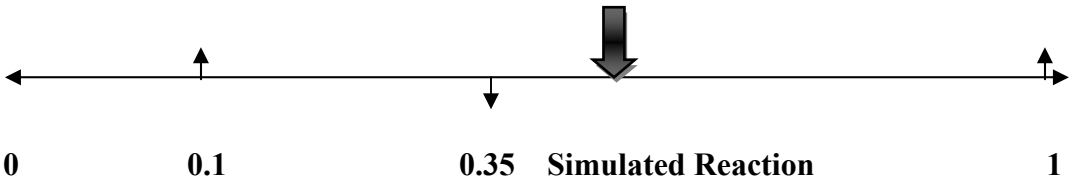

Step 6:

Calculation of time

Another random number (r_2) is chosen between 0 and 1 and used to calculate the time step by the following equation

$$\tau = \frac{1}{R_{sum}} \ln \left(\frac{1}{r_2} \right)$$

The time (t) is updated at every loop with the following relation:

$$t = t + \tau$$

Step 7:

Simulation of Selected Reaction

Once a particular reaction is chosen randomly as in the case of a polymerization reactor, the next step is to carry out the selected reaction by using the language of MATLAB. Many examples are given in order to clearly illustrate the procedure adopted while handling different type of reactions like initiation, equilibrium, propagation, cross propagation, transfer , cross transfer and bimolecular termination.

Example 5: Initiation

Consider the following reaction:

$$I + C \xrightarrow{k_a} PR + CX$$

In this reaction, the initiator and catalyst lose molecules while an increase in the propagating radical and the deactivator/catalyst in the lower valence take is observed. Since Monte Carlo simulation works at the molecular level, we increase and decrease the number of molecules according to the reaction. Thus in this type of reaction we perform the following operation:

- Decrease the number of Initiator molecules by 1: $X_i = X_i - 1$
- Decrease the number of Catalyst molecules by 1: $X_c = X_c - 1$
- Increase the number of the PR molecules by 1: $X_{pr} = X_{pr} + 1$
- Increase the number of CX molecules by 1: $X_{cx} = X_{cx} + 1$

Example 6: Equilibrium

$$D_{r,A} + C \xrightarrow{k_{a,A}} R_{r,A} \bullet + CX$$

As seen from the reaction, there is a decrease in the catalyst and dormant chains while an increase in polymer radical and the lower valence catalyst. We should note that the dormant and the growing polymer radicals are in form of chains, and we represented them as cell matrices earlier. Hence a more sophisticated approach has to be adopted than the one adopted during initiation.

The following operations are performed:

- Decrease the number of catalyst molecules by 1: $X_c = X_c - 1$
- We need to add one molecule to X_{ra} (number of growing radical chain) and reduce one molecule from X_{da}(number of dormant chains) .

  $X_{ra} = X_{ra} + 1;$

  $X_{da} = X_{da} - 1;$

- We need to randomly select one dormant chain from the cell matrix Da and transfer it to the cell Ra. To perform this physical phenomenon in MATLAB, we use the following procedure.

  - Find the total number of chains of the Dormant Radicals :

    ```
    >> LEN = length (Da)
    ```

- Randomly choose one chain among the available chains:

```
>> rvec = randsample(LEN,1)
```

- The randomly chosen chain (rvec) is placed in the growing polymer radical as follows:

```
>> Ra{Xra} = Da{rvec}
```

This ensures that the chain is placed in the new location created before, hence avoiding the overlaying of chains.

- Finally we need to remove the randomly chosen chain (rvec) from Da since it has been placed in Ra. The following command removes the chosen chain from Da.

```
>> Da(rvec) = [ ]
```

Example 7: Propagation

$$R_{r,A}\bullet + M_A \xrightarrow{k_{p,AA}} R_{r+1,A}\bullet$$

The following example shows how propagation reactions are handled in the program. We have a decrease in monomer A and an increase in the chain length of Ra. Hence the following operations are performed.

- Decrease in the number of monomer A by 1 : $X_A = X_A - 1$
- The physical phenomenon is the addition of monomer of the same kind (Monomer A to Radical A) to a particular chain in Ra which increases the chain length by adding one Monomer A unit. To incorporate this physical phenomena in the program, the following operation was done:

- Find the total number of Radical chains :

```
>> LEN = length (Ra)
```

- Randomly choose one chain :

```
>> rvec = randsample (LEN,1)
```

Convert the obtained chain which is a cell matrix type to a normal matrix in order to perform further operations on it, since a cell matrix has access to limited basic operation. Hence the need arises to convert it to a normal matrix at certain junctures.

```
>> vec = cell2mat (Ra (rvec))
```

is the command for such an operation

- Adding the monomer to the particular chain:

```
>> lvec = length (vec) +1
```

- Specifying the type of monomer added (Whether monomer A or B). Monomer A has a indexing of "1" and monomer B has an indexing of "0" in the program. Thus the following assigns that the monomer added is of type A.

```
>> vec (lvec) =1
```

performs the indexing operation.

- Finally we need to have the chain in the cell matrix form due to aforementioned advantages of using a cell matrix. Hence the final part of the program is to convert the normal matrix to a cell matrix and place it in Ra

```
>> Ra(rvec) = vec
```

Example 8: Cross Propagation

$$R_{r,A}\bullet + M_B \xrightarrow{k_{p,AB}} R_{r+1,B}\bullet$$

The programming of cross propagation is slightly different from the previous section since two dissimilar radicals are involved. As emphasized before, a decrease in monomer B and Ra is seen while an increase is observed in Rb.

- Decrease in the number of monomer B by 1 : $X_B = X_B - 1$
- Increase in the number of growing polymer radical (Rb) : $X_{rb} = X_{rb} + 1$
- The physical phenomenon is the addition of monomer of the different kind (Monomer B to Radical A) while creating an increase in the chain length of Rb by adding one Monomer B unit. To incorporate this physical phenomena in the program the following operation was done:
  - Find the total number of Radical chains :

    ```
    >> LEN = length (Ra)
    ```

  - Randomly choose one chain :

    ```
    >> rvec = randsample (LEN,1)
    ```

Convert the obtained chain which is a cell matrix type to a normal matrix in order to perform further operation on it since a cell matrix has access to limited basic operation. Hence the need arises to convert it to a normal matrix at certain junctures.

```
>> vec = cell2mat (Ra (rvec))
```

is the command for such an operation

- Adding the monomer to the particular chain:

```
>> lvec = length (vec) +1
```

- Specifying the type of monomer added (Whether monomer A or B). Monomer A has a indexing of "1" and monomer B has an indexing of "0" in the program. Thus the following ensures that the monomer added is of type A.

`>> vec (lvec) = 0` performs the indexing operation.

- Finally we need to have the chain in the cell matrix form due to aforementioned advantages of using a cell matrix. Hence the final part of the program is to convert the normal matrix to a cell matrix and place it in Ra

```
>> Rb (xrb) = vec
```

➢ Finally the chain which was taken from Ra has to be removed since it has been transferred to Rb.

$X_{ra} = X_{ra} - 1$

`>> Ra (rvec) = [ ]` removes the chain which had been transferred to Rb.

The technique for handling transfer and cross transfer reactions are similar to the propagation reactions and hence will not be discussed.

Example 9: Bimolecular Termination

$$R_{r,A}\bullet + R_{m,A}\bullet \xrightarrow{k_{tc,AA}} P_{r+m}$$

Termination is the process by which two growing polymer radical chains combine and form a dead polymer. The programming is done in the following manner.

- According to the equation, two chains from Ra will combine to form dead polymer and hence Ra should have a minimum of two chains. This check is done as follows

  `>> LEN = length (Ra)` and only if LEN > 2 , the reaction would proceed to completion.

- Two random chains are chosen from Ra as follows:

  ```
  >> rvec1 = randsample (LEN, 1)

  >> rvec2 = randsample (LEN, 1)
  ```

- The following chains are in the cell matrix form and hence need to be converted to a normal matrix in order to perform further operation on them, hence the following code is utilized:

  ```
  >> vec1=cell2mat(Ra(rvec1))
  >> vec2=cell2mat(Ra(rvec2))
  ```

- The number or the length of each chain is calculated as follows:

```
>> lvec1=length(vec1)
>> lvec2=length(vec2)
```

- We have the formation of a dead polymer chain, and hence an increase in the number of dead polymers takes place as follows:

  $X_p = X_p + 1$

- Now the summation of the two growing radical chains takes place, becoming a dead polymer as follows

```
>> P(xp)= lvec1+lvec2
```

- Finally the growing chains which formed the dead polymer should be removed from Ra as follows;

  $X_{ra}=X_{ra}-2$;

```
>> Ra{rvec1}=[ ];
>> Ra{rvec2}=[ ];
```

Thus bimolecular termination reactions are programmed by using the Monte Carlo approach. Other termination reactions can also programmed with a similar methodology or a slightly modified approach as appropriate to the situation. Thus some examples were used to apply the generalized Monte Carlo approach for programming our physical system (ATRcP), hence summarizing the methodology used in achieving the objectives of this thesis.

2.3 Nomenclature

The most important symbols used in this chapter are enumerated below. Even though they have been mentioned earlier, this nomenclature will be helpful for the readers to understand the principles used.

Dra - Dormant chain with end group corresponding to monomer A

Drb - Dormant chain with end group corresponding to monomer B

Da - A cell matrix and the notation used in the program which corresponds to Dra

Db - A cell matrix and the notation used in the program which corresponds to Drb

Rra - Growing Polymer Radicals with end group corresponding to monomer A

Rrb -Growing Polymer Radicals with end group corresponding to monomer B

Ra - A cell matrix and the notation in the program which corresponds to Rra

Rb - A cell matrix and the notation in the program which corresponds to Rrb

LEN - Notation in the program to extract the number of chains in Da,Db, Ra,Rb or P

Rvec - Notation in the program to extract a random chain from Da, Db, Ra, Rb or P

P - Dead Polymer Chains

vec - Notation in the program for converting the cell matrix to normal matrix

lvec - Notation in the program for obtaining the chain length of (vec) or for adding a monomer to (vec)

CHAPTER 3

DYNAMIC MONTE CARLO SIMULATION OF ATOM TRANSFER RADICAL COPOLYMERIZATION IN BATCH REACTOR

3.1 Introduction

The synthesis and design of polymers with well-defined chain structures is a topic of high interest in academia and industry. Controlled radical polymerization (CRP) is fast becoming an important tool for producing polymers with customized microstructures.[1-2] The most well-established mechanisms of CRP are: (1) atom transfer radical polymerization (ATRP),[3,4] (2) nitroxide-mediated polymerization (NMP),[5,6] and (3) reversible addition-fragmentation chain transfer (RAFT).[7,8] Although the application of CRP processes is still limited to academia, they are promising techniques for the industrial production of specialty polymers. At this stage of CRP research, it is imperative to develop reliable mathematical models in order to better understand and improve CRP processes.

Since 1995, significant effort has been directed towards the development, understanding, and application of ATRP to a wide range of monomers. In addition to its ability to control polymer microstructural details, ATRP is very robust toward different

reaction conditions. [9-11] ATRP can also copolymerize a variety of vinyl monomers to form random, gradient, block, and graft copolymers.[12-14] Among these previous chain architectures, gradient copolymers have received considerable interest because they form a new class of materials that have intermediate properties between random and block copolymers.[11]

Several research groups have developed mathematical models for ATRP. The method of moments has been used to study the effect of reactant concentration and rate constants on polymer properties,[15,16] and also used to study the effect of diffusion-controlled reactions using the free volume theory.[17,18] Mathematical models using the concept of pseudo-kinetic rate constants and the method of moments have also been developed to describe ATRP.[19,20]

Even though the method of moments can predict average molecular weights (M_n, M_w, and M_z, for instance) and the polydispersity index (PDI), it cannot predict the complete molecular weight distribution (MWD) and it is well-known that the final properties of the polymer are not only a function of the average properties, but depend on distributions of molecular structural properties such as MWD, copolymer composition distribution (CCD), and sequence length distribution (SLD). The commercial software package PREDICI can be used to model polymerization processes and to predict several polymer microstructural distributions, but it is available only to licensed users, while Monte Carlo simulation is an equally powerful technique that is relatively easy to implement, as will be demonstrated in this thesis. PREDICI has been used to study the kinetics of ATRP, and to model chain end functionality.[21-24]

Several publications show the use of Monte Carlo models for different polymerization processes. [25-27] Recently, Monte Carlo simulation has also been used to study ATRP with mono-functional and bi-functional initiators.[28-30]

In the present study, a Monte Carlo simulation model for ATRP in batch reactors has been developed. The model gives a detailed picture of the microstructure of copolymers produced via such a process, and it can be used to design and optimize the characteristics of the final product.

3.2 Model Development

The methodology used has been clearly explained in Chapter 2. The polymerization mechanism described in chapter 2 is schematically shown in the flow-sheet summarizing the Monte Carlo simulation procedure adopted in this investigation (Figure 3.1).

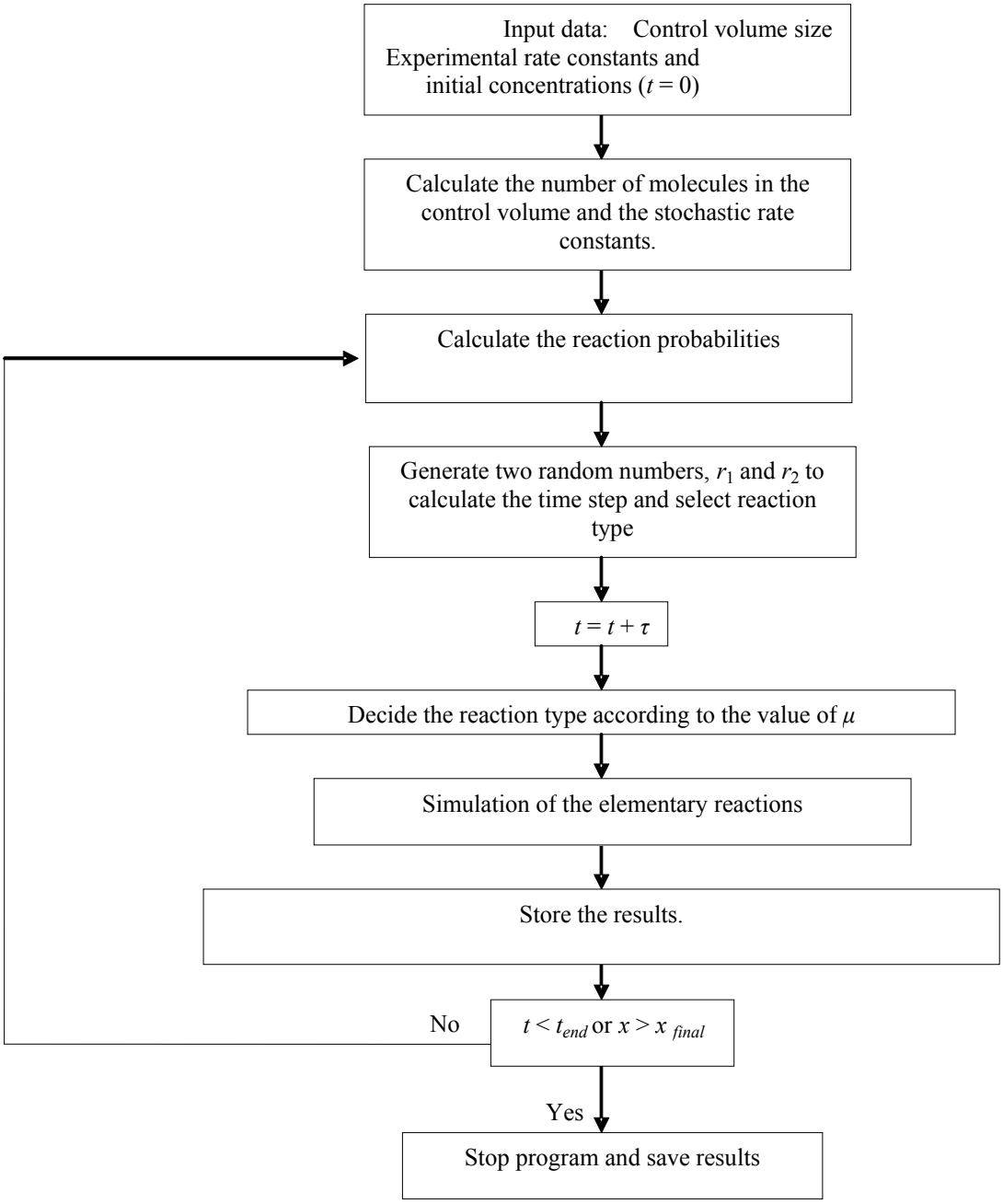

Figure 3.1 Algorithm for Monte Carlo Simulation of ATRcP

3.3 Results and Discussions

We applied our model to describe the copolymerization of styrene and methyl methacrylate, and of acrylonitrile and methyl methacrylate. These comonomer combinations were chosen because they have significantly different reactivity ratios, which will lead to the production of copolymers with distinct CCDs and SLDs. Reaction rate constants were kept constant during the simulations; that is, we neglected diffusion effects.

During living polymerization, the polymer average chain length increases linearly with monomer conversion, the polydispersity index approaches unity and, as a result, the molecular weight distribution is narrow, as shown in Figures 2.a to 2.c.

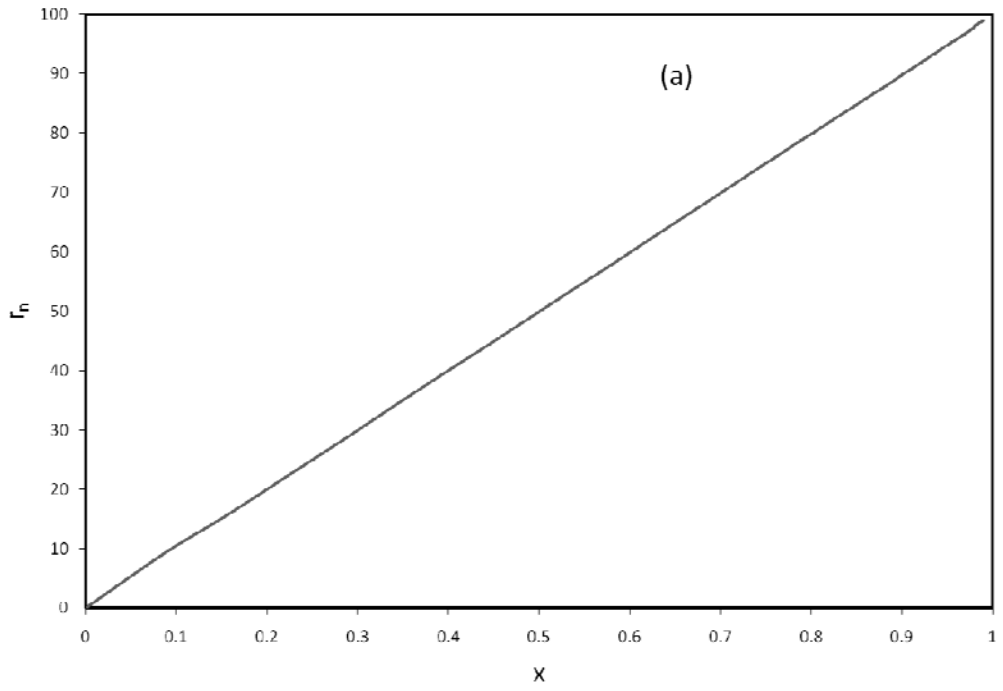

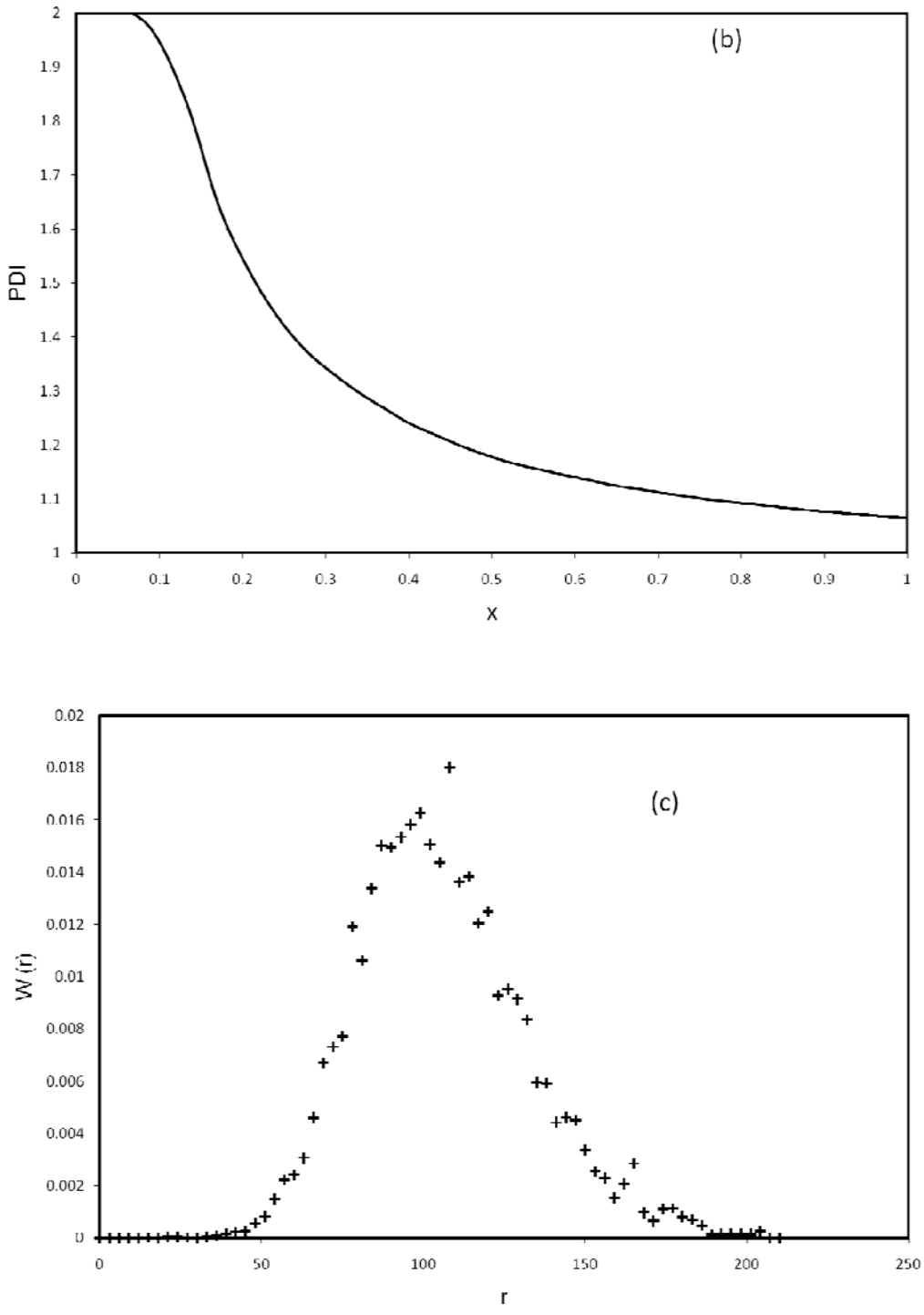

Figure 3.2 Monte Carlo simulation results for the copolymerization of styrene and methyl methacrylate : (a) number average chain length (r_n) as a function of conversion (x), (b) PDI as a function of conversion, and (c) chain length distribution when conversion is $x = 0.99$. The initial comonomer molar fractions in the reactor were $f_{0,St} = 0.5$, $f_{0,MMA} = 0.5$.

Table 3.1 Kinetic rate constants and physical properties for the copolymerization of styrene (A) and methyl methacrylate (B).

Parameter	Value	Reference
$k_{p\mathrm{AA}}$	$4.266\times10^{7}\exp(-7769/RT)$ (L/mol s)	38
$k_{p\mathrm{BB}}$	$(2.95\times10^{7}\exp(-4353/RT)/60)$ (L/mol s)	42
r_{A}	0.52	40
r_{B}	0.46	40
$k_{tc\mathrm{AA}}$	$(k_{\mathrm{pAA}})^{2}\times1.1\times10^{-5}\exp(12452.2/RT)$ (L/mol s)	41
$k_{td\mathrm{BB}}$	$9.80\times10^{7}\exp(-701/RT)$ (L/mol s)	39
$k_{td\mathrm{AA}}$	0	37
$k_{tc\mathrm{BB}}$	0	37
$k_{tr\mathrm{A}}$	$(k_{\mathrm{pAA}})\times2.198\times10^{-1}\exp(-2820/T)$ (L/mol s)	41
$k_{tr\mathrm{B}}$	$(k_{\mathrm{pBB}})\times((9.48\times10^{3}\times\exp(-13880/(RT)))/60)$ (L/mol s)	37
$k_{a\mathrm{A}}$	0.45 (L/mol s)	43
$k_{d\mathrm{A}}$	1.15×10^{7} (L/mol s)	44
$k_{a\mathrm{B}}$	0.055 (L/mol s)	43
$k_{d\mathrm{B}}$	8×10^{7} (L/mol s)	44
MW_{A}	104.14 (g/mol)	
MW_{B}	100.13 (g/mol)	
Initiator concentration	0.087 (mol/L)	
Catalyst concentration	0.087 (mol/L)	
Total monomer concentration	8.7 (mol/L)	
Polymerization temperature	110 °C	

Table 3.2 Kinetic rate constants and physical properties for the copolymerization of acrylonitrile (A) and methyl methacrylate (B).

Parameter	Value	Reference
$k_{p\mathrm{AA}}$	$1.05\times10^{8}\exp(-3663/RT)$ (L/mol s)	45
$k_{p\mathrm{BB}}$	$4.92\times10^{5}\exp(-4353/RT)$ (L/mol s)	38
r_{A}	0.14	46
r_{B}	1.3	46
$k_{tc\mathrm{AA}}$	$3.30\times10^{12}\exp(-5400/RT)$ (L/mol s)	47
$k_{td\mathrm{BB}}$	$9.80\times10^{7}\exp(-701/RT)$ (L/mol s)	39
$k_{td\mathrm{AA}}$	0	37
$k_{tc\mathrm{BB}}$	0	37
$k_{tr\mathrm{A}}$	$4.62\times10^{4}\times\exp(-5837/RT)$ (L/mol s)	37
$k_{tr\mathrm{B}}$	$(kp_{\mathrm{BB}})\times(9.48\times10^{3}\times\exp(-13880/(RT)/60)$ (L/mol s)	37
$k_{a\mathrm{A}}$	0.1 (L/mol s)	This Study
$k_{d\mathrm{A}}$	1×10^{8} (L/mol s)	This Study
$k_{a\mathrm{B}}$	0.5 (L/mol s)	This Study
$k_{d\mathrm{B}}$	1×10^{7} (L/mol s)	This Study
MW_{A}	53.15 (g/mol)	
MW_{B}	100.13 (g/mol)	
Initiator concentration	0.087 (mol/L)	
Catalyst concentration	0.087 (mol/L)	
Total monomer concentration	8.7 (mol/L)	
Polymerization temperature	90 °C	

Figure 3.3 shows the cumulative molar fraction of methyl methacrylate (MMA) in poly(acrylonitrile-co-methyl methacrylate) (AN-MMA) and poly(styrene-co-methyl methacrylate) (St-MMA). We can clearly see that in the St-MMA

copolymer, the cumulative molar fraction of MMA remains almost constant throughout the polymerization. However, for the AN-MMA copolymer, the MMA molar fraction decreases from 0.5 to 0.3.

Figure 3.4 shows the instantaneous molar fraction of MMA in AN-MMA and St-MMA copolymers. The instantaneous molar fraction of MMA in these copolymers differs significantly because of the difference in the reactivity ratios of the comonomer pairs. Because styrene and methyl methacrylate have very close reactivity ratios (0.53 and 0.46) the molar fraction of MMA does not change significantly with conversion. On the other hand, the molar fraction of MMA in AN-MMA copolymers decreases with conversion because the reactivity ratios (0.14 and 1.3) of the two comonomers are very different. Figure 3.4 shows that no more MMA is incorporated in the chains after a total monomer conversion of approximately 0.8. A similar trend is observed when the molar fraction of MMA is plotted as a function of the average chain length. The comonomer composition drift in this case leads to the formation of a gradient copolymer with a terminal block composed of only acrylonitrile units.

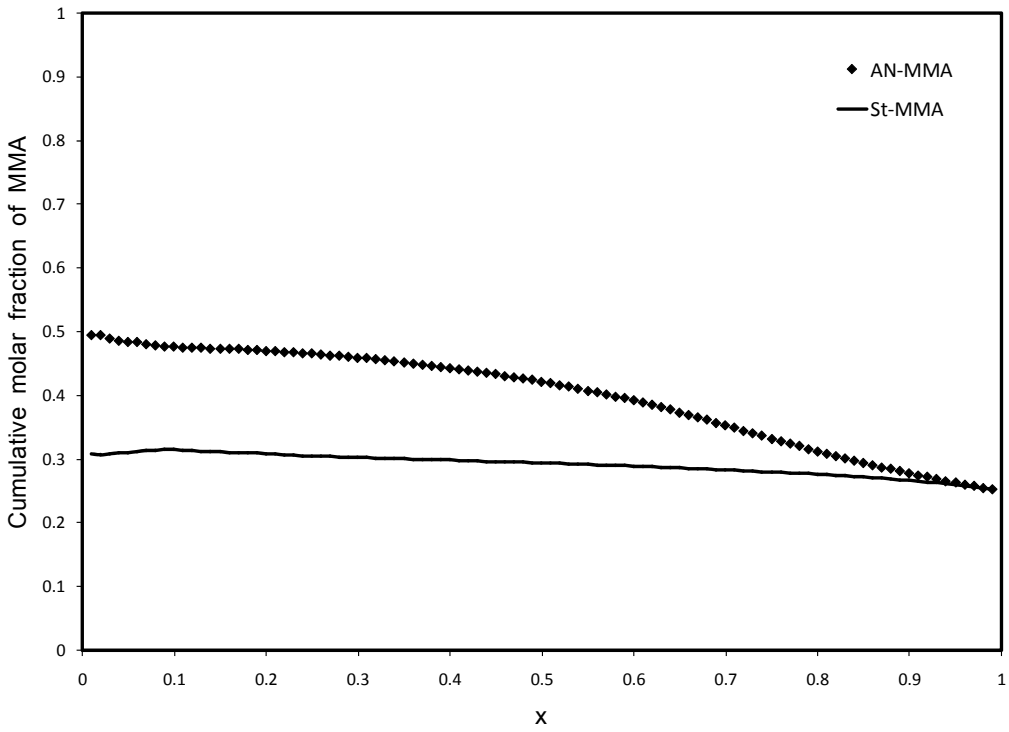

Figure 3.3**.** Cumulative molar fraction of MMA in AN-MMA and St-MMA copolymers as a function of total comonomer conversion. The initial comonomer molar fractions in the reactor were $f_{0,MMA} = 0.25$ and $f_{0,AN} = 0.75$ or $f_{0,St} = 0.75$.

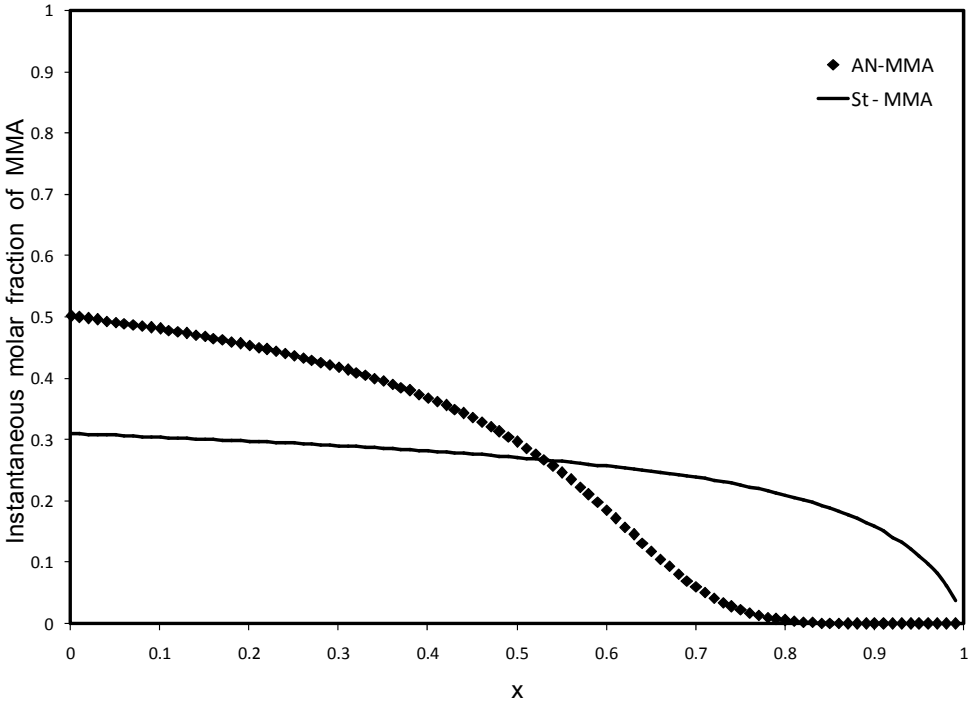

Figure 3.4. Instantaneous molar fraction of MMA in AN-MMA and St-MMA copolymers as a function of total comonomer conversion. The initial monomer molar fractions in the reactor were $f_{0,MMA} = 0.25$ and $f_{0,AN} = 0.75$ or $f_{0,St} = 0.75$.

The comonomer sequence length distribution is usually characterized by its distribution of diads, triads, tetrads, and higher comonomer sequences, measured by NMR spectroscopy. Our model can be use to predict the time evolution of any comonomer sequence, since it stores the microstructural information of the copolymer chains as they are produced during the simulation. Our Monte Carlo program records the chain length, the copolymer composition and the sequence of the repeating units of each chain. The program saves the total number of diads and triads during the formation of the chain. The sum of all the diads and triads is calculated and used to compute the cumulative fraction of all diads and triads in the polymer. The same procedure can be easily applied to predict tetrads and higher comonomer sequence lengths, if necessary.

Figures 3.5 and 3.6 shows that Monte Carlo simulation can be used to predict the cumulative fractions of homodiads and homotriads of styrene and acrylonitrile as a function of total conversion. In agreement with the results shown in Figures 3.3 and 3.4, the fraction of styrene homodiads and homotriads does not change significantly with conversion. On the other hand, the fractions of acrylonitrile homodiads and homotriads increases with total conversion, confirming that the composition of the polymeric chains shifts from random methyl methacrylate and acrylonitrile to pure blocks of acrylonitrile at the end of the polymerization.

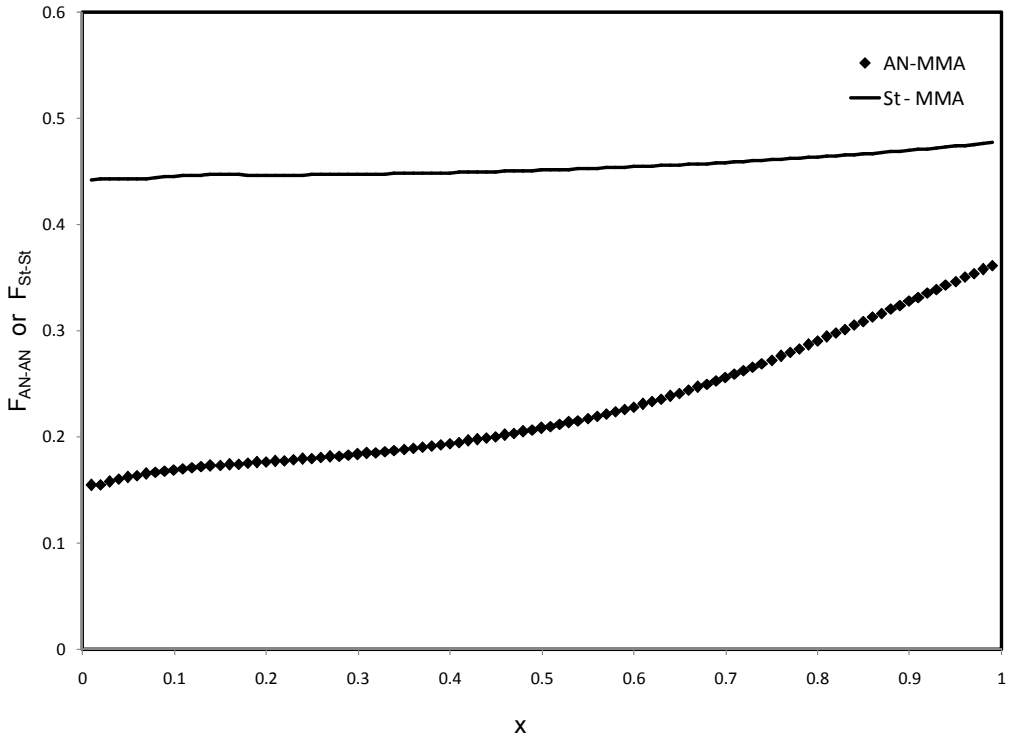

Figure 3.5. Cumulative fraction of homodiads as a function of total comonomer conversion. The initial comonomer molar fractions are $f_{0,MMA} = 0.25$ and $f_{0,AN} = 0.75$ or $f_{0,St} = 0.75$.

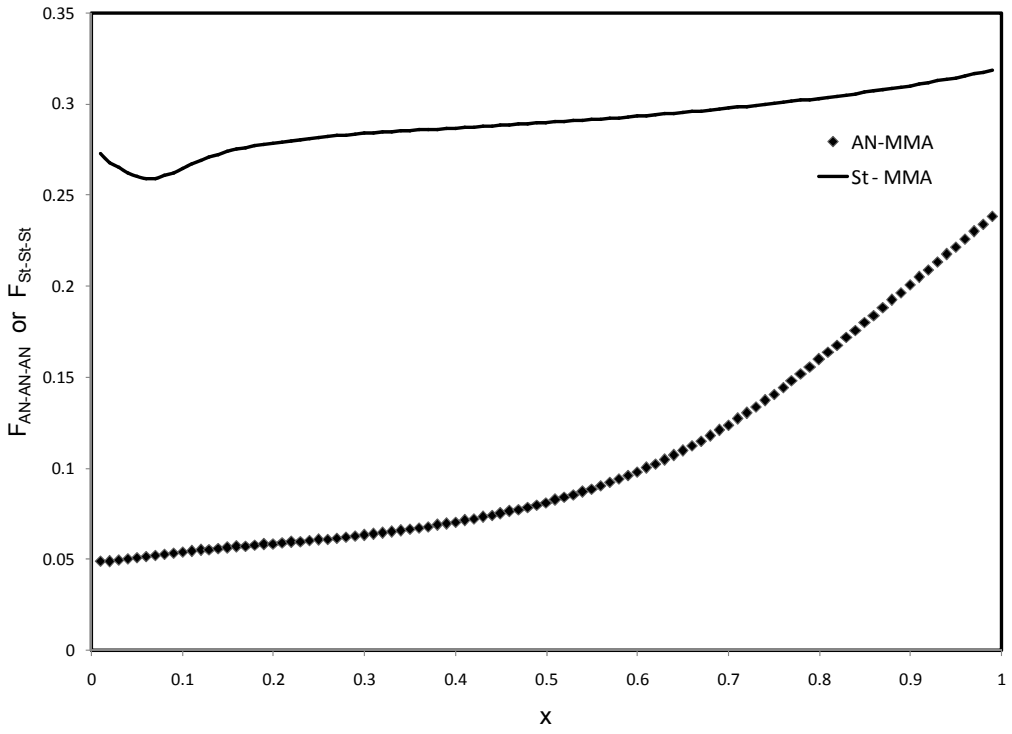

Figure 3.6. Cumulative fraction of homotriads as a function of total comonomer conversion. The initial comonomer molar fractions are $f_{0,MMA} = 0.25$ and $f_{0,AN} = 0.75$ or $f_{0,St} = 0.75$.

For a given set of reactivity ratios, the copolymer composition can be controlled by varying the initial molar fraction of each comonomer in the batch reactor. The initial comonomer molar fractions were varied for the copolymerization of acrylonitrile and methyl methacrylate to illustrate its effect on the cumulative and instantaneous molar fraction of acrylonitrile in the copolymer (Figures 7 and 8) and comonomer sequence length distribution (Figures 9 and 10). Figure 7 shows that for an initial molar fraction of acrylonitrile of 0.25, the cumulative molar fraction of methyl methacrylate does not change significantly, whereas, when the initial molar fraction of acrylonitrile is raised to 0.75, the cumulative molar fraction of methyl methacrylate decreases significantly. From Figure 8, it is obvious that, to form

gradient copolymers, one should increase the initial molar fraction of acrylonitrile in the reactor.

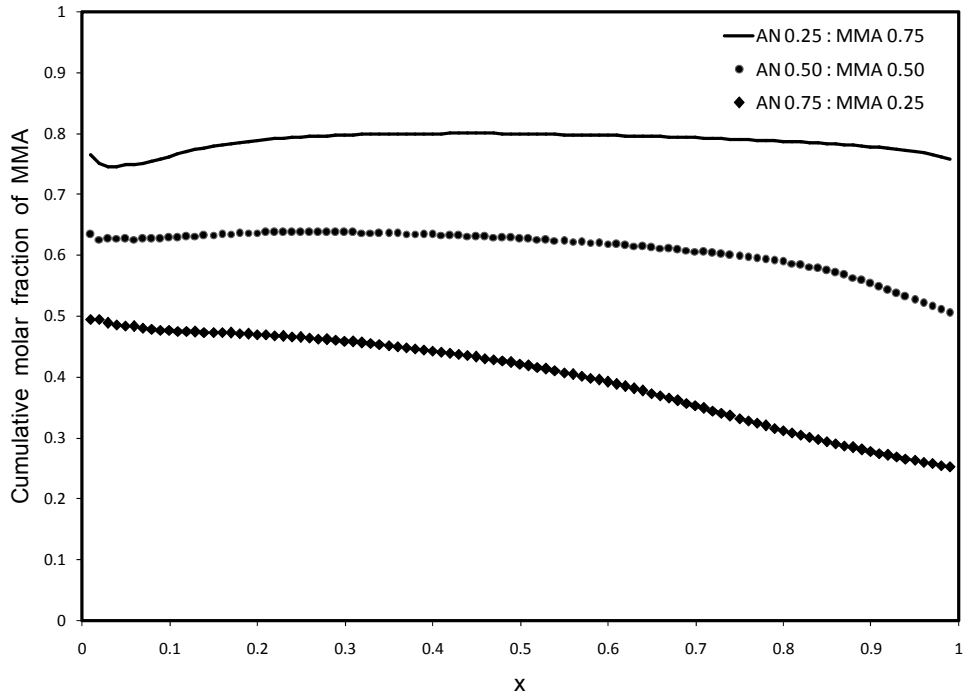

Figure 3.7**.** Cumulative molar fraction of MMA in AN-MMA copolymers as a function of total comonomer conversion and initial comonomer fractions.

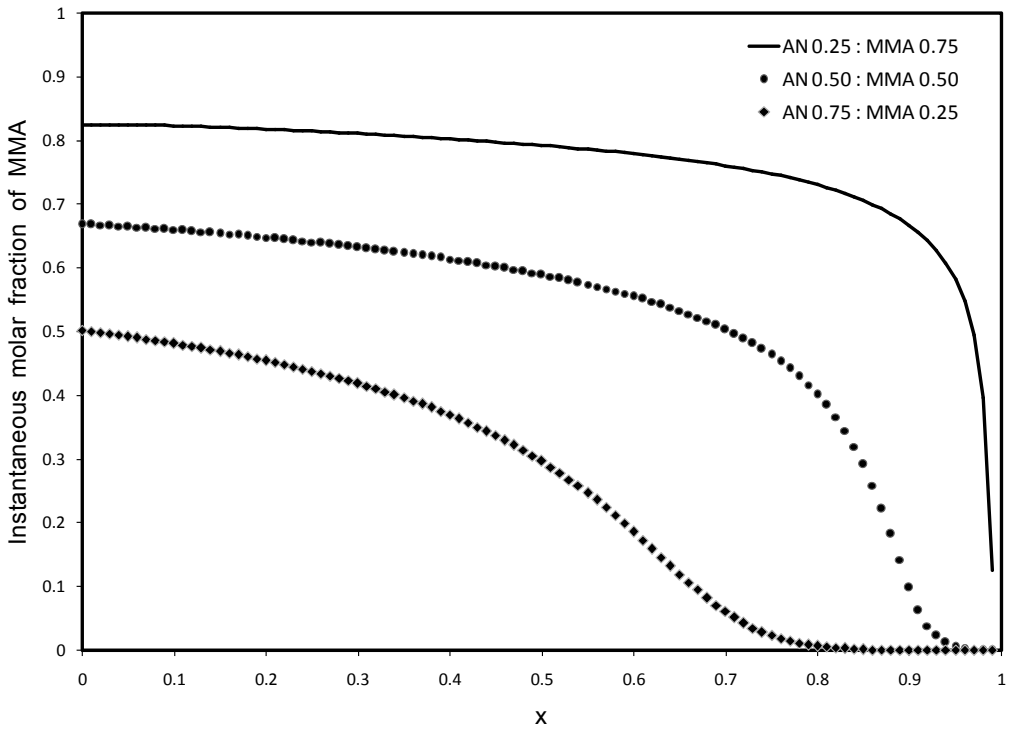

Figure 3.8**.** Instantaneous molar fraction of MMA in AN-MMA copolymers as a function of total comonomer conversion.

Figures 3.9 and 3.10 shows the cumulative acrylonitrile homodiads and homotriads in AN-MMA copolymers made with different initial comonomer fractions. We observe that, only when the initial comonomer molar fractions fed to the reactor are $f_{0,MMA}$ = 0.75 and $f_{0,AN}$ = 0.25, there is a significant change in homodiads and homotriads with increasing conversion.

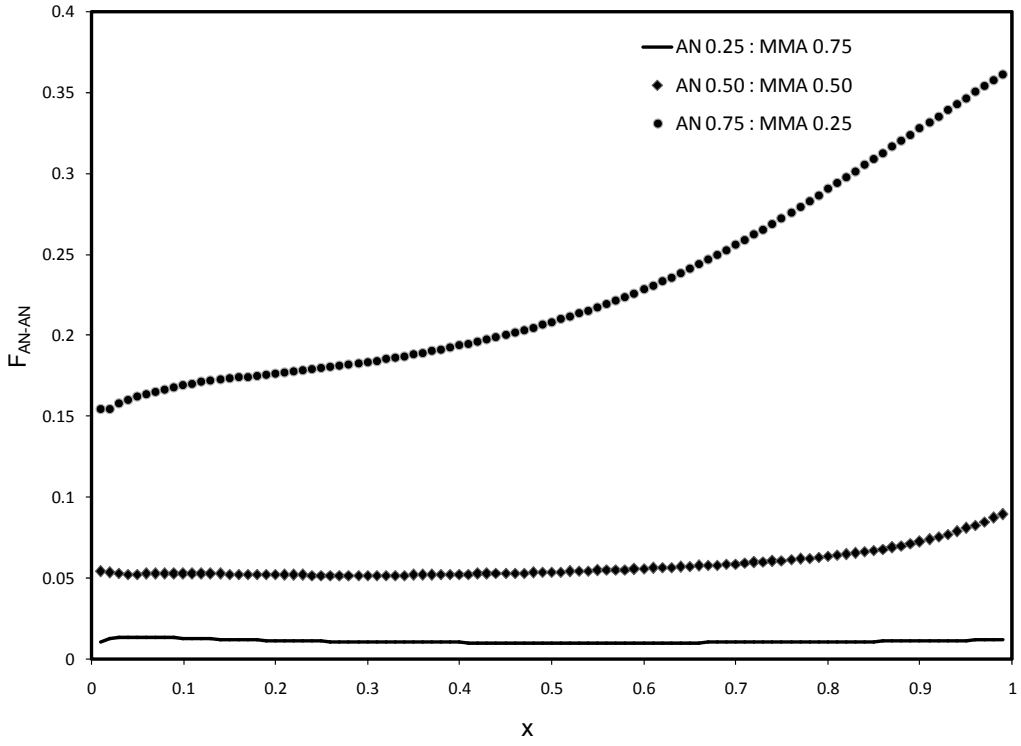

Figure 3.9. Cumulative fraction of AN homodiads in AN-MMA as a function of total comonomer conversion with various initial comonomer compositions.

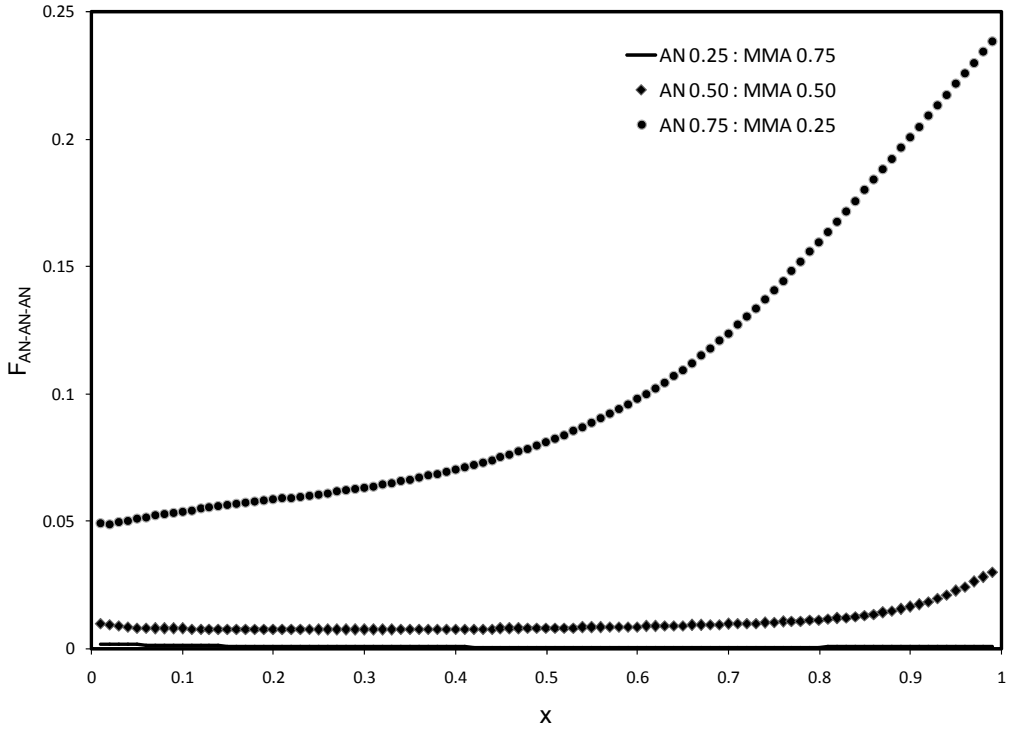

Figure 3.10. Cumulative fraction of homotriads of AN in AN-MMA as a function of total comonomer conversion with various initial comonomer compositions.

Figure 3.11 shows the cumulative fractions of diads and triads as a function of total comonomer conversion for St-MMA copolymers. Figure 3.11.a shows that, even though the cumulative fraction of St-St diads increases slightly with conversion, the St-MMA and MMA-MMA diads do not decrease significantly. Figure 3.11.b shows that there is no significant change in any of the cumulative triad fractions for this system. Therefore, gradient copolymers are not produced in this case.

Figure 3.12 shows the cumulative fraction of diads and triads as a function of total comonomer conversion for AN-MMA copolymers. Figure 3.12.a demonstrates that not only does the cumulative fraction of AN-AN diads increase, but also that the AN-MMA and MMA-MMA diads decrease with conversion. In Figure 3.12.b also shows that the AN-AN-AN triads increase, while the other triads either decrease or remain the same with increasing conversion. This confirms that a gradient copolymer is produced during the copolymerization of MMA and AN under these conditions.

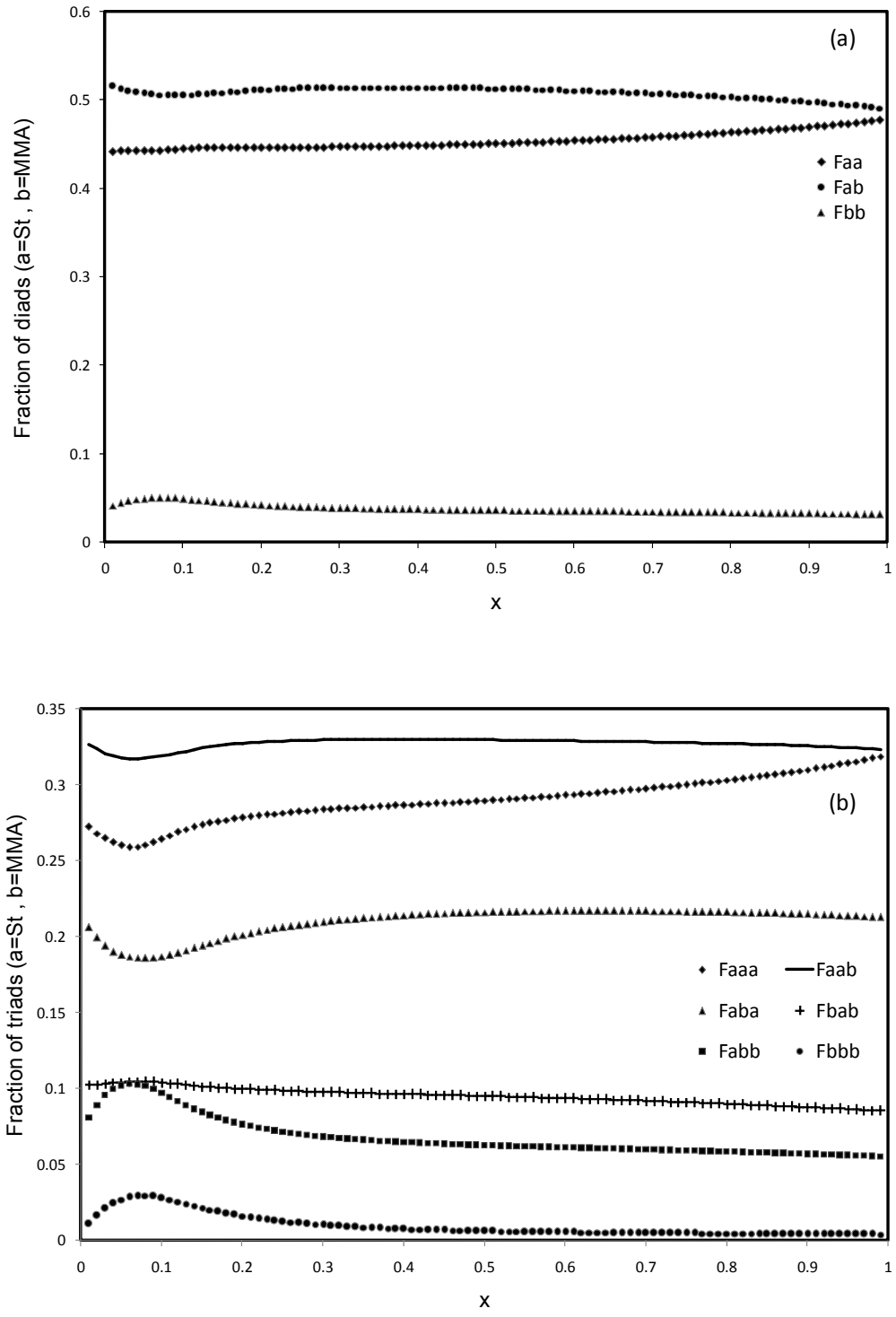

Figure 3.11. Cumulative diads and triad fractions as a function of total comonomer conversion for St-MMA copolymerization. The initial comonomer molar fractions are $f_{0,MMA} = 0.25$ and $f_{0,St} = 0.75$.

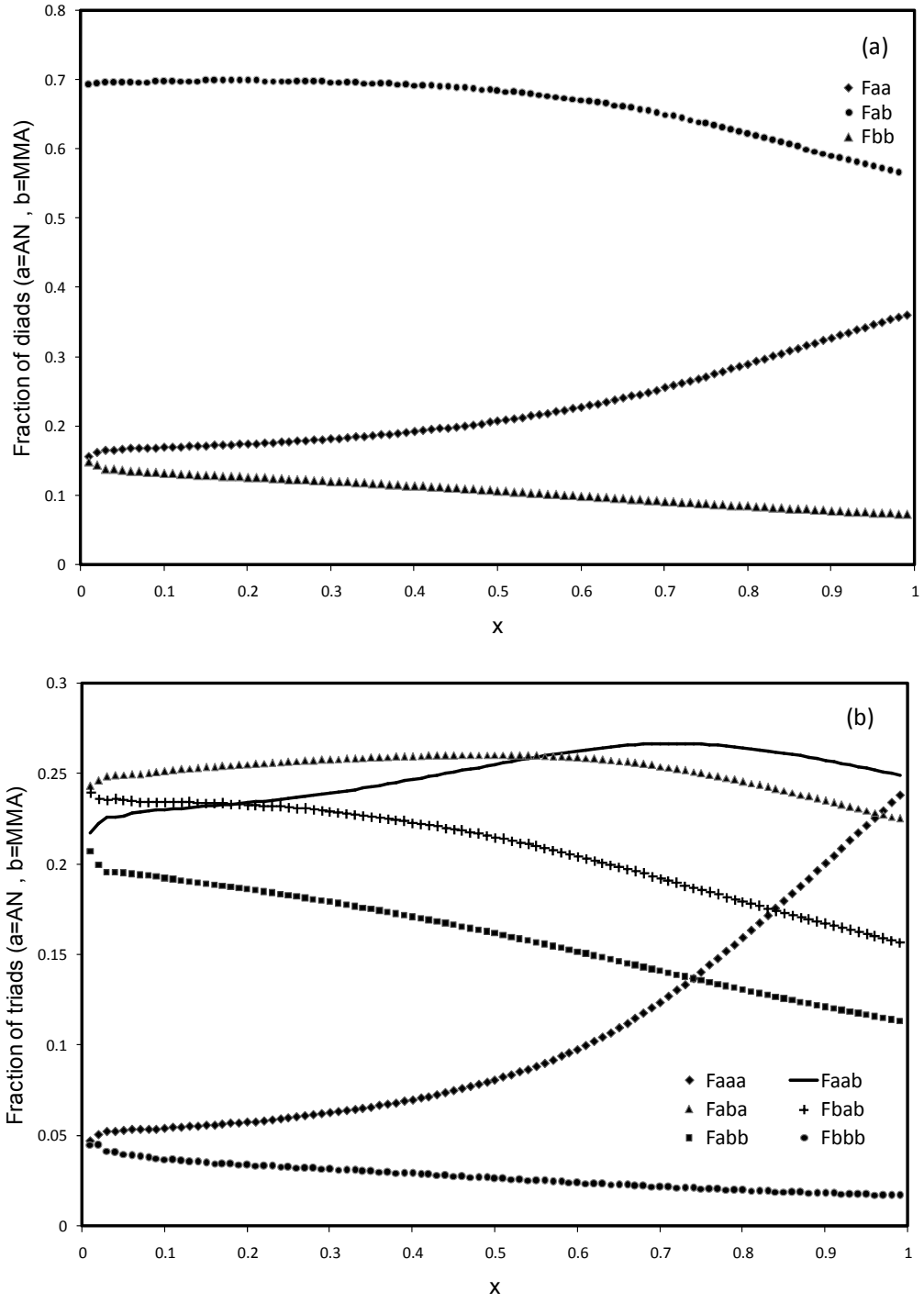

Figure 3.12. Cumulative diad and triad fractions as a function of total comonomer conversion for AN-MMA copolymerization. The initial comonomer molar fractions are $f_{0,MMA} = 0.25$ and $f_{0,AN} = 0.75$.

Figure 3.13 depicts the CCDs of St-MMA and AN-MMA copolymers. Figure 3.13.a shows that the CCDs of St-MMA copolymers made with three different initial comonomer molar fractions are unimodal and narrow. The reactivity ratio of styrene and MMA are similar and, therefore, changes in initial comonomer molar fractions just shift the CCD average to a different value.

Figure 3.13.b indicates that, even though all the CCDs of the AN-MMA copolymers are also unimodal, they become broader as the initial concentration of acrylonitrile increases. This broadening is caused by the difference in reactivity ratios of acrylonitrile and methyl methacrylate, since "blocky" copolymers also have broader CCDs than random copolymers of similar chain lengths.

Finally, Table 3.3 shows the standard deviations for the molar concentrations of styrene and acrylonitrile in the CCDs shown in Figure 3.13, quantifying the broadening effect caused by the acrylonitrile blocks for copolymers made with a high AN:MMA ratio in a batch reactor.

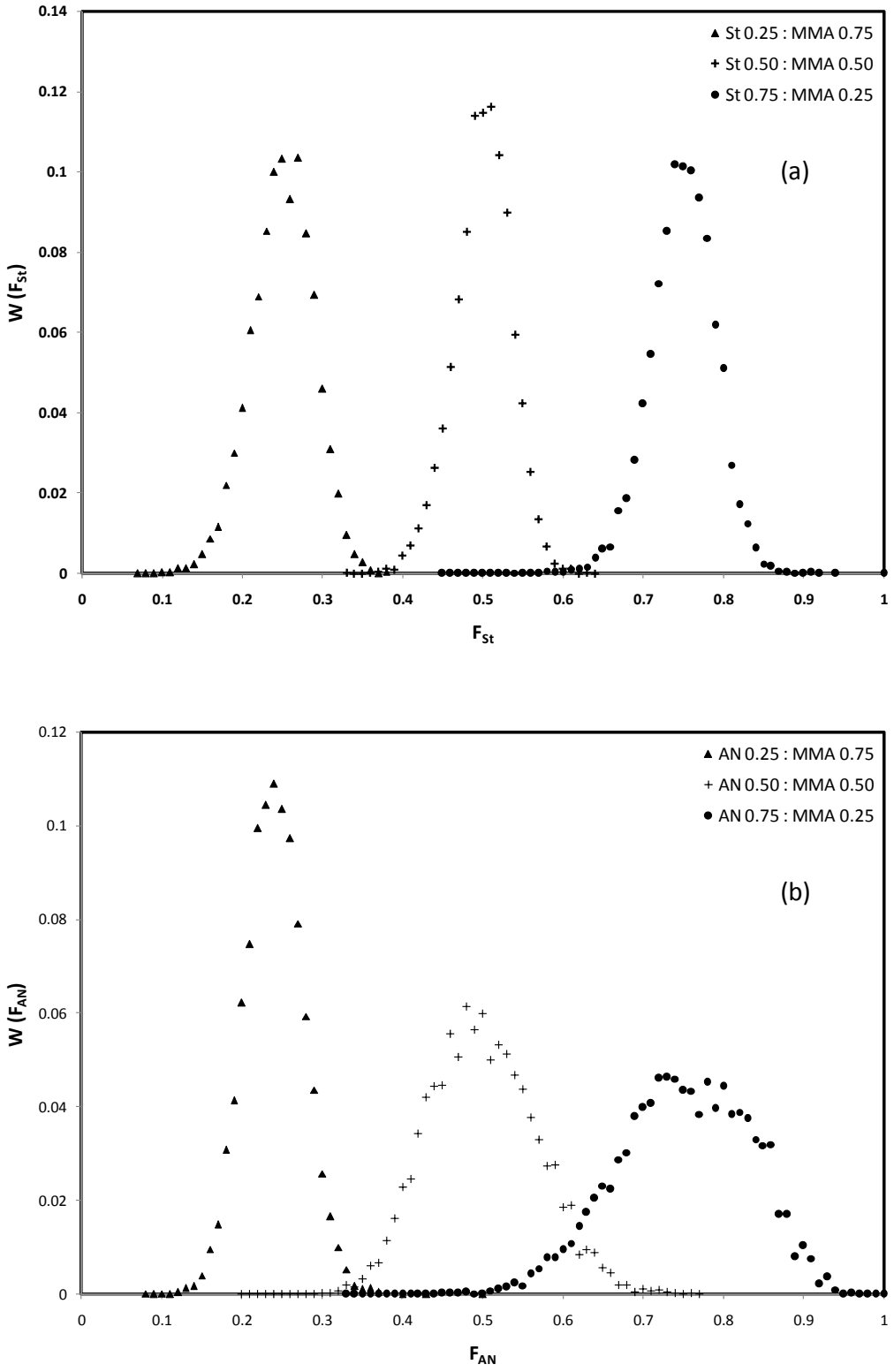

Figure 3.13. Chemical composition distributions of St-MMA and AN-MMA copolymers for a total monomer conversion of $x = 0.995$.

Table 3.3. Standard deviation (σ) of the molar fractions of styrene in the St-MMA copolymers and acrylonitrile in the AN-MMA copolymers shown in Figure 13.

St:MMA molar ratio	Average St molar fraction	σ
0.25:0.75	0.23	0.094
0.50:0.50	0.49	0.094
0.75:0.25	0.72	0.139
AN:MMA molar ratio	**Average AN molar fraction**	**σ**
0.25:0.75	0.24	0.106
0.50:0.50	0.49	0.169
0.75:0.25	0.67	0.198

3.4 Conclusions

We have developed a dynamic Monte Carlo model for the simulation of atom transfer radical copolymerization. The model can predict monomer conversion, average molecular weight, polydispersity index, and copolymer composition as a function of polymerization time in batch reactors. Two copolymers, poly(styrene-*co*-methyl methacrylate) and poly(acrylonitrile-*co*-methyl methacrylate), were chosen to demonstrate the effect of reactivity ratios and initial comonomer molar ratios on the copolymer composition as a function of time or monomer conversion.

The simulations show that the instantaneous molar fraction of methyl methacrylate does not change significantly for poly(styrene-*co*-methyl methacrylate) copolymers made in a batch reactor starting with different comonomer molar ratios, as methyl methacrylate and styrene have close reactivity ratios (0.53 and 0.46) and, therefore, produce nearly random copolymer chains. On the other hand, the instantaneous molar fraction of methyl methacrylate in poly(acrylonitrile-*co*-methyl methacrylate) decreases with conversion, and it reaches zero at around 80% of the total monomer conversion. There is a clear difference in the reactivity ratios (0.14 and 1.3) for this system. Composition drift, in this case, leads to the formation of gradient copolymer chains. The simulation for the varying monomer feed composition showed that the chance of forming gradient acrylonitrile-methyl methacrylate copolymers increases when the initial molar fraction of acrylonitrile is much higher than that of methyl methacrylate.

More importantly, we have shown, for the first time, how dynamic Monte Carlo simulation can be used to describe the time evolution of several microstructural

distributions, such as MWD, CCD and SLD, of copolymer made with ATRP, thus becoming an important tool in product design and optimization.

3.5 References

[1] K. Matyjaszewski, *Prog Polym Sci*. **2005**, *30*, 858.

[2] K.A. Davis, K. Matyaszewski, *Adv Polym Sci.* **2002**, *159,* 2.

[3] K. Matyjaszewski, J. Xia, *Chem Rev.* **2001**, *101*, 2921.

[4] M. Kamigaito, T. Ando, M. Sawamoto, *Chem Rev* **2001**,*101*:3689.

[5] D. Benoit , V. Chaplinski , R. Braslau, C.J. Hawker, *J Am Chem Soc* **1999,** *121*, 3904.

[6] M. Rodlert, E. Harth, I. Rees , C.J. Hawker, *J Polym Sci Polym Chem Ed* **2000,** *38*,4749.

[7] J. Chiefari , Y.K.Chong, F. Ercole , J. Krstina, J. Jeffery ,T.P.T Le ,R.T.A. Mayadunne , C.F. Meijs, C.L.Moad, G. Moad , E. Rizzardo , S.H.Thang. *Macromolecules.* **1998**, *31*, 5559.

[8] G. Moad, J. Chiefari, Y.K. Chong, J. Krstina , R.T.A Mayadunne , A. Postma, E. Rizzardo , S.H. Thang, *Polym Int.* **2000**, *49*, 993.

[9] K. Matyjaszewski, *J Macromol Sci Pure Appl Chem* **1997**, *A34*, 1785.

[10] K. Matyjaszewski , J. Xia, *Handbook of radical polymerization*. New York: Wiley; 2002. p. 523.

[11] K. Matyjaszewski, M.J. Ziegler, S.V. Arehart, D. Gresztra, T. Pakula, *J Phys Org Chem.* **2000**, *13,* 775.

[12] S.V. Arehart, D. Greszta, K. Matyjaszewski, *Polym Prepr Am Chem Soc Div Polym Chem*. **1997**, *38*,705.

[13] G. Chen , Z.Wu , J. Wu , Z.Li , F. Li , *Macromolecules*. **2000**, *33*, 232.

[14] H. Uegaki , Y. Kotani , M. Kamigaito , M. Sawamoto *Macromolecules*. **1998**, *31*,6756.

[15] M. Al-Harthi , J. Soares, L. Simon, *Macromol Theory Simul*. **2006**, *15*, 198.

[16] S. Zhu, *Macromol Theory Simul*. **1999**, *8*,29.

[17] O. Delgadillo-Velazquez, E. Vivaldo-Lima, I.A. Quintero-Ortega, S.Zhu, *AIChE J*. **2002**,*48*, 2597.

[18] M. Al-Harthi, J. Soares, L.Simon, *Macromol Chem Phys*. **2006**, *207*, 469.

[19] M. Al-Harthi, J. Soares, L.Simon, *Macromol React Eng*. **2007**,*1,* 468.

[20] M. Zhang, W.H. Ray, *J Appl Polym Sci*. **2002**,86,1630.

[21] Z.Szablan, A.A. Toy, A.Terrenoire, T.P. Davis, M.H. Stenzel, A.H.E. Muller, C. Barner-Kowollik, *J Polym Sci Polym Chem*. **2006**, *44*, 3692.

[22] D.A. Shipp, K. Matyjaszewski, *Macromolecules.* **2000**, *33*, 1553.

[23] J.Lutz, K. Matyjaszewski *Macromol Chem Phys*. **2002**, *203*, 1385.

[24] Y. Fu, A. Mirzaei, M.F. Cunningham, R.A. Hutchinson, *Macromol React Eng.* **2007**, *1,* 425.

[25] H. Tobita, *Macromol Theory Simul.* **2003**, *12*, 32.

[26] J. Lu, H. Zhang, Y. Yang, *Makro Chemie Theory Simul*. **1993**, *2,* 747.

[27] J. He, H. Zhang, J. Chen, Y. Yang, *Macromolecules*. **1997**, *30*, 8010.

[28] M. Al-Harthi, J. Soares, L. Simon, *Macromol React Eng* **2007**, *1*,95.

[29] M. Al-Harthi, J.Soares, L. Simon, *Macromol Symp Polym React Eng*. **2006**, *243*, 83.

[30] M. Al-Harthi, J. Soares, L. Simon, *Macromol Mat Eng*. *2006*, *291*, 993.

[31] D.Gillespie, *J Phys Chem*. **1977**, *81,* 2340.

[32] S.V.Arehart, K. Matyjazewski, *Macromolecules.***1999,** *32*, 2221

[33] José Luis de la Fuente, Marta Fernández-García, Marina Fernández-Sanz, Enrique López Madruga, *Macromolecules.***2001,** *34,*5833

[34] S. Zhu, R. Wang,Y. Luo, B. Li, *AIChe J*. **2007**, *53*, 174

[35] H. Tobita, A. E. Hamielec,*Macromolecules.* **1989,** *22,* 3098

[36] S. Zhu, A. E. Hamielec, *Macromolecules.* **1993**, *26*, 3131

[37] A. Keramopoulos, C. Kiparissides, *Macromolecules* 2002, *35*, 4155.

[38] M. Buback, R.G. Gilbert, R.A. Hutchinson, B. Klumperman, F. Kuchata , B.G. Manders, K.F. O'Driscoll, G.T. Russell, Schweer *J Macromol Chem Phys*. **1995**, *196*, 3267.

[39] D. Achilias, D. Kiparissides, *Macromolecules*. **1992**, *25*, 3739.

[40] H. Suzuki, V. Mathot, *Macromolecules*. **1989**, *22*, 1380.

[41] A. Hui, A.E. Hamielec, *J Appl Polym Sci*. **1972**, *16*, 749.

[42] F.R. Mayo, J.M. Lewis, *J.Am.Chem.Sco*. **1944**,*66*,1594

[43] K. Olmo, A. Goto,T. Fukuda, J. Xia, K. Matyjazewski, *Macromolecules*. **1998**, *31*, 2699.

[44] M. Zhang,H. Ray, *J.Appl.Poly.Sci*. **2002**, *86*, 1630.

[45] I.M. Yaraskavitch, J.L.Brash, A.E. Hamielec, **Polymer, 1987**, *28*, 489.

[46] J. Brandrub, E. Immergut, E. Grulke, *Polymer Handbook*. NewYork: Wiley; **1999**.

[47] T.P.Pittman-Bejger, Real-Time Control and Optimization of Batch Free-Radical Copolymerization Reactors. Ph.D. Thesis: University of Minnesota; **1982**.

CHAPTER 4

DYNAMIC MONTE CARLO SIMULATION OF ATOM TRANSFER RADICAL COPOLYMERIZATION IN SEMIBATCH REACTOR

4.1 Introduction

Controlled radical polymerization (CRP) can be used to produce polymers with well-defined molecular architectures including block, graft and star polymers.[1-4] There are three main CRP mechanisms: (1) nitroxide-mediated polymerization (NMP),[5,6] (2) reversible addition-fragmentation chain transfer (RAFT),[7,8] (3) and atom transfer radical polymerization (ATRP).[3,9]

Several CRP characteristics have been elucidated with the help of mathematical models using the method of moments, Monte Carlo simulation and the software package PREDICI. The method of moments has been used to describe NMP [10, 11] ATRP [12-14] and RAFT [15] in batch reactors and it has also been used to simulate ATRP and RAFT in semibatch reactors. [16, 17] PREDICI has been used to simulate CRP processes in both batch and semibatch reactors. [18]

The method of moments can describe monomer conversion, average molecular weights and copolymer composition as a function of polymerization time, but it cannot predict the distributions of molecular weight (MWD) and chemical composition (CCD). PREDICI solves the polymer population balances numerically and can predict both MWD and CCD. However, this commercial software is available only for users who have acquired it. On the other hand, Monte Carlo simulation is a powerful tool that can simulate any polymer microstructural distribution and is relatively simple to implement, making it very attractive for academic and industrial use.

As one of the most successful living/controlled polymerization methods, ATRP has drawn increasing attention since its first applications in 1995.[19,20] A conventional ATRP system is composed of a monomer, an initiator with a transferable (pseudo) halogen, and a transition metal catalyst. ATRP can be used under mild reaction conditions to produce well-defined polymers with controlled topology, composition, and functionality. [21, 22] ATRP is also used to produce random, block, graft or gradient copolymers. [23, 24]

There are considerable differences between conventional free radical copolymerization and ATRP. In free radical copolymerization, polymer chains grow and terminate within seconds. Since the polymer chains are generated at different times during the polymerization, they will have different compositions if composition drift takes place. As a consequence, the final product made by free radical polymerization in a batch reactor may have a rather broad CCD because of intermolecular heterogeneity. Contrarily, in ATRP most chains are generated at the start of the polymerization and grow simultaneously. As a consequence, composition drift leads to intramolecular

heterogeneity, but no intermolecular heterogeneity. These copolymers are named gradient copolymers and their synthesis has been discussed in the literature. [25-27]

In a batch process, the chemical composition of gradient copolymers is mainly affected by the comonomer reactivity ratios and initial composition. A semi-batch process allows more flexibility to control the copolymer composition since the concentration of each comonomer, and consequently that of the copolymer chains, can be changed precisely by feeding the comonomers at specified flow rates to the reactor.

In the present study, a dynamic Monte Carlo model has been developed to study ATRP in a semibatch reactor. The model has been applied to study gradient copolymer formation, and it can be used to monitor custom-specific molecular properties. To our knowledge, this is the first time that a dynamic Monte Carlo model has been used to describe ATRP using semi-batch reactors.

4.2 Model Description

The kinetic parameters used here are the same parameters as for the batch copolymeriation as shown in Tables 4.1 and 4.2. The methodology used has been dealt in chapter 2.

Table 4.1. Kinetic rate constants and physical properties for styrene (1) -methyl methacrylate (2) copolymerization at 383K.

Parameter	Value	Reference
$k_{p\mathrm{AA}}$	$4.266\times10^{7}\exp(-7769/RT)$ (L/mol s)	30

$k_{p\mathrm{BB}}$	$2.95\times10^{7}\exp(-4353/RT)/60$ (L/mol s)	39
r_A	0.52	32
r_{B}	0.46	32
$k_{tc\mathrm{AA}}$	$(k_{\mathrm{pAA}})^2\times1.1\times10^{-5}\exp(12452.2/RT)$ (L/mol s)	33
$k_{td\mathrm{BB}}$	$9.80\times10^{7}\exp(-701/RT)$ (L/mol s)	31
$k_{td\mathrm{AA}}$	0	29
$k_{tc\mathrm{BB}}$	0	29
$k_{tr\mathrm{A}}$	$(k_{\mathrm{pAA}})\times2.198\times10^{-1}\exp(-2820/\mathrm{R}T)$ (L/mol s)	33
$k_{tr\mathrm{B}}$	$(k_{\mathrm{pBB}})\times((9.48\times10^{3}\times\exp(-13880/(RT)))/60)$ (L/mol s)	29
$k_{a\mathrm{A}}$	0.45 (L/mol s)	34
$k_{d\mathrm{A}}$	1.15×10^{7} (L/mol s)	35
$k_{a\mathrm{B}}$	0.055 (L/mol s)	34
$k_{d\mathrm{B}}$	8×10^{7} (L/mol s)	35
Initial Catalyst Concentration	0.087 mol/L	
Initial Initiator	0.087 mol/L	

Concentration	
Total Monomer Concentration	8.7 mol/L
MW_A	104.14 (g/mol)
MW_B	100.13 (g/mol)

Table 4.2. Kinetic rate constants and physical properties for the acrylonitrile (1) - methyl methacrylate (2) copolymerization at 363K.

Parameter	**Value**	**Reference**
$k_{p\mathrm{AA}}$	$1.05\times10^{8}\exp(-3663/RT)$ (L/mol s)	36
$k_{p\mathrm{BB}}$	$4.92\times10^{5}\exp(-4353/RT)$ (L/mol s)	30
r_A	0.14	37
r_B	1.3	37
$k_{tc\mathrm{AA}}$	$3.30\times10^{12}\exp(-5400/RT)$ (L/mol s)	38
$k_{td\mathrm{BB}}$	$9.80\times10^{7}\exp(-701/RT)$ (L/mol s)	31
$k_{td\mathrm{AA}}$	0	29
$k_{tc\mathrm{BB}}$	0	29

k_{trA}	$4.62\times10^{4}\times\exp(-5837/RT)$ (L/mol s)	29
k_{trB}	$(k_{pBB})\times(9.48\times10^{3}\times\exp(-13880/(RT)/60)$ (L/mol s)	29
k_{aA}	0.1 (L/mol s)	This Study
k_{dA}	1×10^{8} (L/mol s)	This Study
k_{aB}	0.5 (L/mol s)	This Study
k_{dB}	1×10^{7} (L/mol s)	This Study
Initial Catalyst Concentration	0.087 mol/L	
Initial Initiator Concentration	0.087 mol/L	
Total Monomer Concentration	8.7 mol/L	
MW_A	53.15 (g/mol)	
MW_B	100.13 (g/mol)	

4.3 Results and Discussion

In batch copolymerization using controlled/living polymerization, a gradient copolymer is produced only if comonomer composition drift is significant, that is, when the difference between the reactivity ratios of the comonomers is large and/or the initial comonomer concentrations are very different.

In the present work we used a Monte Carlo model to describe the copolymerization of styrene and methylmethacrylate (St-MMA) or acrylonitrile and methylmethacrylate (AN-MMA) in a semibatch reactor. St-MMA and AN-MMA were selected for this investigation because they have very different reactivity ratios. The reactivity ratios of St-MMA are very close, while a larger difference is observed for the AN-MMA system. Styrene and MMAS are also commonly used monomers in ATRP. We compared the effect of using different initial comonomer concentrations and of slowly adding styrene, acrylonitrile or methyl methacrylate into the reactor as a side stream during the polymerization. The respective initial concentrations were kept constant and all volume effects have been ignored. We assumed that the autoclave reactor was isothermal and well-mixed. The copolymerization of AN and MMA was simulated at a temperature of 363K but that of St and MMA at a temperature of 383K. A control volume of 1×10^{-19}L has been used in all simulations. During semibatch operation we assumed that the flow of the monomers was such as to keep their concentrations constant in the reactor throughout the polymerization. The flow rate was not explicitly used in the simulation.

Figure 4.1 compares the polydispersity index (PDI) of AN-MMA copolymers made in semibatch and batch reactors. Two different initial comonomer molar ratios (AN: MMA = 25:75 and 50:50) were simulated. For the semibatch simulations, the acrylonitrile concentration was kept constant by slowly feeding the comonomer to the reactor as the polymerization proceeded. Both the batch and semibatch reactors made copolymers with PDIs that followed the same trend: the PDI was initially high and then it approached a value of approximately 1.1, as commonly observed in ATRP processes.

Figure 4.2 shows the instantaneous and cumulative molar fraction of AN in the copolymer as a function of polymerization time respectively. Figure 4.2.a shows gradient copolymers are not made in the batch reactor when AN:MMA molar ratio is 25:75, but when AN:MMA is changed to 50:50, gradient copolymers will be produced for longer polymerization times. On the other hand, gradient copolymers are formed in the semibatch reactor for both initial AN:MMA molar ratios at a shorter polymerization time. The reason for that is apparent: AN is fed continuously to the reactor to keep its concentration constant, while the concentration of MMA decreases to zero at the end of the polymerization. Therefore, the AN:MMA ratio at the end of the polymerization under batch operation may differ significantly from that of semibatch operation.

Figure 4.2.b shows the cumulative molar fraction of acrylonitrile in the copolymer as a function of polymerization time. It clearly indicates the formation of gradient copolymers in a semibatch reactor. Both initial molar concentrations show the formation of gradient copolymers. The AN:MMA molar ratio of 25:75 does not produce a gradient but, when AN:MMA is changed to 50:50, gradient copolymers are formed. A longer AN

block is formed while using a semibatch than in batch reactors as inferred from Figure 2. Thus better gradient copolymers can be produced by using semibatch reactors.

Figures 4.3.a and 4.3.b compare the chain length distribution (CLD) of AN-MMA copolymers made in batch and semibatch reactors for the two initial comonomer ratios. For an AN:MMA molar ratio of 25:75, the CLD of the copolymer made in the batch reactor is shifted to lower molecular weights. However, when AN:MMA is changed to 50:50, an opposite behavior is observed and the CLD of the copolymer made in the batch reactor is shifted to lower values. In the latter case, the semibatch reactor can be used to produce a copolymer with higher molecular weight average without increasing the PDI. This is due to the higher propagation constant associated with AN. Hence, when AN concentration increases, the rate of propagation also increases, thereby producing copolymer with higher molecular weight at a given polymerization time.

Figure 4.4 compares the CCDs of AN-MMA copolymers made in batch and semibatch reactors. It is apparent that the CCDs of copolymers made in the batch reactor are narrower than those made in the semibatch reactor for these simulation conditions. The standard deviation values are given in Table 4.3. In addition, the copolymers made in the semibatch reactor will always have a higher molar fraction of acrylonitrile, as expected. This is the opposite behavior that would have been observed in conventional free radical polymerization, where the CCD would be narrower for the semi-batch operation. In the latter case, the combination of chain termination and comonomer drift may result in very broad CCDs, since chains made in the beginning of the polymerization will have different chemical compositions from those made at the end of the polymerization. In controlled free radical polymerization, on the other hand, the

monomer composition drift will be reflected along the polymer chain (that is, as a gradient), but the CCD remains narrow during batch operation. Curiously, under semi-batch operation (no composition drift), the CCD of polymers made by controlled living polymerization will become broader, because of the continuous feeding of acrylonitrile.

The batch and semibatch simulation for polymerization of 50AN:50MMA both show broad CCDs with a clear shift towards lower AN fractions for the semibatch process. This indicates the formation of blocky or gradient polymers as predicted from Figure 4.2.

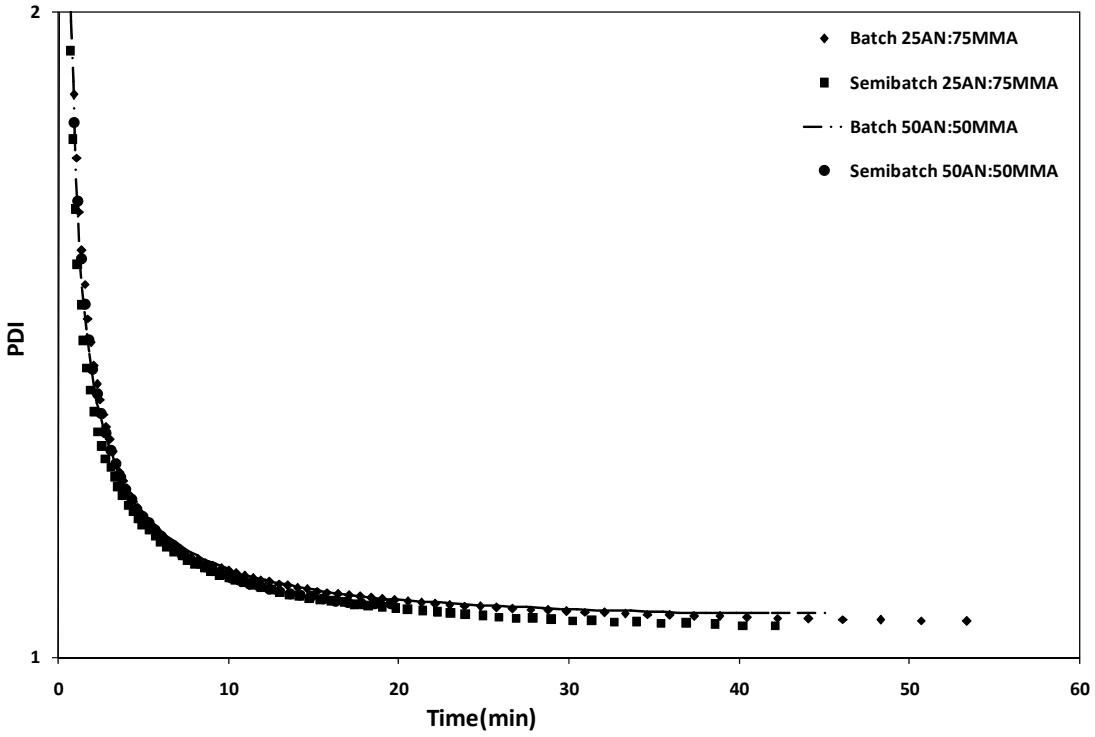

Figure 4.1. PDI as a function of time for the copolymerization of AN and MMA in batch and semibatch reactors. The AN concentration was kept constant during the simulation of the semibatch reactor.

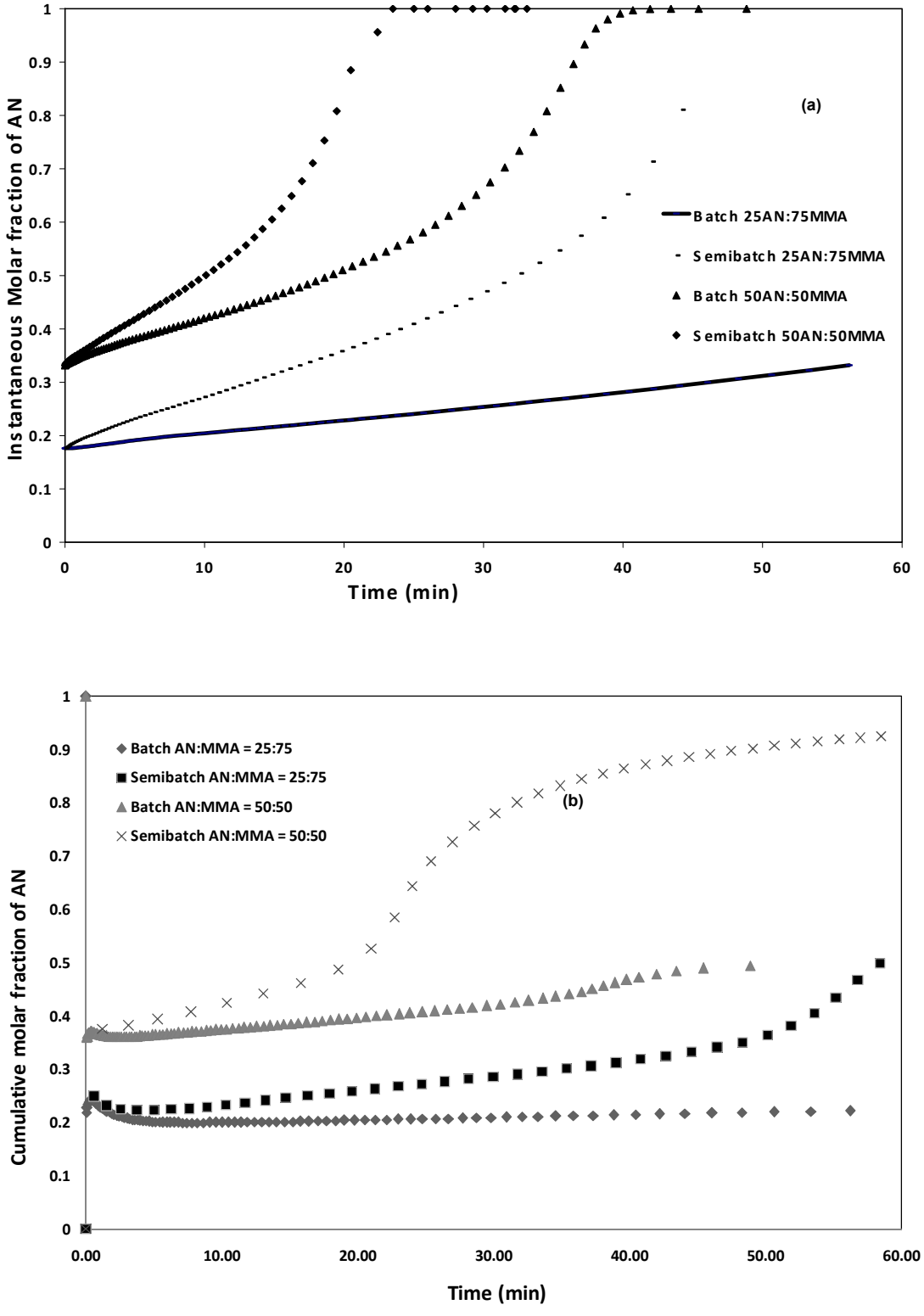

Figure 4.2 (a) Instantaneous molar fraction of AN in AN-MMA copolymers as a function of polymerization time in batch and semibatch reactors.

(b) Cumulative molar fraction of AN-MMA copolymers as a function of polymerization time in batch and semibatch reactors.

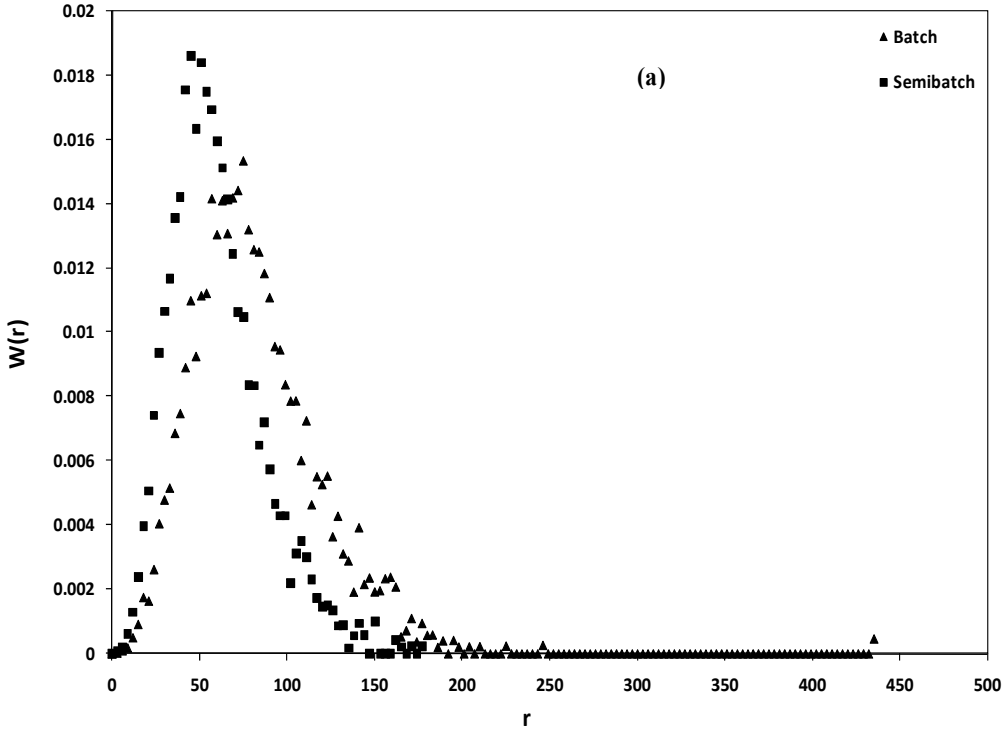

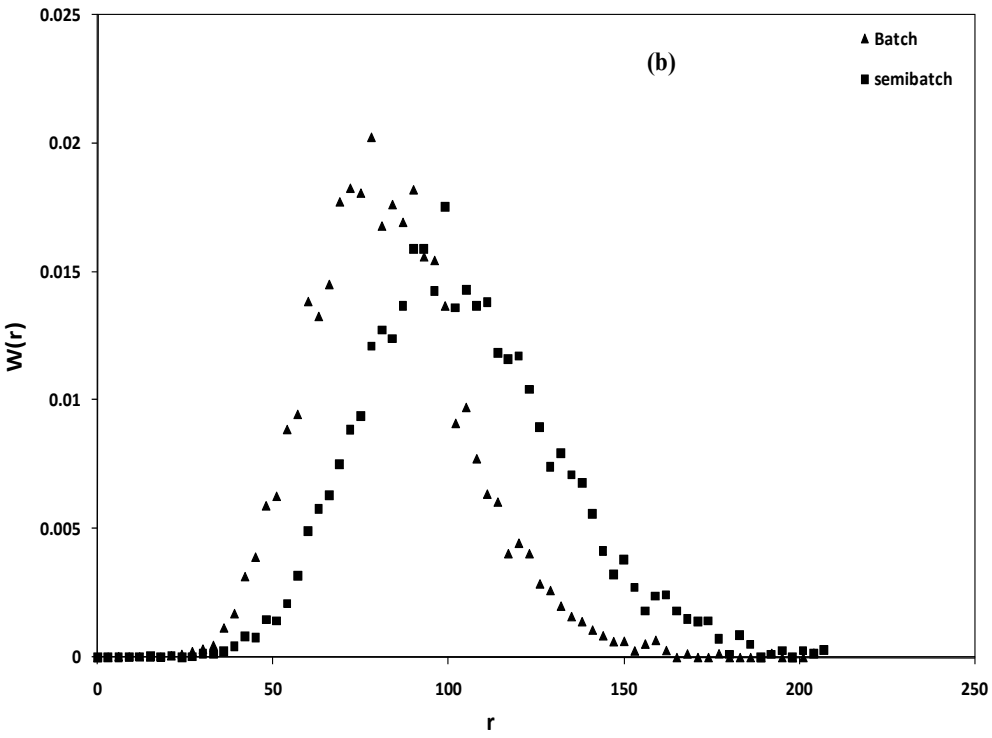

Figure 4.3. Chain length distribution of AN-MMA copolymers made in batch and semibatch reactors. (a) AN:MMA = 25/75 (b) AN:MMA = 50/50. Polymerization time = 50 min.

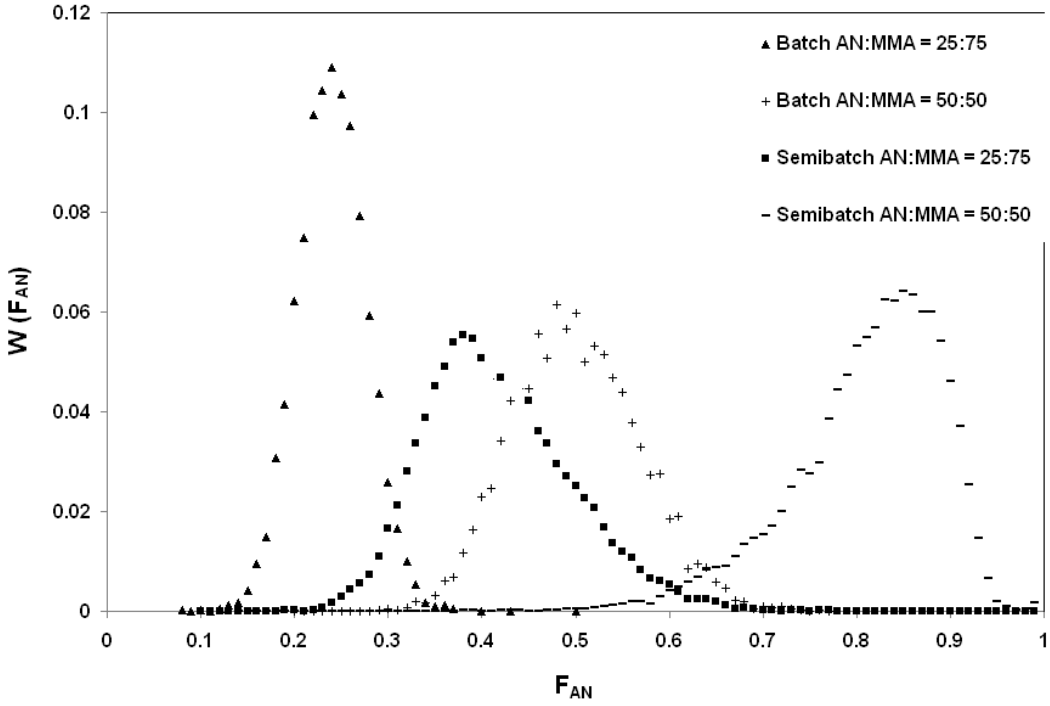

Figure 4.4 Chemical composition distributions of AN-MMA copolymers made in batch and semibatch reactors . Polymerization time = 30 min.

Semibatch reactors can be used to produce custom-made gradient copolymers in a more controlled way than batch reactors. Figure 4.5a shows that the length of the AN terminal block increases as the AN:MMA ratio varies from 25:75 to 50:50. This is a great advantage over batch reactors operated with the same initial AN:MMA ratios. Figure 4.5b shows a plot of number average chain length, which clearly shows the difference in the average molecular weight for different concentration, thereby allowing control over the molecular weight and the gradient nature of the copolymer. Thus flexibility in producing tailor-made copolymers is highly possible by using semibatch.

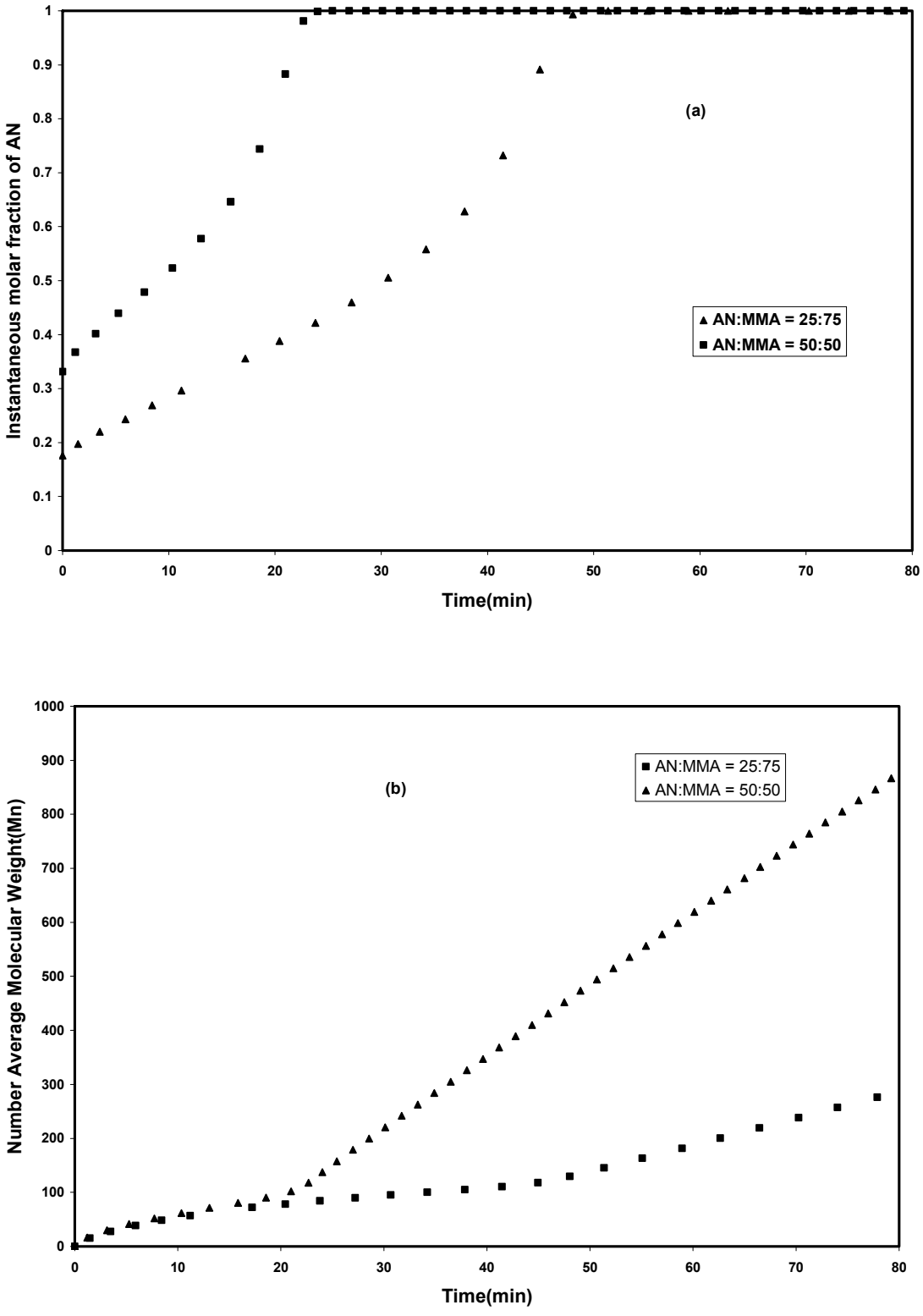

Figure 4. 5. (a) Instantaneous molar fraction of AN in AN-MMA copolymers as a function of polymerization time for a semibatch reactor. (b) Number average molecular

weight as a function of time. The AN concentration was kept constant during the simulations.

We have shown in a previous chapter that St-MMA gradient polymers are not produced effectively in batch reactors because of their similar reactivity ratios (Table 1).[40] In this case, the only resource is the use of semibatch reactors with the continuous feed of at least one of the comonomers.

Figure 4.6 demonstrates that the PDI of St-MMA copolymers approaches unity in a semi-batch reactor when either styrene or MMA are fed as side streams during the polymerization. This guarantees that the living nature of the polymerization is not affected by the comonomer feed policy.

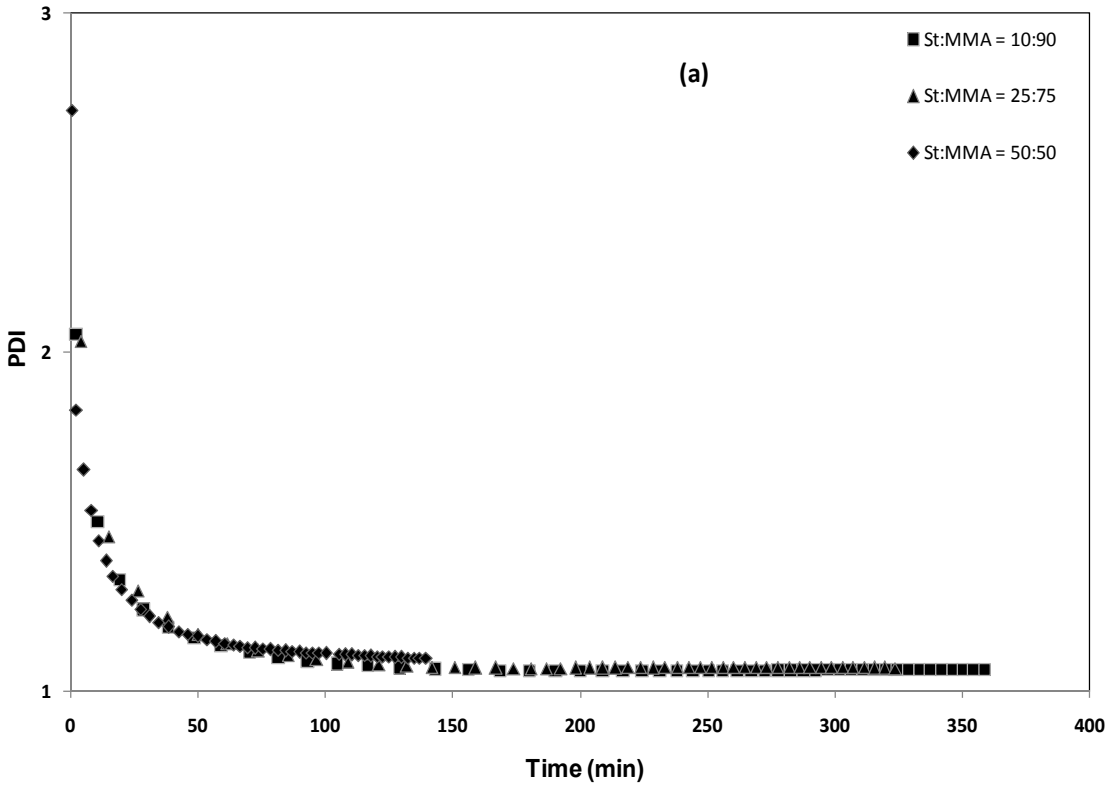

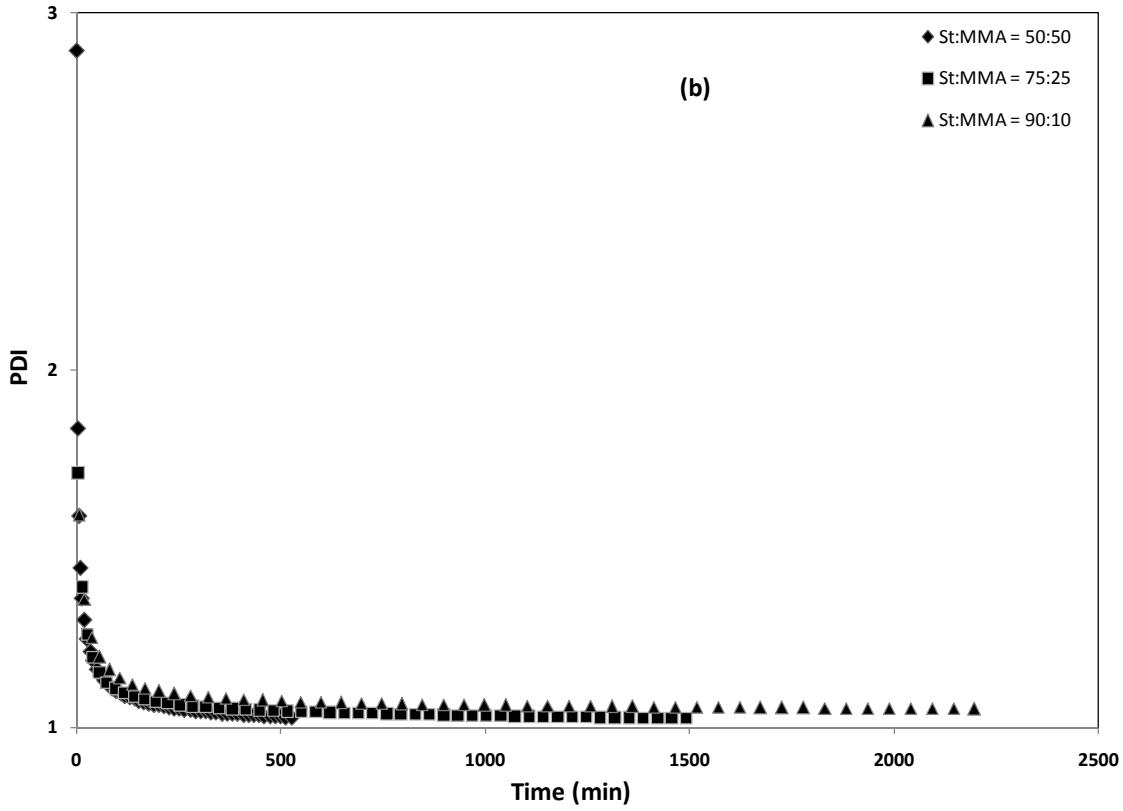

Figure 4.6. PDI as a function of time for St-MMA copolymers: (a) constant St concentration, (b) constant MMA concentration.

Figure 4.7 compares the CLDs of St-MMA copolymers made in a semibatch reactor with an initial composition of St:MMA = 10:90 when either styrene or MMA are fed continuously during the polymerization to keep their concentrations constant. Both feed policies produce polymer with narrow CLD. Figure 4.8 shows similar results for an initial composition of St:MMA = 25:75. Figure 4.6 confirms that the PDI of these copolymers is small for all the cases, thus proving in agreement with our CLD predictions. This is due to the effect of the equilibrium constant: MMA having a higher equilibrium constant highly favors the transition between dormant and active sites, hence enabling a narrower chain length distribution. Also, a higher molecular weight is obtained

when St is fed in semibatch mode. Figures 4.7 and 4.8 show a clear shift of the CCD towards the right, predicting a higher molecular weight polymer.

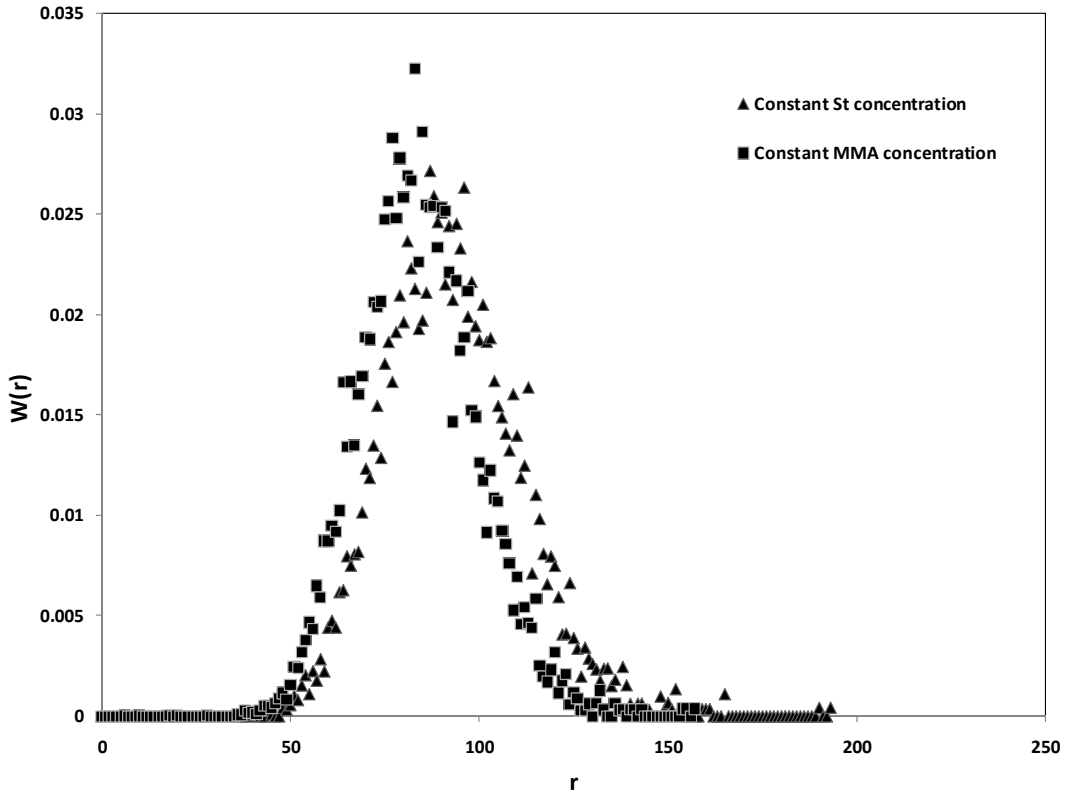

Figure 4.7. Chain length distribution for St-MMA made in a semibatch reactor with St-MMA = 10:90. Polymerization time = 300 minutes.

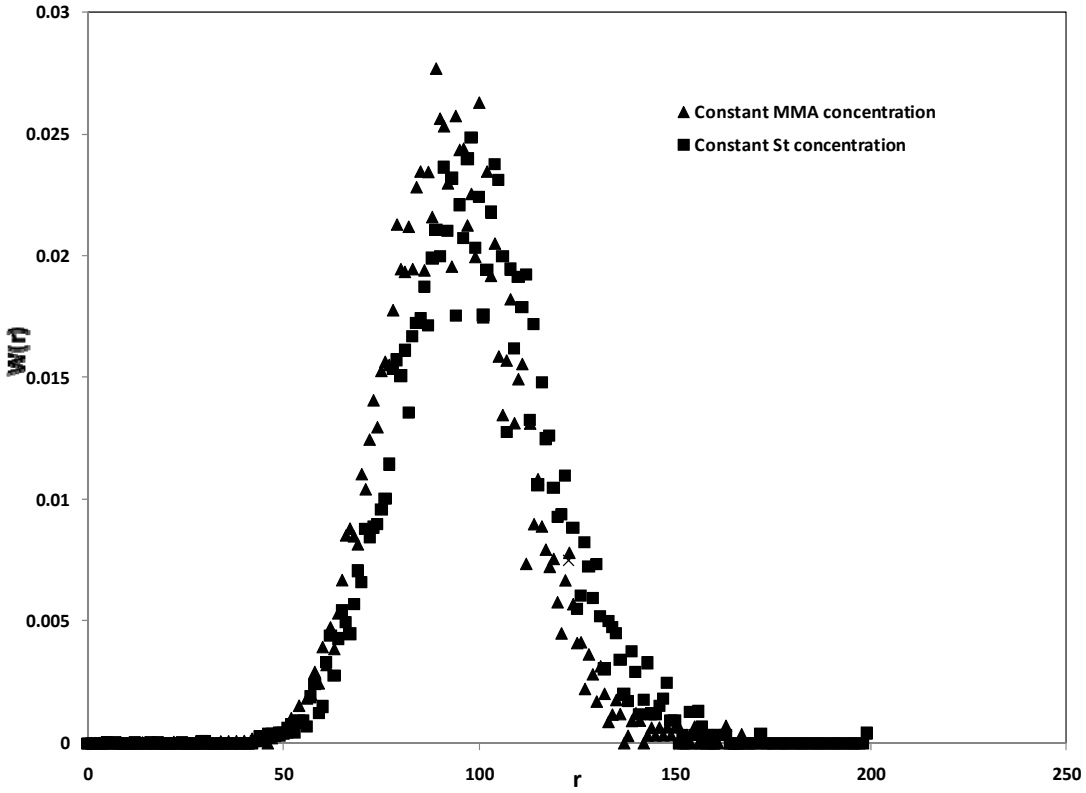

Figure 4.8. Chain length distribution for St-MMA made in a semibatch reactor with St-MMA = 25:75. Polymerization time = 300 minutes.

Figure 4.9.a shows the instantaneous molar fraction of styrene in the copolymer as a function of polymerization time for three initial St:MMA ratios. Styrene is charged continuously into the reactor as a side stream, and MMA is fed into the reactor only at the beginning of the polymerization. Gradient copolymers are produced in all the three cases. However, as the initial styrene molar fraction is reduced, the time required to start forming blocks of pure styrene increases.

In Figure 4.9.b the feed policy is reversed, with MMA being fed continuously and styrene only at the start of the polymerization. Similarly, as the initial MMA molar fraction is reduced, the time for the formation of pure MMA blocks increases. However,

the polymerization time required for the formation of the MMA blocks is much higher than that required for the formation of the styrene blocks depicted in Figure 4.9.a. Thus using MMA as the sidestream is not the ideal option to produce gradient polymers in shorter polymerization runs.

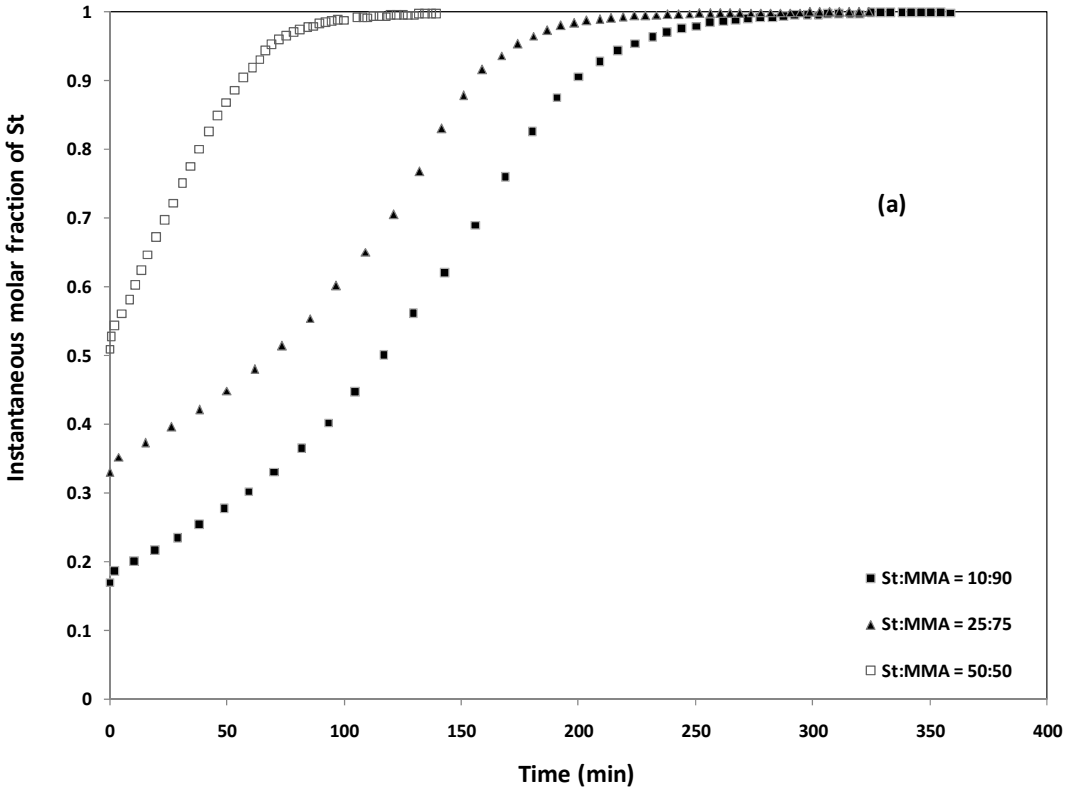

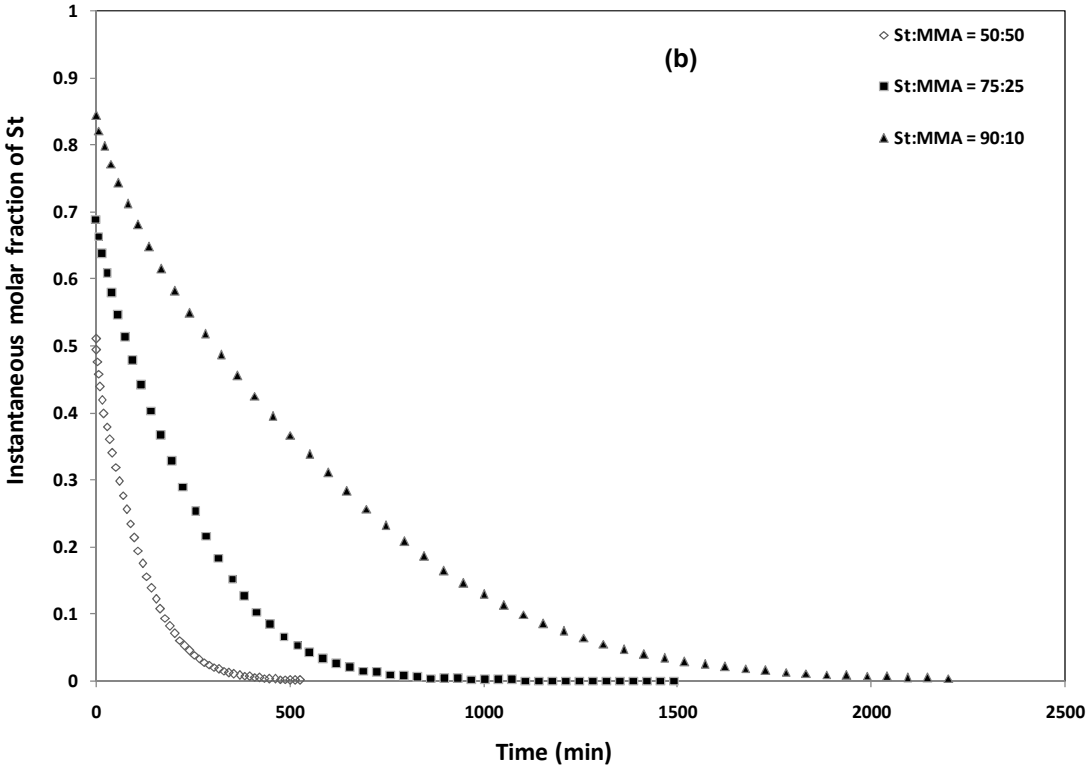

Figure 4.9. Instantaneous molar fraction of styrene in St-MMA copolymers: (a) constant St concentration (b) constant MMA concentration.

Figure 4.10 shows how the CLD of St-MMA copolymers, with constant feed of styrene and an initial equimolar concentration of St and MMA, moves towards higher values as the polymerization time increases, due to the living nature of the polymerization.

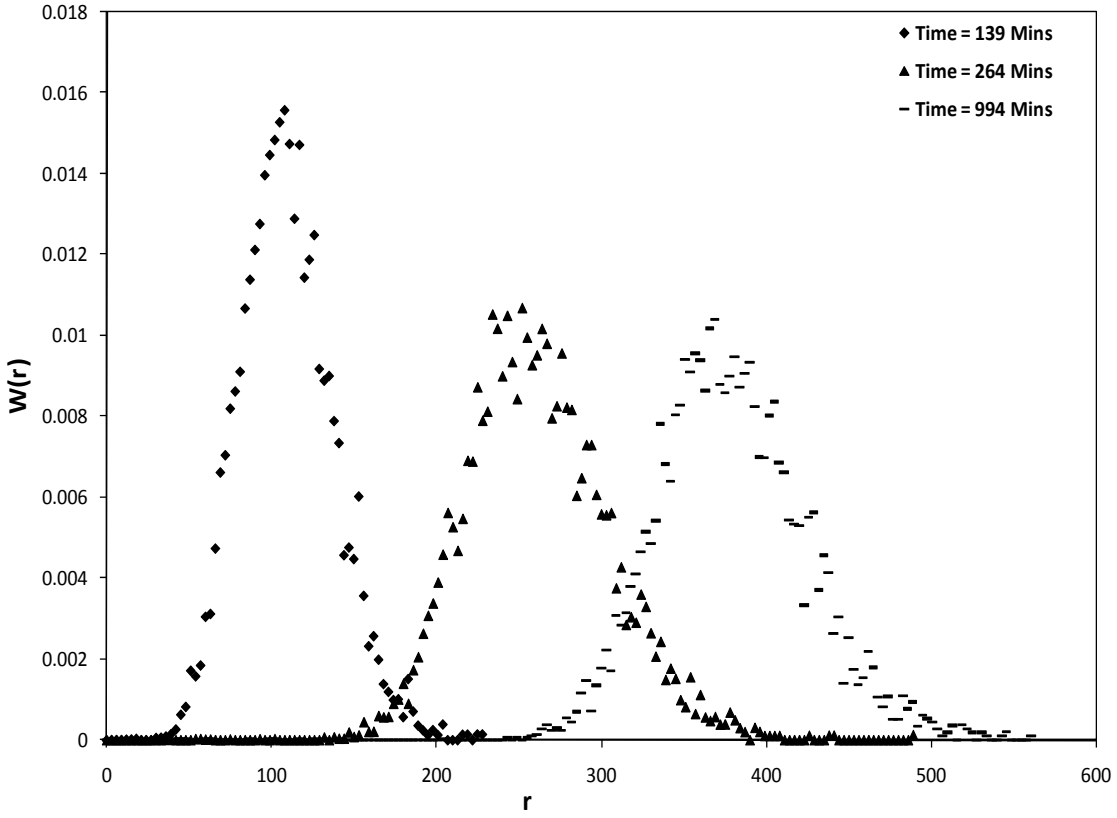

Figure 4.10. Chain length distributions for St-MMA copolymers (St:MMA = 50:50) at three different polymerization times (t_1 = 139 min, t_2 = 264 min, t_3 = 994 min).

Figures 4.11.a and 4.11.b show the CCDs of St–MMA copolymers made with several initial St:MMA ratios and different feed policies. The standard deviations for all the CCDs are given in Table 4.3. Copolymers made with an initial St:MMA ratio of 10:90 and continuous feed of styrene have the broadest CCD, as evident from the σ values reported in Table 4.3 and by visual inspection of the distributions presented in Figure 4.11.a and 4.11.b. On the other hand, when MMA was fed to the reactor, the breadth of the CCDs remained unaltered for the three simulated cases.

Table 4.3. Standard deviation (σ) of the molar fractions for St-MMA and AN-MMA polymerizations in a semibatch reactor.

Initial St:MMA Molar Ratio	Side-stream	σ
0.1:0.9	St	0.1
0.25: 0.75	St	0.079
0.50:0.50	St	0.05
0.50:0.50	MMA	0.04
0.75:0.25	MMA	0.04
0.9:0.1	MMA	0.04
Initial AN:MMA Molar Ratio		
0.1:0.9	AN	0.04
0.25:0.75	AN	0.08
0.50:0.50	AN	0.1
0.50:0.50	MMA	0.03
0.75:0.25	MMA	0.03
0.9:0.1	MMA	0.03

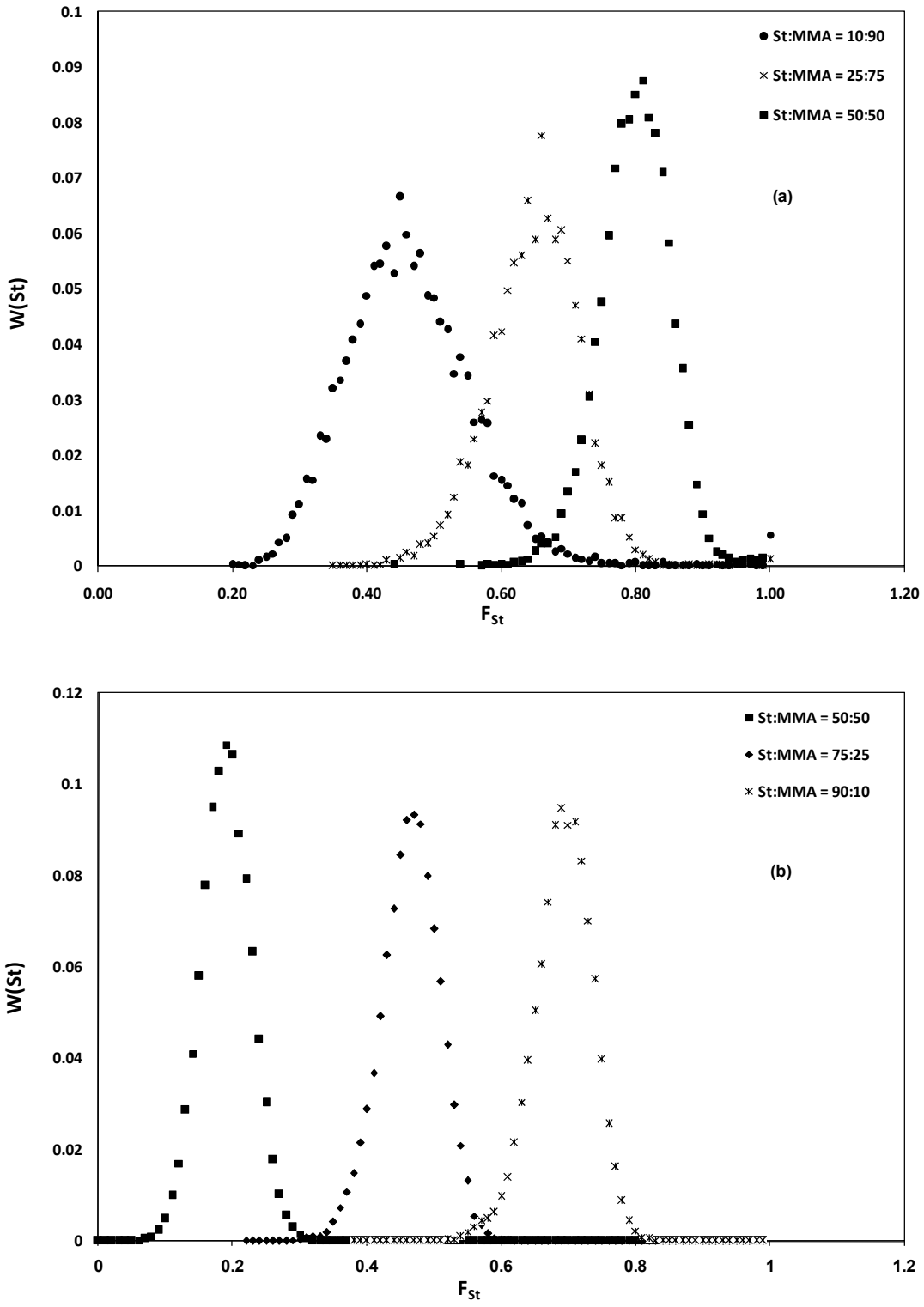

Figure 4.11. Chemical composition distributions of St-MMA copolymers made in a semibatch reactor: a) constant styrene concentration, b) constant MMA concentration. Polymerization time = 300 minutes.

The comonomer sequence distribution is characterized by its diads, triads, tetrads, and higher sequences, generally measured by NMR spectroscopy. Our Monte Carlo simulation program can also predict these sequences. Figures 4.12 to 4.17 show model predictions for diads and triads of styrene/MMA copolymers as a function of time when styrene is fed continuously to the reactor. Long polymerization times are needed to make gradient copolymers when MMA is fed to the reactor, as shown in Figure 4.9b. Therefore, it is more convenient to produce gradient polymer when styrene is fed as the sidestream. This may be attributed to the reactivity ratio of styrene, which is slightly higher than MMA. Figures 4.12 to 4.17 clearly show that styrene diads and triads increase with increasing time for all initial monomer concentrations. Comparing these results with those reported in our batch polymerization simulation paper (Chapter 2) [40] remarkable improvement in the formation of styrene diads and triads is inferred. The batch results show no formation of gradient polymers at all concentrations used, while our results predict the formation of gradient polymers for all the concentrations. Figures 4.12 to 4.17 were simulated at a maximum polymerization time of 100 minutes to better understand the formation of various diads and triads at a shorter timescale. A clear increase in AN-AN blocks is found for all concentrations except 25-75, but an increase in the timescale would result in the formation of gradient. The MMA-MMA blocks decreases for all concentration. Considering the homotriads, the AN-AN-AN blocks increases for all concentration within the timescale of 100 minutes, while a sharp decrease in the MMA-MMA-MMA triblocks are found for all concentration. An increase in the fraction of block copolymers is also found in our study. Clearly all the concentrations form gradient polymers, while a St:MMA molar ratio of 50:50 forms a

better gradient at the least polymerization time. Hence the semibatch process can be very well utilized for making gradient polymers with styrene as the sidestream.

Researchers have tried to use semibatch reactors in controlled radical polymerization, e.g. Cunningham et.al. used semibatch reactors for controlled radical polymerization experiments.[41,42] Our research provides more understanding in the area of gradient copolymers, which is a subject matter of considerable current interest. Unfortunately, there are no published experimental data describing the semibatch polymerization of these comonomers. However, we are very confident on the predictive abilities of our model, since we have applied a similar approach to model the polymerization of styrene [43] and these model results agree very well with our experimental findings.

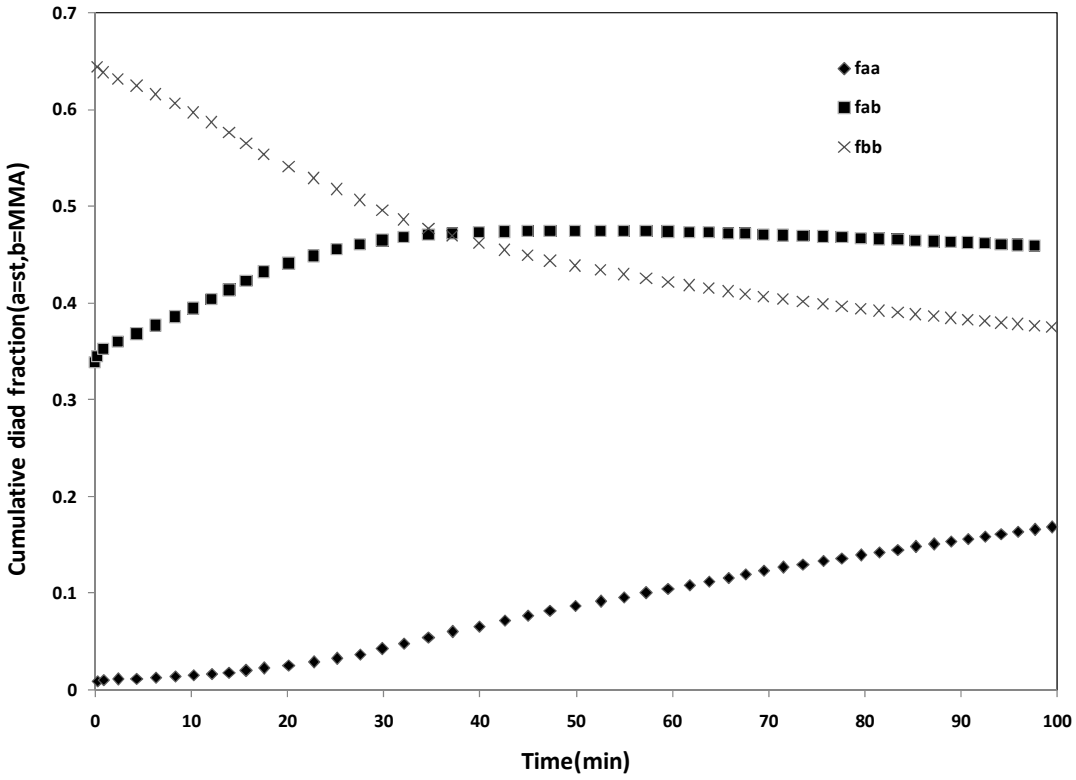

Figure 4.12. Cumulative diad fraction as a function of time for St-MMA system. The initial comonomer molar fractions are $f_{0,MMA} = 0.90$ and $f_{0,St} = 0.10$.

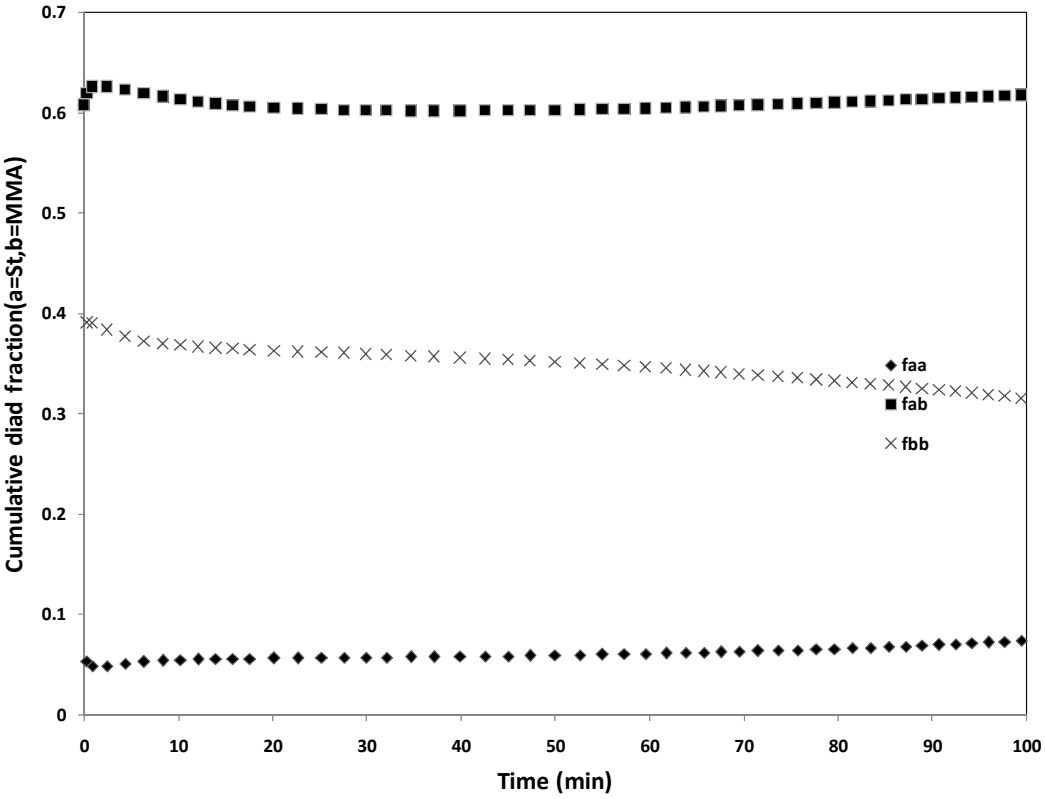

Figure 4.13. Cumulative fraction of homodiads as a function of time for St-MMA system. The initial comonomer molar fractions are $f_{0,MMA} = 0.75$ and $f_{0,St} = 0.25$.

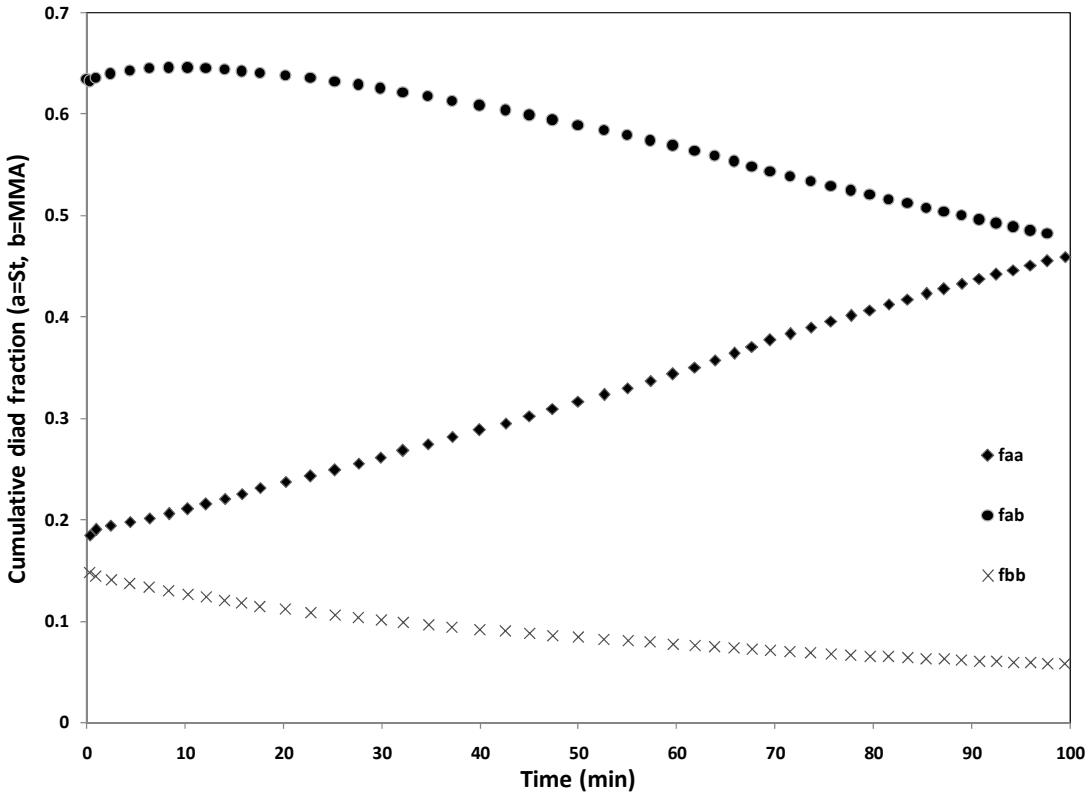

Figure 4.14. Cumulative diad fraction as a function of time for St-MMA system. The initial comonomer molar fractions are $f_{0,MMA} = 0.50$ and $f_{0,St} = 0.50$.

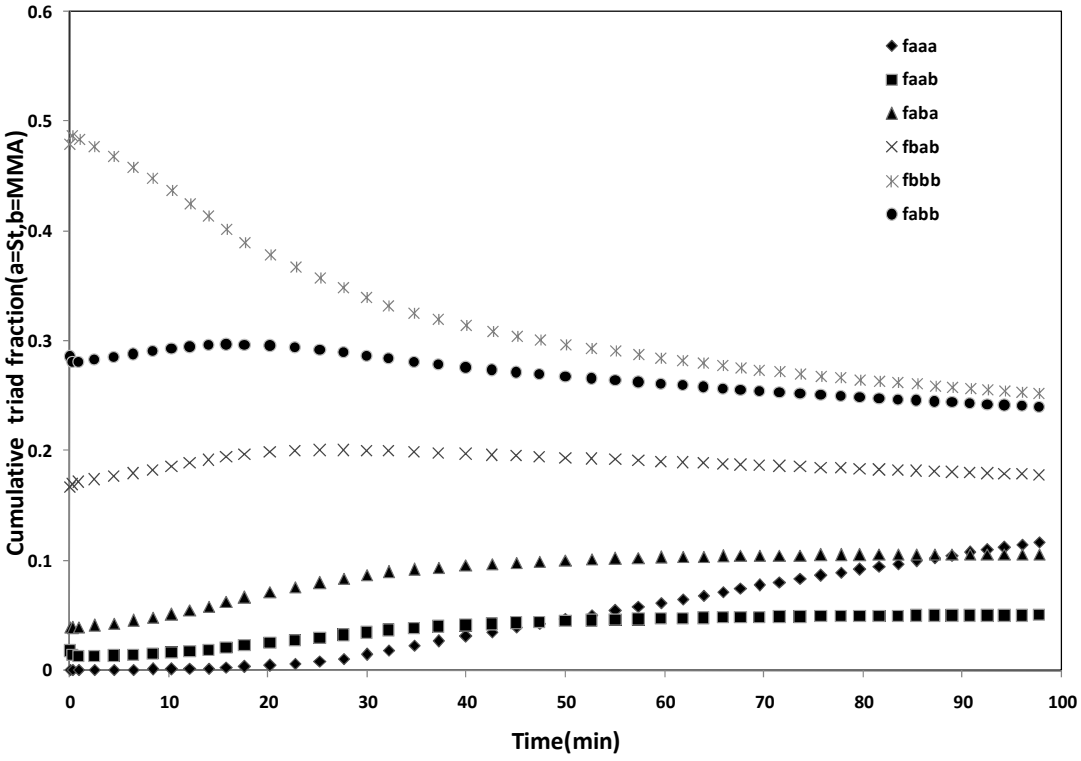

Figure 4.15. Cumulative triad fraction as a function of time for St-MMA system. The initial comonomer molar fractions are $f_{0,MMA} = 0.90$ and $f_{0,St} = 0.10$.

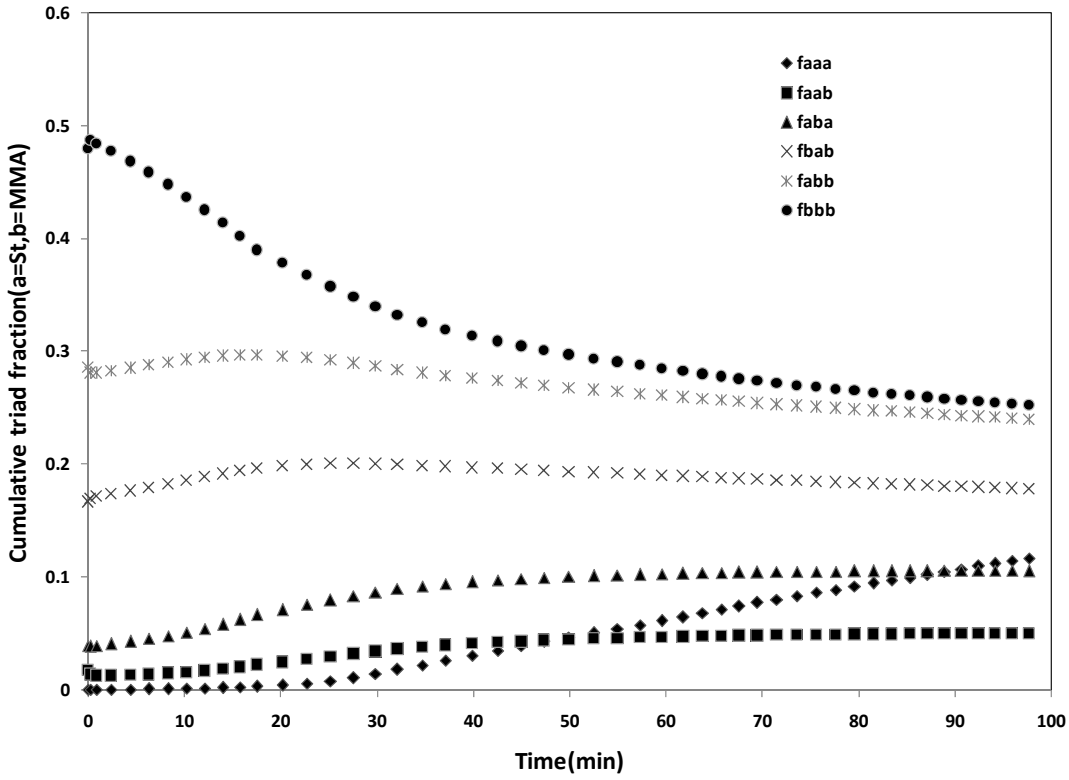

Figure 4.16. Cumulative triad fraction as a function of time for St-MMA system. The initial comonomer molar fractions are $f_{0,MMA} = 0.75$ and $f_{0,St} = 0.25$.

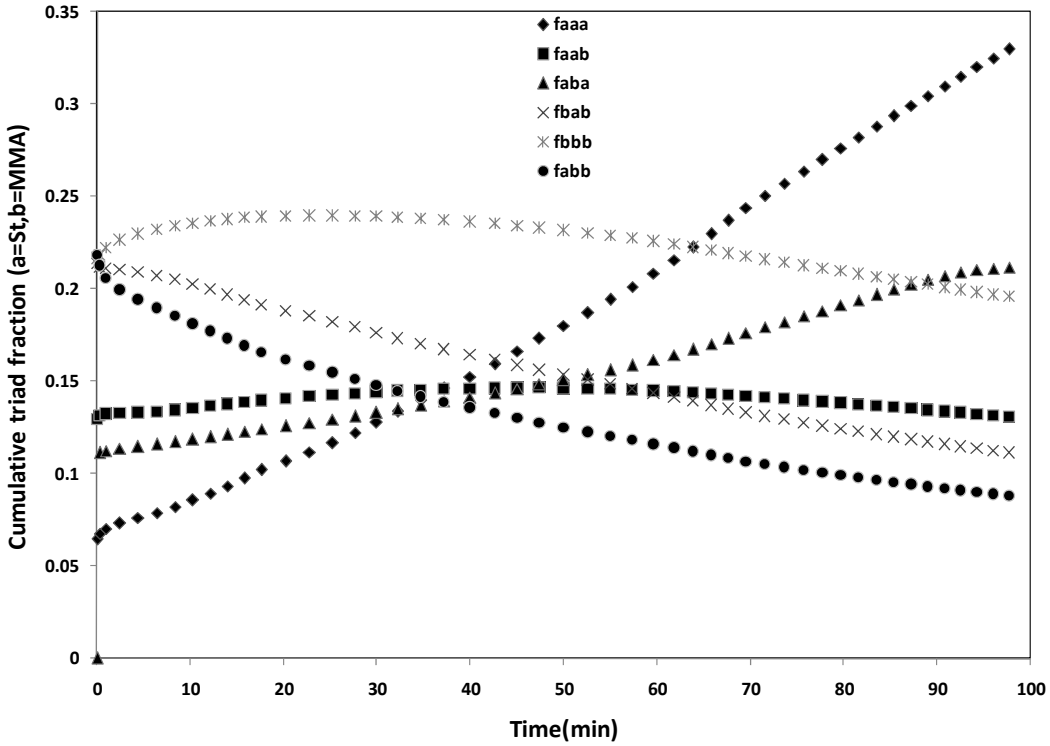

Figure 4.17. Cumulative triad fraction as a function of time for St-MMA system. The initial comonomer molar fractions are $f_{0,MMA} = 0.50$ and $f_{0,St} = 0.50$.

4.4 Conclusions

We have developed a dynamic model for the simulation of atom transfer radical copolymerization by using Monte Carlo simulation. The model can predict average molecular weight, polydispersity index, MWD, CCD, SLD and copolymer composition as a function of polymerization time in semibatch reactors. Two case studies (styrene-co-methyl methacrylate and acrylonitrile-co-methyl methacrylate) were chosen to demonstrate the effect of semibatch method and monomer feed composition.

The simulation clearly showed the impact of using semibatch for the formation of gradient copolymers. The system utilizing styrene as semibatch showed that increasing the styrene content formed a gradient, while increasing the MMA content also formed a gradient at the expense of high polymerization time, but it produced a narrow molecular distribution. The AN-MMA system followed the same trend. The gradient was formed in a shorter polymerization time while employing AN as the sidestream. Even though the batch process also produced gradient polymers, the semibatch utilized less polymerization time and lower concentration of AN than its batch counterpart. The vital fact is the production of gradient polymers with great control enhancing the use of semibatch technology. The model also showed its capability to produce tailor-made gradient polymers.

4.5 References

[1] A.Goto, T.Fakuda, *Prog. Polym. Sci*. **2004** , *29,* 329.

[2] K.ADavis, K.Matyaszewski, *Adv. Polym. Sci.* **2002**, *159,* 1.

[3] M.Kamigaito, T.Ando, M.Sawamto, *Chem. Rev.* **2001**, *101,* 3689.

[4] K.Matyjaszewski, *Prog. Polym. Sci.* **2005**, *30*, 858.

[5] D.Benoit, V.Chaplinski, R.Braslau, C.J.Hawker, *J. Am. Chem. Soc.* **1999**, *121,* 3904.

[6] M.Rodlert, E.Harth, I.Rees, C.J.Hawker, *J. Polym. Sci. Polym. Chem. Ed.* **2000**, *38,* 4749.

[7] G.Moad, J.Chiefary, Y.K. Chong, J.Krstina, R.T.A.Mayadunne, A.Postma, E.Rizzardo, S.H.Thang, *Polym. Int.* **2000**, *49,* 993.

[8] J.Chiefary, Y.K.Chong, F.Ercole, C.Moad, G.Moad, E.Rizzardo, S.H.Thang, *Macromolecules.* 1998, *31*, 5559.

[9] K.Matyjaszewski, J.Xia, *Chem. Rev*. **2001**, *101,* 2921.

[10] S.Zhu, *J Polym Sci Part B: Polym Phys.* **1999**, *37*,2692.

[11] A.Butte, G.Storti, M.Morbidelli, *Chem Eng Sci* **1999**, *54*, 3225.

[12] S.Zhu, *Macromol.Theory Simul*. **1999**, *8,29*.

[13] M. Al-Harthi, J. Soares, L. Simon, *MacromolTheory Simul* **2006**, *15*, 198.

[14] M.Al-Harthi, J.Soares, L. Simon, *Macromol Chem Phys.* **2006**, *207*, 469

[15] L. Li, J. He, Y.Yang, Chem*. J. Chin Univ.* **2000**, *21,* 1146.

[16] S. Zhu, R. Wang,Y. Luo, B. Li, *AIChe J*. **2007**, *53*, 174

[17] S. Zhu, R. Wang,Y. Luo, B. Li, X.Sun, *Macromol. Theory Simul*. **2006**, *15*, 356

[18] Y. Fu, A. Mirzaei, M.F. Cunningham, R.A. Hutchinson, *Macromol. React. Eng*. **2007**, *1,* 425.

[19] K. Matyjaszewski, *J. Macromol. Sci., Pure Appl. Chem.* **1997**, *A34,* 1785.

[20] K. Matyjaszewski, J. Xia, "*Handbook of radical polymerization*", T. Davis, K. Matyjaszewski, Eds., Wiley, New York 2002, p523.

[21] M. Hideharu, A.H.E Muller, *Prog. Polym. Sci*. **2003**, *28,* 1403.

[22] S. Arehart, *Polym. Prepr. (Am. Chem. Soc., Div. Polym. Chem.)*. **1997**, *38,* 705.

[23] G. Chen, *Macromolecules*. **2000**, *32,* 232.

[24] H. Uegaki, *Macromolecules.* **1998**, *31,* 6756.

[25] K. Matyjaszewski, M.J. Ziegler, S.V. Arehart, D. Gresztra, T. Pakula, *J. Phys. Org. Chem.* **2000**, *13, 7*75.

[26] M.J. Ziegler, K. Matyjaszewski, *Macromolecules.* **2001**, *34,* 415.

[27] K. Karaky, E. Pere, C. Pouchan, G.H. Khoukh, J. Francois, J. Desbrieres, L. Billion, *New J. Chem.* **2006**, *30,* 698.

[28] D. Gillespie, *J. Phys. Chem.* **1977**, *81,* 2340.

[29] A. Keramopoulos, C. Kiparissides, *Macromolecules*. **2002**, *35,* 4155.

[30] M. Buback, R. Hutchinson, R. Klumperman, B. Kuchata, F. Manders, B. O'Driscoll, K. Russell, G. Schweer, *J. Macromol. Chem. Phys.* **1995**, *196,* 3267.

[31] D.S. Achilias, C. Kiparissides, *Macromolecules*. **1992**, *25,* 3739.

[32] H. Suzuki, V.B.Mathot, *Macromolecules.* **1989**, *22,* 1380.

[33] A.W. Hui, A.E.Hamielec, *J. Appl. Polym. Sci.* **1972**, *16,* 749.

[34] K.Olmo, A. Goto, T. Fukuda, J. Xia, K. Matyjazewski, *Macromolecules*. **1998**, *31*, 2699.

[35] M. Zhang,H. Ray, *J.Appl.Poly.Sci*,**2002**, *86*, 1630.

[36] I.M. Yaraskavitch, J. Brash, L, A.E. Hamielec, *Polymer*. **1987**, *28,* 489

[37] J. Brandrub, E. Immergut, E. Grulke, Eds. *Polymer Handbook*, 4th ed.; Wiley: New York, **1999**.

[38] Pittman-Bejger, Real-Time Control and Optimization of Batch Free-Radical Copolymerization Reactors. Ph.D. Thesis, University of Minnesota, 1982.

[39] F.R. Mayo, J.M.Lewis, *J.Am.Chem.Sco*, **1944**,*66*,1594

[40] M. Al-Harthi, S.H. Abbasi, J.Masihullah, J. Soares, *Macromolecular Theory and Simulation*, submitted.

[41] Y. Fu, M.F. Cunningham, R.A. Hutchinson *Macromolecular Symposia.* **2007***, 259*, 151

[42] Y. Fu, M.F Cunningham, R.A. Hutchinson, *Macromolecular Reaction Engineering*. **2007**, *1*, 243

[43] M. Al-Harthi, L.S. Cheng, J. Soares, L. Simon, *J.Polym.Sci: Part A: Polym Chem*. **2007**, *45*, 2212

CHAPTER 5

EFFECT OF DIFFUSION CONTROLLED REACTIONS ON ATOM TRANSFER RADICAL COPOLYMERIZATION

5.1 Introduction

The development of controlled/living radical polymerization (CLRP) for the synthesis of polymers with controlled architecture, molecular weight and narrow polydispersity index (PDI) is a major area of interest in the field of polymer science and engineering. A polymerization process is "living" when the growing chains do not experience permanent termination and/or transfer during the course of the polymerization. Living polymers are primarily synthesized by using one of the three predominant methods of CLRP, namely: (1) atom transfer radical polymerization (ATRP), (2) nitroxide-mediated polymerization (NMP) and (3) reversible addition fragmentation chain transfer processes (RAFT). Among the three methods, ATRP is the most successful method to produce a variety of polymers in a controlled manner. [1, 2] A conventional ATRP system is composed of a monomer, an initiator with a transferable (pseudo) halogen, and a transition metal catalyst. The major distinction between free

radical polymerization (FRP) and ATRP is the dynamic equilibration between growing free radical and the dormant species.

Copolymers possess outstanding chemical and mechanical properties leading to numerous applications. They can be further enhanced by an additional control of molecular weight, PDI and chain topology. As stated in the literature [3] "ATRP provides a distinct advantage over the other techniques in synthesizing block copolymers in any order (with halogen exchange) which is not possible for other CLRP methods. Difficulties in polymerization of methacrylates by NMP method [4] and in the production of end-group functionalized polymers by NMP and RAFT [5] makes ATRP an ideal option to synthesis copolymers". Hence it is justified to use ATRP for our case.

The literature available on the synthesis of copolymers using ATRP is on the increase in recent years. [6, 7, 8] However, there are fewer studies on modeling of atom transfer radical copolymerization (ATRcP). [9, 10] But until now the modeling of ATRcP has been done without attention to the effect of diffusion controlled reaction on the process or by considering only diffusion limited termination reactions. It is evident in polymerization reactions, besides the conventional chemical kinetics associated with the polymerization mechanism. Physical phenomena related to the diffusion of various chemical reactive species also play an important role. In FRP, as the reaction goes from zero to complete conversion, the viscosity of the reacting mixture increases by several orders of magnitude. An auto acceleration in rate begins at 30 – 50% conversion caused by drastic decrease in the rate of chain termination due to severe diffusional limitations. Evidence of diffusion effects on reactivity and polymerization has been apparent since early experimental studies. [11, 12, 13] Since then a large number of papers have been

published on the effect of diffusion controlled phenomena on FRP kinetics. North [14], Mita and Horrie [15], O'Driscoll [16], Litvinenko and Kaminsky [17] and Dube et al. [18] wrote interesting reviews. Recently, interesting work has been done in the field of diffusion controlled free radical polymerization [19, 20, 21] emphasizing the effect of diffusion in polymerization. However, there is no agreement in the literature about diffusion effects in CLRP. For instance, the auto-acceleration phenomenon that appears in conventional FRP seems to be absent in CLRP. Some authors suggest that only the termination constant may be affected by diffusion limitations at high monomer conversions,[22,23,24,25] while others say that all the rate constants may be affected in controlled free radical polymerizations[26,27]. Al-Harthi et al. [28] predicted the variation of the conversion, PDI and number average molecular weight when diffusion limitations are present for homopolymerzation by using a bifunctional initiator. Zhu et al. [29] produced the same results while using a mono functional initiator. Both groups of researchers concluded that diffusion may play a role in ATRP and required experimental data at high conversion to verify the importance of diffusion controlled reactions in ATRP. Thus it is important to evaluate the validity of these suggestions with a mathematical model that can quantify these effects for ATRcP.

5.2 Free Volume Theory

A plethora of models have been developed to quantify the effect of diffusion controlled phenomena on polymerization reactions. Gregory and John [30] stated that **"**For the past 20-25 years, most attempts to explain this phenomenon have fallen into one of the two categories: entanglement pictures and free volume pictures. However, the theory

that onset of entanglement causes gel effect is incorrect as it fails to predict trends concerning the effect of temperature, polymer concentration and molecular weight on the gel effect onset conversion. [31] The free theory fares much better [32] when critically tested. [33]". Hence the free volume theory is a good way to find the effect of diffusion controlled reaction in ATRcP.

The free volume theory works on the principle that the free volume of the reaction medium varies throughout the reaction as a function of monomer conversion. As the conversion increases, the viscosity of the reaction medium increases and its free volume decreases, therefore slowing down the diffusion of the species in the reactor. Termination reactions occur between two large polymer radicals, and they are limited by the rates at which the polymer radical ends meet each other. As a result, the termination rate constant depends on the length of the polymer radical, and it is inversely proportional to the viscosity of the medium. Propagation, activation, and deactivation reactions become diffusion controlled when the polymerization medium becomes very viscous, at high monomer conversion. In solution polymerization, the solvent acts as a diluent, which in turn decreases the viscosity of the reaction mixture, delaying or eliminating diffusion limitations. Using this theory, all the rate constants can be correlated to the change of the free volume of the reaction media. During polymerization, the free volume of the reaction mixture depends on the volume of the components present in the system. The total volume is calculated as

$$v_f = \sum_{i=1}^{\#\,of\ components} \left[0.025 + \alpha_i (T - T_{gi})\right] \frac{V_i}{V_t} \qquad (1)$$

where α_i is the expansion coefficient for component *i,* T and T_{gi} are the polymerization temperature and glass transition temperature of component *i*, and V_i and V_t are the volume of component *i* and the total volume.

Among the elementary reactions present in ATRcP, only chain termination involves reactions between two large polymer radicals. Therefore, the model for the termination rate constant is a function of the PDI of the polymer radicals. Equation shows the expression used to correct the termination rate constant due to diffusion

$$k_t = k_{t0}\left(pdi\right)^{x/2} \exp\left[-B_t\left(\frac{1}{v_f}-\frac{1}{v_{f0}}\right)\right] \tag{2}$$

where x is monomer conversion, B_t is a dimensionless adjustable parameter, $k_{t,0}$ is the termination rate constant at the beginning of the polymerization, and v_{f0} is the fractional free volume at the beginning of the polymerization. The expressions for the propagation, activation, and deactivation reaction rate constants are shown in the following equations:

$$k_p = k_{p0} \exp\left[-Bp\left(\frac{1}{v_f}-\frac{1}{v_{f0}}\right)\right] \tag{3}$$

$$k_a = k_{a0} \exp\left[-Ba\left(\frac{1}{v_f}-\frac{1}{v_{f0}}\right)\right] \tag{4}$$

$$k_d = k_{d0} \exp\left[-Bb\left(\frac{1}{v_f} - \frac{1}{v_{f0}} \right) \right] \quad (5)$$

where B_p, B_a, and B_b are dimensionless adjustable parameters for propagation, activation, and deactivation reactions, respectively, and the subscript ‘‘0’’ indicates the initial value of each reaction rate constant.

The method of moments has been used to describe the effect of diffusion controlled reactions in ATRP. The effect of diffusion on reactions such as bimolecular termination, deactivation, activation and propagation was investigated. Its effect on the monomer conversion, PDI and average molecular weights as a function of polymerization time or conversion was investigated using the method of moments. [28,29] A thorough investigation into the available literature indicates the lack of papers that has predicted the molecular weight distribution (MWD) and chemical composition distribution (CCD). Even though PDI has been described, it can be misleading with regard to the microstructural properties. Hence the prediction of MWD is highly important for process such as ATRcP. On the other hand, Monte Carlo simulation is a powerful tool that can simulate any polymer microstructural distribution, and it is relatively simple to implement, making it very attractive for academic and industrial use.

In the present study, a dynamic Monte Carlo model has been developed to study the effect of diffusion controlled reactions (Bimolecular termination, deactivation and propagation) in ATRcP. The model has been applied to study qualitatively the individual and combined effects of diffusion controlled reactions. Properties such as PDI, MWD and

CCD are described along with the prediction of conversion and number average molecular weight. The ability of the mathematical model to describe diffusion controlled reactions in ATRcP will be validated by its application to two systems, including styrene-acrylonitrile (SAN) and styrene-methyl methacrylate (St-MMA). To our knowledge this is the first attempt to predict the variation of MWD, CCD, conversion, and average molecular weight by taking into account simultaneously the free volume dependence of all termination, deactivation and propagation rate constants in ATRcP. This is also the first attempt at using dynamic Monte Carlo simulation to describe diffusion controlled ATRcP. This is also the first attempt at using Monte Carlo simulation to describe diffusion controlled ATRP.

5.3 Model Description

We have followed Gillespie's algorithm for dynamic Monte Carlo simulation as explained in chapter 2. [34] Tables 5.1 lists the numerical values of the kinetic rate constants, reactivity ratios and diffusional parameters used in our simulations.

Table 5.1. Kinetic rate constants and physical properties for styrene (A) - methyl methacrylate (B) copolymerization at a temperature of 383 K.

Parameter	Value	Reference
$k_{p\mathrm{AA}}$	$4.266\times10^{7}\exp(-7769/RT)$ (L/mol s)	36
$k_{p\mathrm{BB}}$	$4.92\times10^{5}\exp(-4353/RT)$ (L/mol s)	37

r_A	0.52	38
r_B	0.46	38
$k_{tc}AA$	$(k_{p11})^2 \times 1.1 \times 10^{-5}$ exp(12452.2/RT) (L/mol s)	39
$k_{td}BB$	9.80×10^7exp(-701/RT) (L/mol s)	37
$k_{td}AA$	0	40
$k_{tc}BB$	0	40
$k_{tr}A$	$(k_{p11}) \times 2.198 \times 10^{-1}$exp(-2820/$T$) (L/mol s)	35
$k_{tr}B$	$(k_{p22}) \times ((9.48 \times 10^3 \times \exp(-13880/(RT)))/60)$ (L/mol s)	35
Initial Catalyst Concentration	0.087 mol/L	
Initial Initiator Concentration	0.087 mol/L	
Total Monomer Concentration	8.7 mol/L	
MW_A	104.14 (g/mol)	
MW_B	103.13 (g/mol)	
T_{gma}, T_{gmb}, K	185,159.15	19

densitymA(g/m^3)	$0.9236-0.887 \times 10^{-3} \times (T-273.15)$	19
densitymB(g/m^3)	$0.968-1.225 \times 10^{-3} \times (T-273.15)$	19
α_A	6.2×10^{-3}	19
α_B	2.9×10^{-4}	19

5.4 Results and Discussion

In the free volume theory, the rate constants vary exponentially with the total free volume of the mixture. An equimolar mixture of St-MMA was used to study the effect of diffusion controlled reactions on the conversion, PDI, MWD, Mn and CCD. Two different equilibrium constants were chosen to understand the effect of diffusion on the microstructural properties. The chemically controlled rate constants for all the reactions at 383 K were used from the literature (see Table 5.1). A control volume of 1×10^{-19}L has been used in all simulations. The ratio of the initial molar concentrations of monomer, initiator, and activator was 100:1:1. The free volume parameters B_t, B_p, and B_b were varied over a range of values wide enough to have a significant impact on the reaction rate constants. Glass transition temperatures and thermal expansion coefficients used in this study are also shown in Table 5.1. All the parameters used fall well within the accepted range predicted in the literature. [28, 29, 41]

A system with a lower equilibrium constant was chosen to see the effect of the dimensionless adjustable parameter B_t. Bimolecular termination is the first reaction to be affected by diffusion after a conversion of 30% -50%. Thus to start with, the value of B_t was varied to find the effect of diffusion on the targeted parameters. An increase in the conversion is seen when B_t is increased. Diffusion controlled termination decreases the termination rate constant considerably, and the termination rate constant goes to zero at high conversion. This leads to a decrease in radicals terminating with each other and greatly aids the propagation reactions. Thus an increase in the monomer conversion is seen when diffusion controlled termination increases i.e increasing the free volume parameter B_t. The number average molecular weight (Mn) also increases as the value of B_t increases. This is also due to the increase in the propagation reactions taking place. The deactivation/activation reactions may also be increased. A higher number of dormant species will also shift the equilibrium towards activation/ propagation reactions to take place. Thus an increase in the conversion and Mn are observed when the value of B_t increases as shown in Figure 5.1.a and 5.1.b. An attempt has been made to understand the effect of diffusion on CCD. The diffusion controlled termination reactions do not show a distinct difference for the three values of B_t. But a slightly higher weight fraction of styrene is obtained for B_t value of 1. This can be inferred from the standard deviation value in Table 5.2, thus showing that diffusion controlled termination might increase the styrene content in the obtained polymer. Figure 5.1c represents the above mentioned results graphically. The PDI of the system does not vary significantly with the increase in the value B_t hence proving that the system is well controlled. The PDI of the system falls considerably for all the cases due to the lower equilibrium constant as seen from Figure

5.1.d. In this case, the number of dormant chains formed is very high compared to the dead polymer due to high equilibrium constant and the effect of diffusion on termination reactions. The MWD is narrow for all the values of B_t verifying our results obtained for PDI. The distribution is uniform for all values of B_t as seen from Figure 5.1.e.

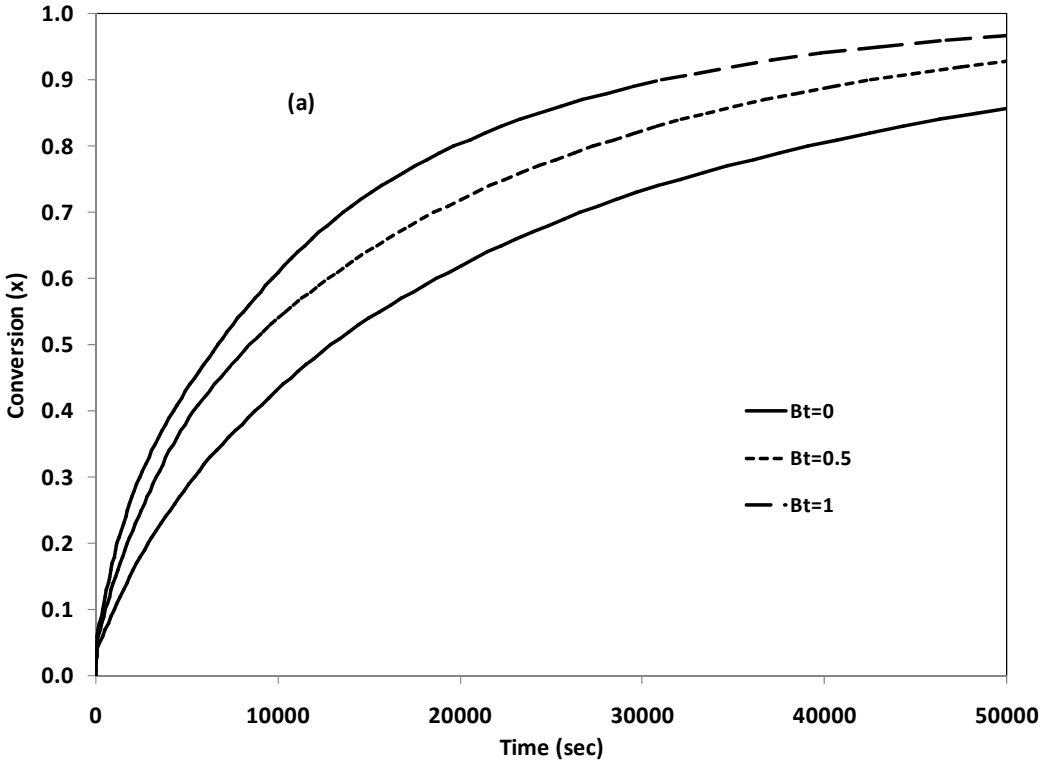

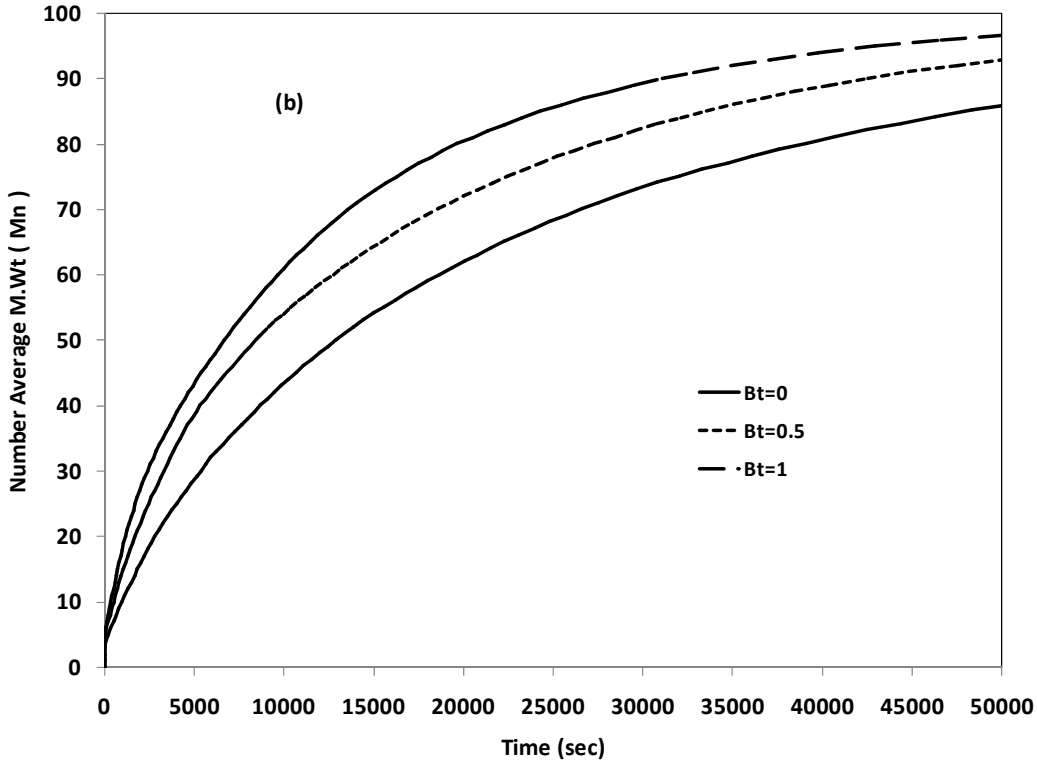
(b)
Number Average M.Wt (Mn)
Time (sec)
Bt=0
Bt=0.5
Bt=1
0
10
20
30
40
50
60
70
80
90
100
0
5000
10000
15000
20000
25000
30000
35000
40000
45000
50000

(c)

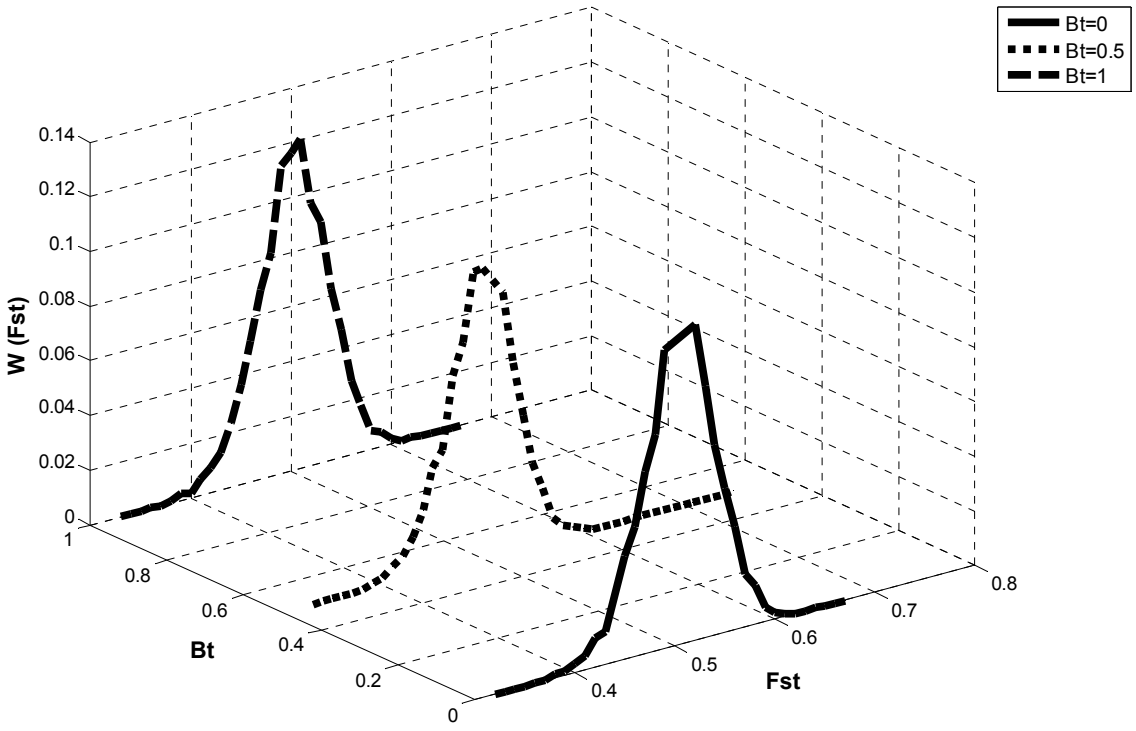
Bt=0
Bt=0.5
Bt=1
W (Fst)
0.14
0.12
0.1
0.08
0.06
0.04
0.02
0
Bt
1
0.8
0.6
0.4
0.2
0
Fst
0.4
0.5
0.6
0.7
0.8

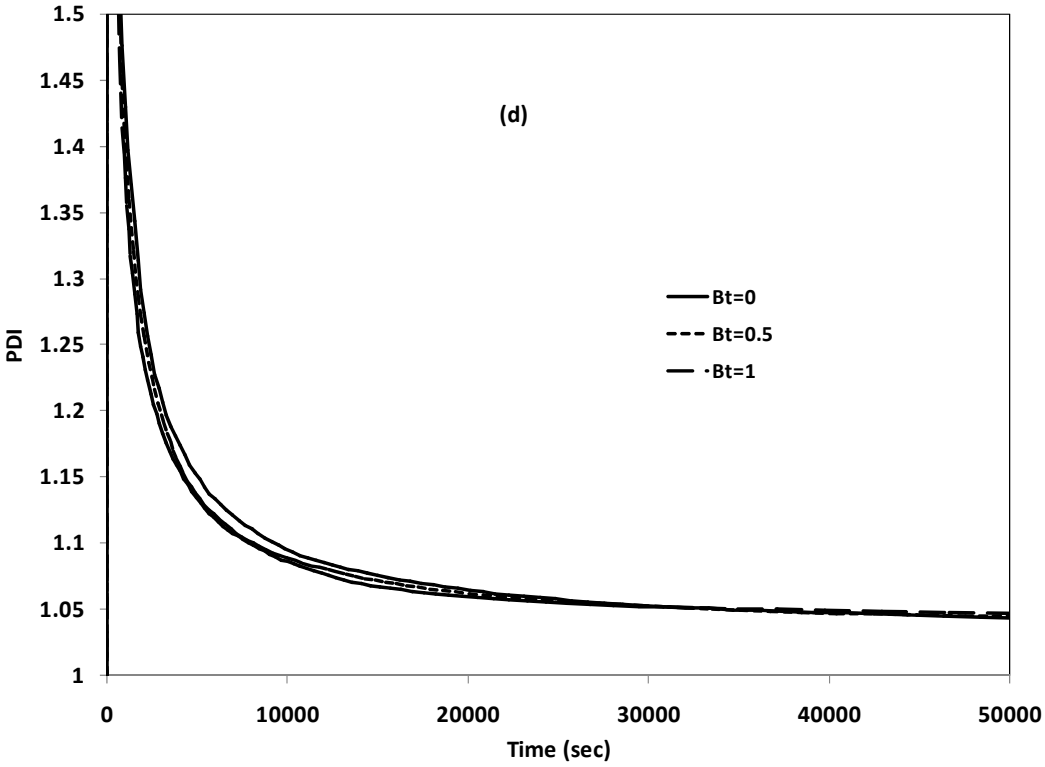
(d)
PDI
Time (sec)
Bt=0
Bt=0.5
Bt=1
1.5
1.45
1.4
1.35
1.3
1.25
1.2
1.15
1.1
1.05
1
0
10000
20000
30000
40000
50000

(e)

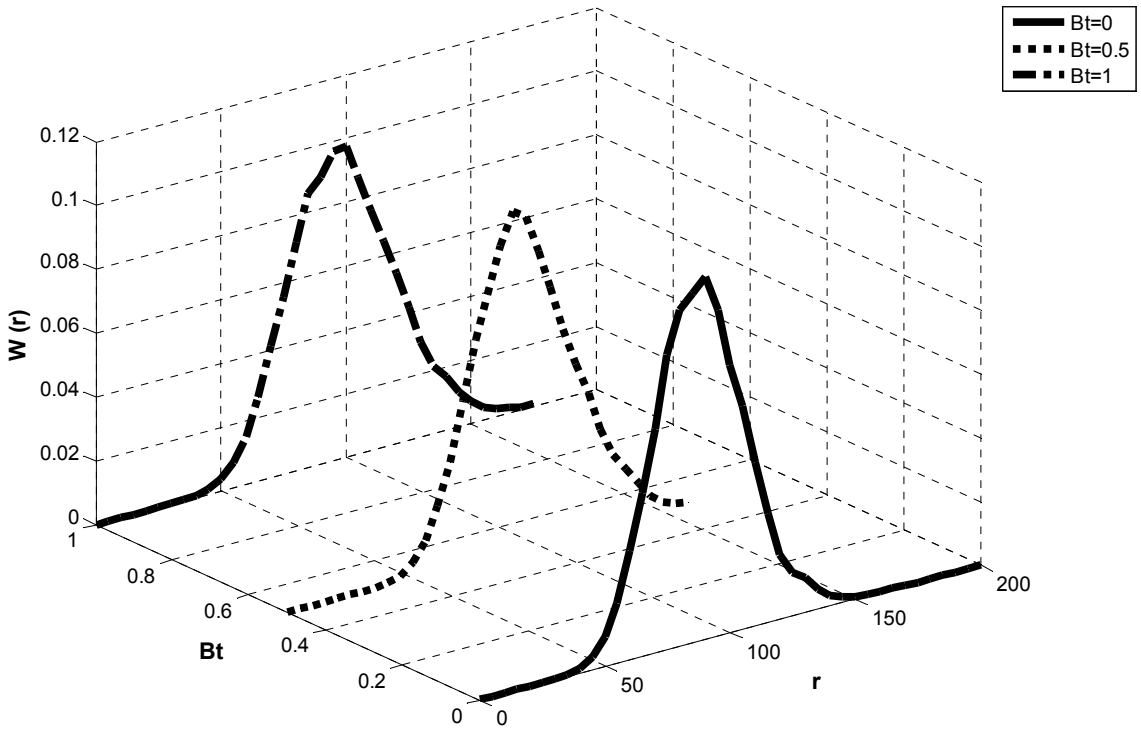

Figure 5.1. Monte Carlo Simulation results for the copolymerization of St-MMA. Effect of diffusion limitation on the termination rate constant: (a) monomer conversion as a function of time, (b) Number Average M.Wt (Mn) as a function of time, (c) chemical composition distribution (d) PDI as a function of time, (e) Molecular weight distribution.The initial comonomer molar fractions in the reactor were $f_{0,St} = 0.5$, $f_{0,MMA} = 0.5$. The equilibrium constant *(Keq)* is 6.87×10^{-10}. *(Bb=Bp=0)*

Since the PDI shown in Figure 5.1.d does not show any change or deviation in the profile for all the three values of B_t, a comparison is made with another system with a higher equilibrium constant. Such a change in the equilibrium constant is easily brought about by changing the catalyst in a real time process. A change in the equilibrium constant changes the livingness of the system and a viable option to study the effect of

diffusion controlled termination reactions. Only PDI and conversion results are reproduced to avoid redundancy in results and to show the deviation from the system which has a lower equilibrium constant. When the value of B_t is increased, the conversion increases and it needs a shorter time to reach maximum conversion. This is a known fact that a system with higher equibrium constant needs lesser polymerization time. A significant change in the PDI is observed as the value of B_t increases. This was absent in the previous system (lower *Keq*). The PDI is well above 1.5 and hence represents an uncontrolled ATRcP. The copolymerization process changes from a completely well controlled to an uncontrolled system in this case. A higher number of bimolecular termination takes place, producing more dead polymers. Hence diffusion controlled termination reactions for a system with higher Keq reduces the livingness while considerably decreasing the polymerization time as inferred from Figure 5.2. Thus the effect of diffusion controlled termination increases with an increase in the value of the equilibrium constant.

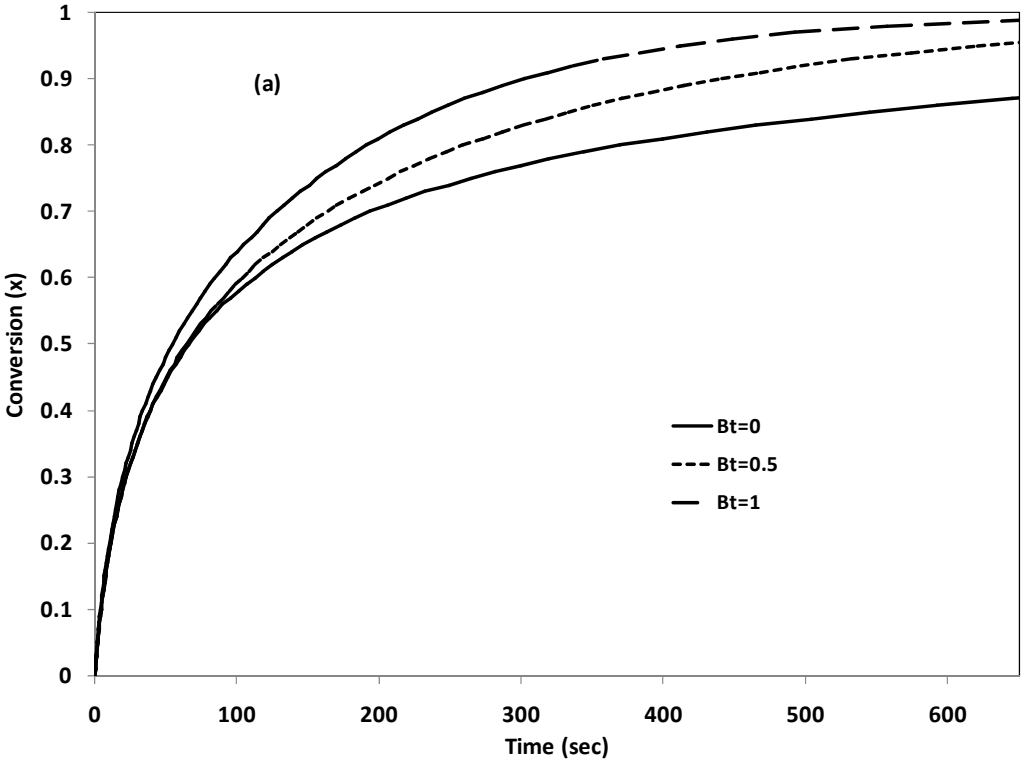
(a)
Conversion (x)
Time (sec)
Bt=0
Bt=0.5
Bt=1
0
0.1
0.2
0.3
0.4
0.5
0.6
0.7
0.8
0.9
1
0
100
200
300
400
500
600

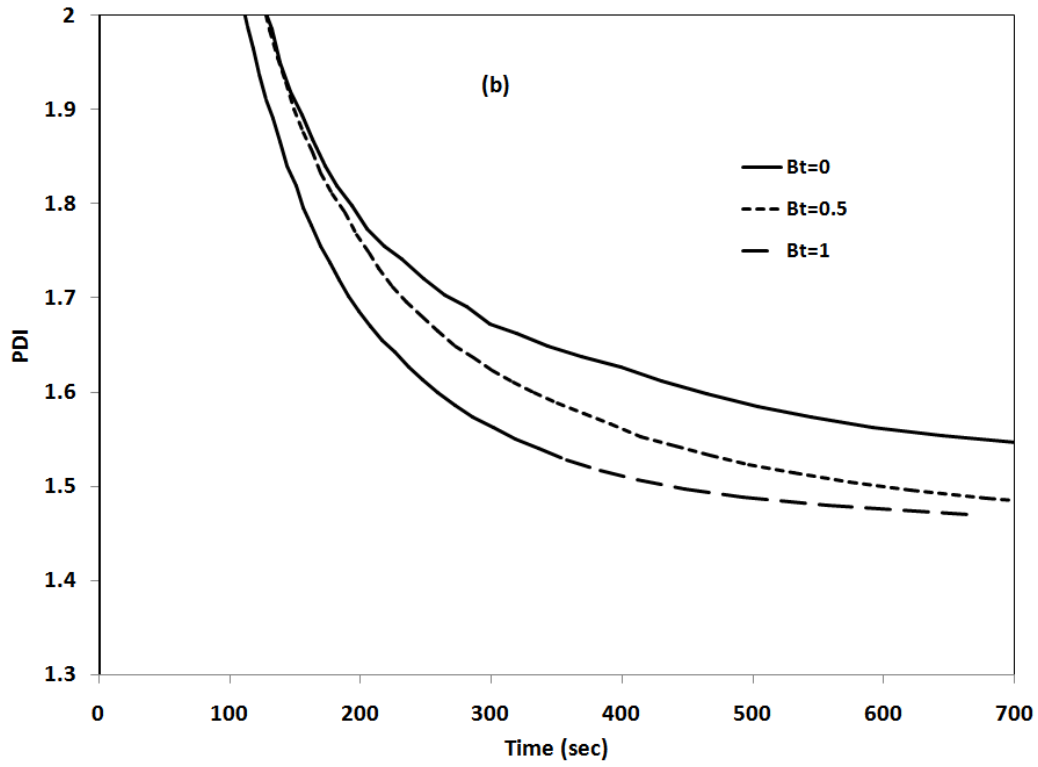

Figure 5.2. Monte Carlo Simulation results for the copolymerization of St-MMA. Effect of diffusion limitation on the termination rate constant: (a) monomer conversion as a function of time, (b) PDI as a function of time. The initial comonomer molar fractions in the reactor were $f_{0,St} = 0.5, f_{0,MMA} = 0.5$. The equilibrium constant *(Keq)* is 5.5×10^{-5}. *(Bb=Bp=0)*

Diffusion controlled deactivation has a similar effect to diffusion controlled termination reactions. A general idea of diffusion phenomena indicates that termination reactions would become diffusion controlled before deactivation. Hence an increase in the monomer conversion is expected when both bimolecular termination and deactivation reactions are diffusion controlled. Figure 5.3.a shows a clear increase in the conversion as the value of B_b increases. Figure 5.3.b shows the increase in the value of Mn as B_b increases. As expected when both deactivation and termination reactions are diffusion

controlled, a sharp decrease in the rate of both the termination and deactivation constant is observed, hence shifting the equilibrium towards more propagation reactions. Thus monomer conversion is increased, which in turn increases the Mn. The PDI also varies for the three values of B_b. Closer examination indicates that diffusion affects the PDI at high conversion. Diffusion increases the PDI of the system as the value of B_b increases. This is highly logical since the deactivation reactions are reduced considerably due to diffusion, and it is also verified from the MWD. Figure 5.3.c clarifies our proposition on PDI since the MWD broadens as value of B_d increases. Again the CCD seems to be affected when the value of B_b is maximum at 0.25. A high peak is obtained with a narrower distribution of styrene at the value of 0.25 which can be inferred from Figure 5.3.e. Thus diffusion seems to reduce the styrene content in the polymer. Comparing Figure 5.1.c and 5.3.e, a considerable decrease in the molar fraction of styrene is obtained when deactivation reactions are diffusion controlled. The standard deviation values in Table 5.2 converge to the fact that a lower molar fraction is obtained when B_b is 0.25. A profound effect is found when deactivation reactions are diffusion controlled at high values of B_b.

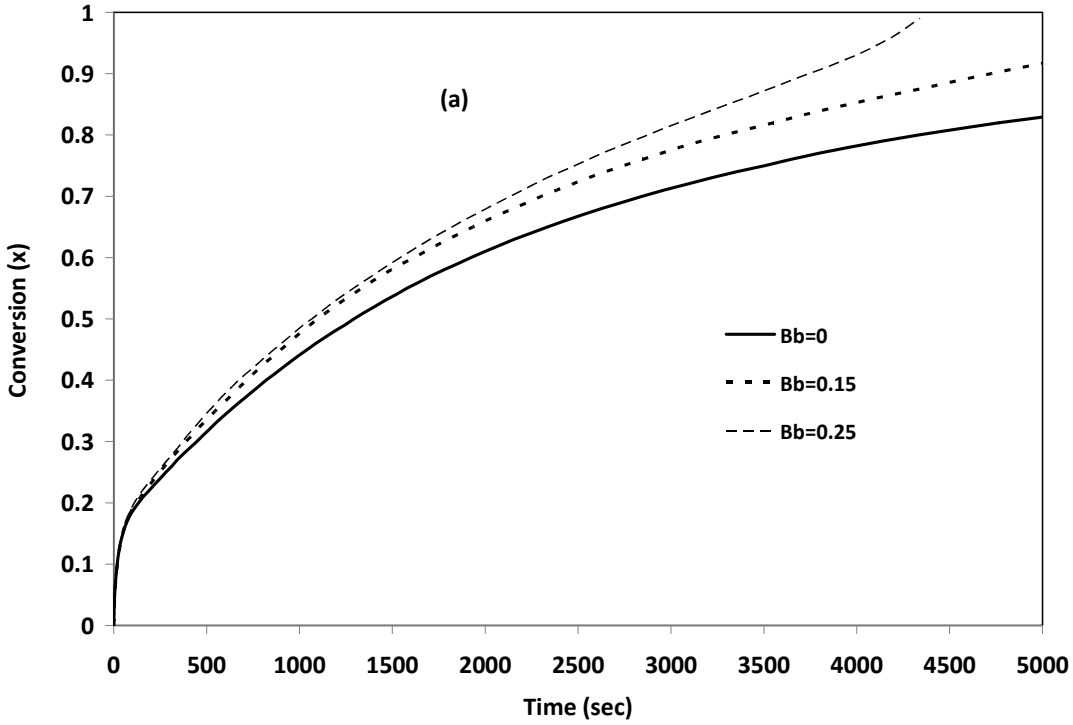
(a)
Conversion (x)
Time (sec)
Bb=0
Bb=0.15
Bb=0.25
0
0.1
0.2
0.3
0.4
0.5
0.6
0.7
0.8
0.9
1
0
500
1000
1500
2000
2500
3000
3500
4000
4500
5000

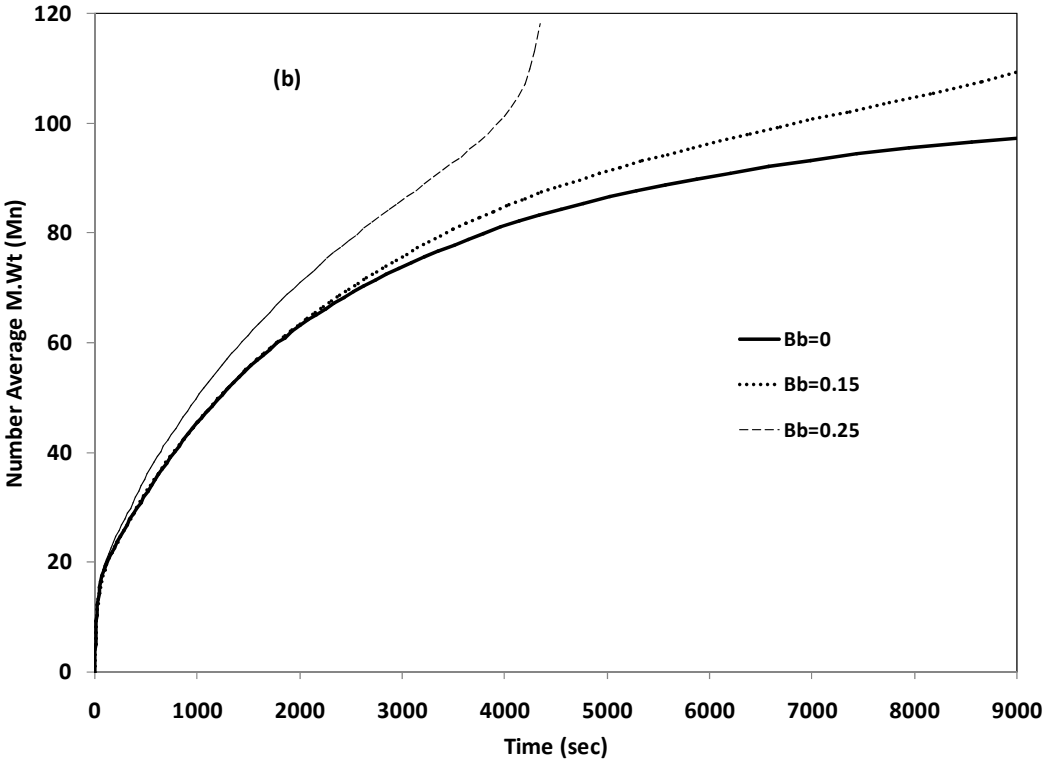
(b)
Number Average M.Wt (Mn)
Time (sec)
Bb=0
Bb=0.15
Bb=0.25
0
20
40
60
80
100
120
0
1000
2000
3000
4000
5000
6000
7000
8000
9000

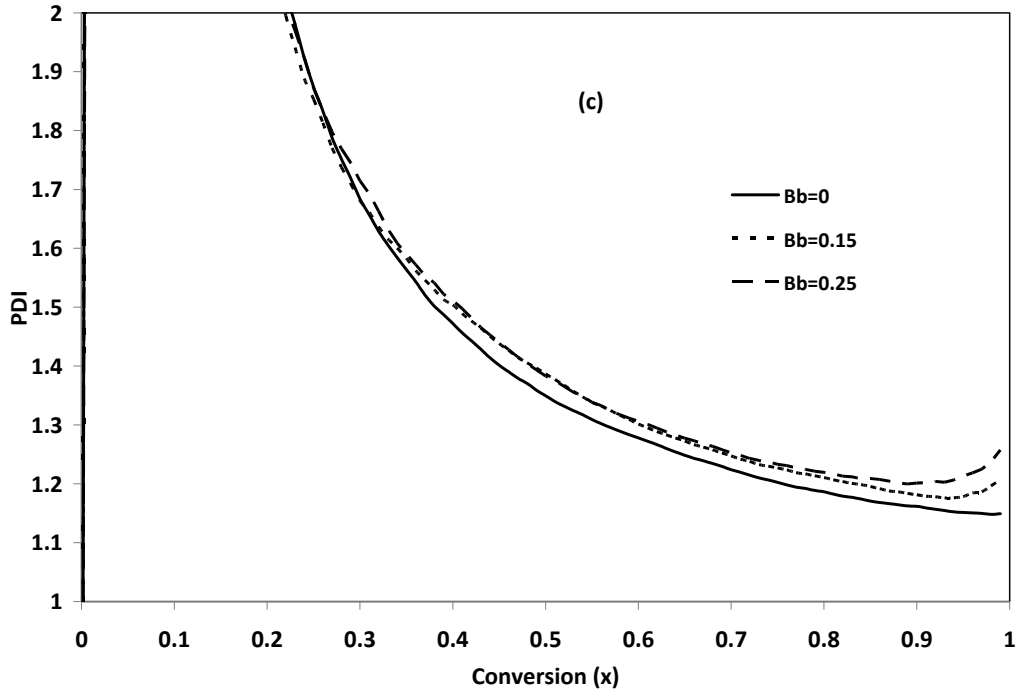
(c)
PDI
Conversion (x)
Bb=0
Bb=0.15
Bb=0.25
1
1.1
1.2
1.3
1.4
1.5
1.6
1.7
1.8
1.9
2
0
0.1
0.2
0.3
0.4
0.5
0.6
0.7
0.8
0.9
1

(d)

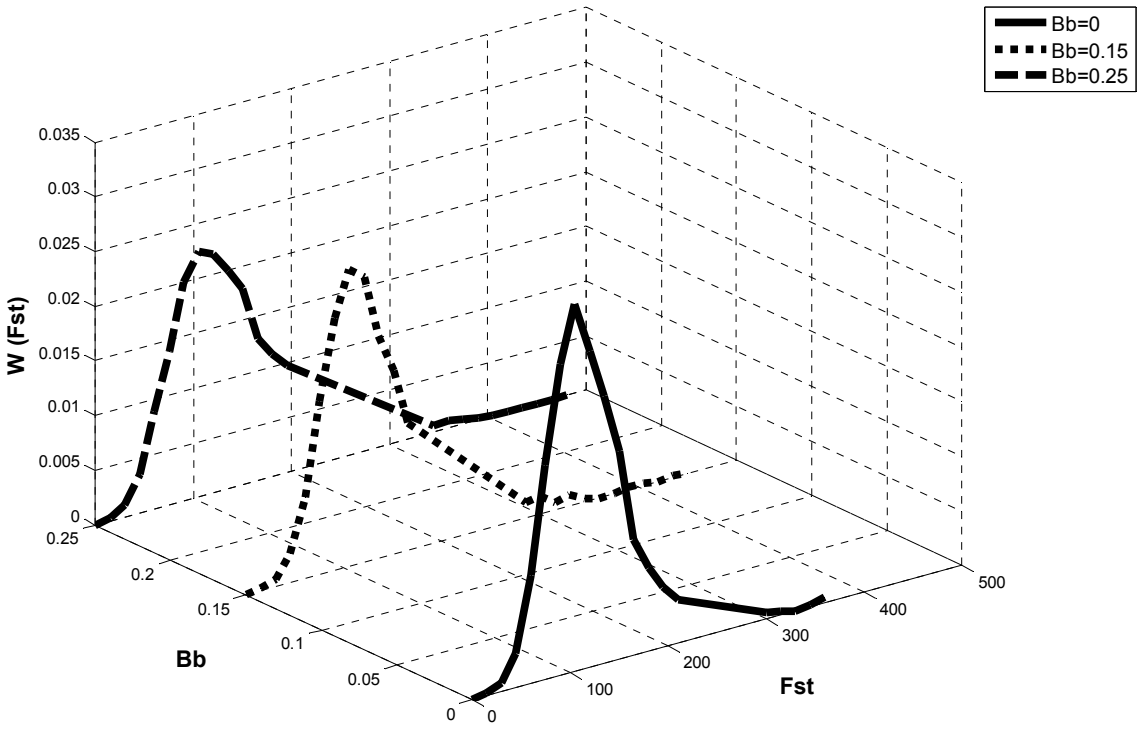
Bb=0
Bb=0.15
Bb=0.25
W (Fst)
0.035
0.03
0.025
0.02
0.015
0.01
0.005
0
Bb
0.25
0.2
0.15
0.1
0.05
0
Fst
0
100
200
300
400
500

(e)

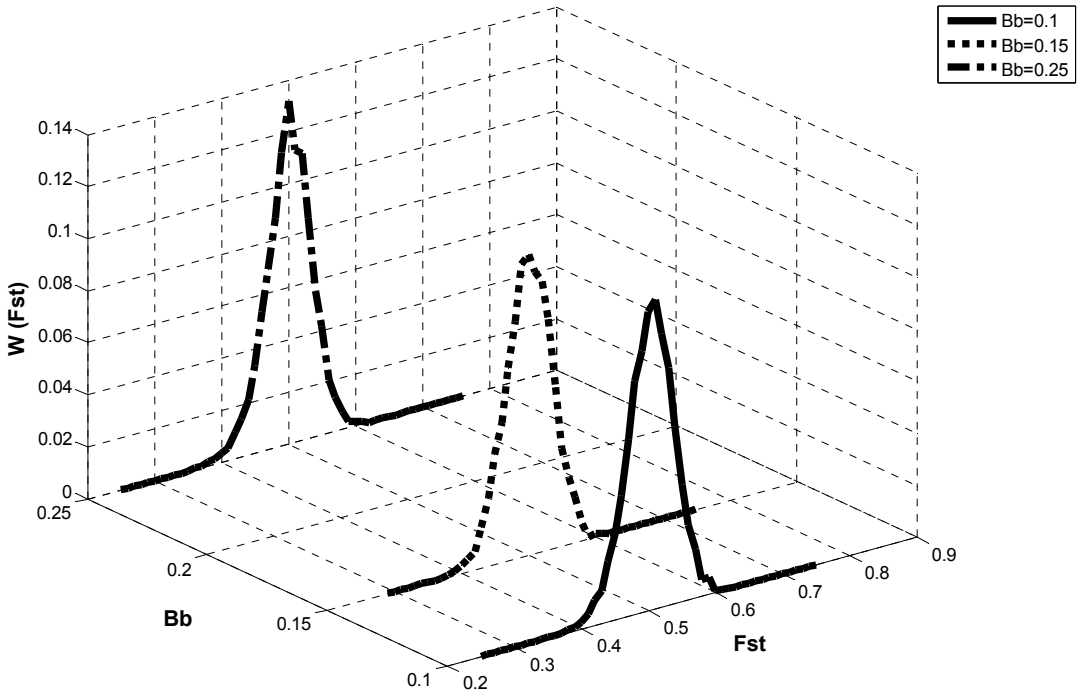

Figure 5.3. Monte Carlo Simulation results for the copolymerization of St-MMA. Effect of diffusion limitation on the deactivation rate constant on: (a) monomer conversion as a function of time, (b) number Average M.Wt (Mn) as a function of time, (c) PDI as a function of time (d) molecular weight distribution, (e) chemical composition distribution. The initial comonomer molar fractions in the reactor were $f_{0,St} = 0.5, f_{0,MMA} = 0.5$. The equilibrium constant *(Keq)* is 6.87×10^{-10}. ***(Bt=0.1, Bp=0)***

When diffusion limits the propagation reactions, a decrease in the conversion and Mn is observed as the value of B_p increases. Since propagation reactions are diffusion controlled, a decrease in monomer consumption happens during polymerization. Hence a reduction in the conversion and Mn is observed as shown in Figure 5.4.a and 5.4.b. The PDI increases as the value of B_p increases. The MWD clearly depicts the slight broadening in the profile, indicating the increase in the value of PDI as B_p goes from 0.1

to 0.5. The CCDs seem to have a similar trend except for the fact that at high values of B_p, a narrower distribution is obtained, indicating a lesser molar fraction of styrene. The standard deviation values have been shown in Table 5.2. The above mentioned results are shown in Figure 5.4.e.

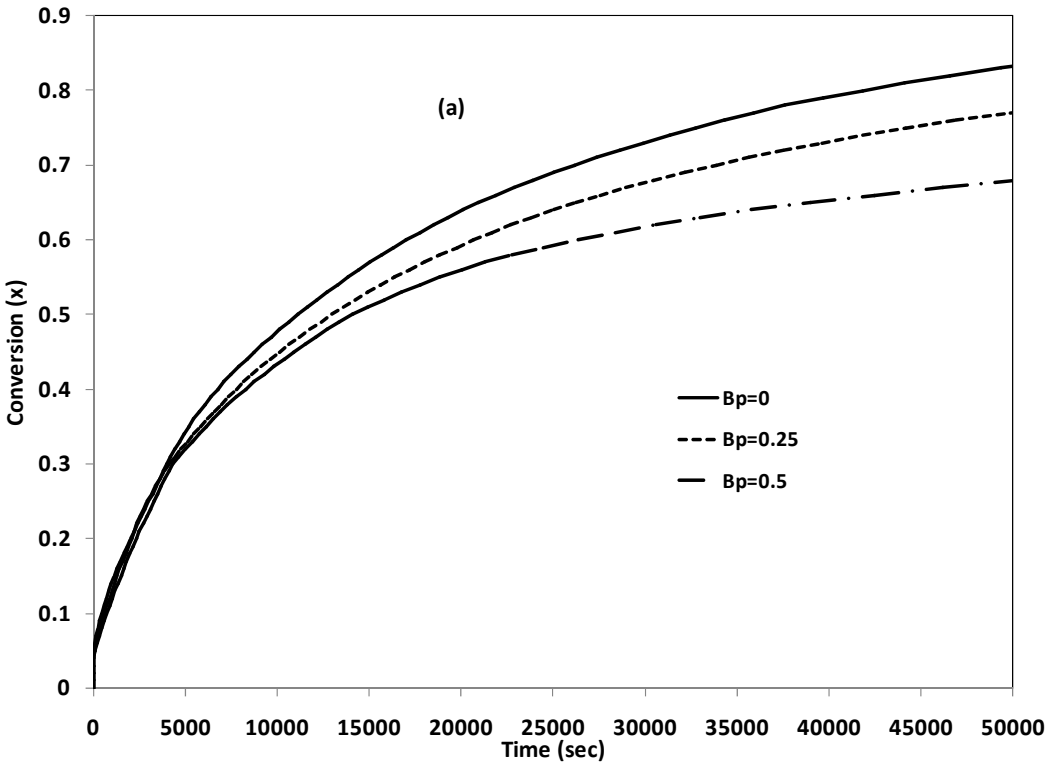

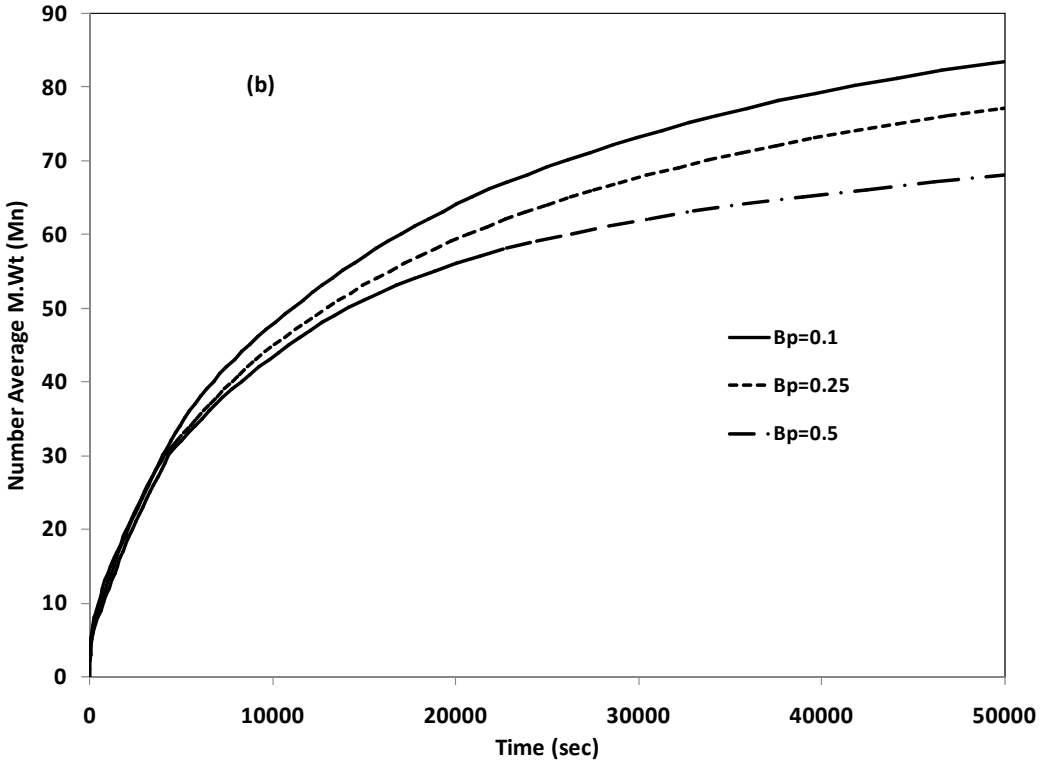
(b)
Number Average M.Wt (Mn)
Time (sec)
Bp=0.1
Bp=0.25
Bp=0.5
0
10
20
30
40
50
60
70
80
90
0
10000
20000
30000
40000
50000

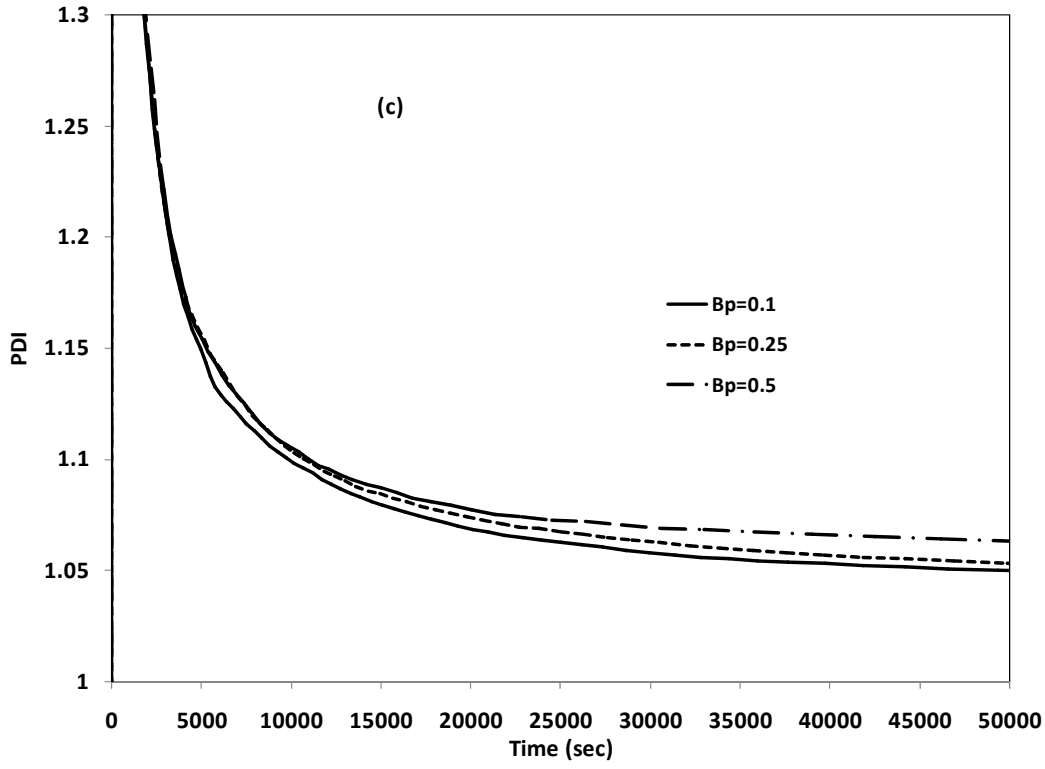
(c)
PDI
Time (sec)
Bp=0.1
Bp=0.25
Bp=0.5
1
1.05
1.1
1.15
1.2
1.25
1.3
0
5000
10000
15000
20000
25000
30000
35000
40000
45000
50000

(d)

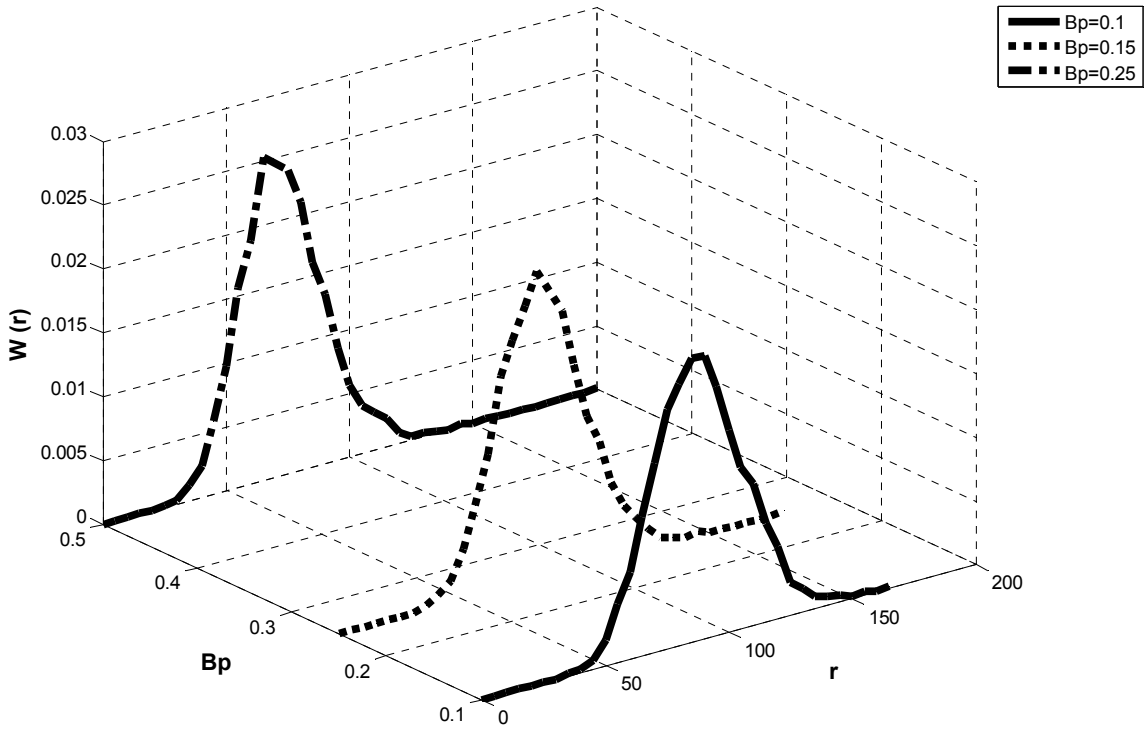
Bp=0.1
Bp=0.15
Bp=0.25
W (r)
0.03
0.025
0.02
0.015
0.01
0.005
0
0.5
0.4
0.3
0.2
0.1
Bp
0
50
100
150
200
r

(e)

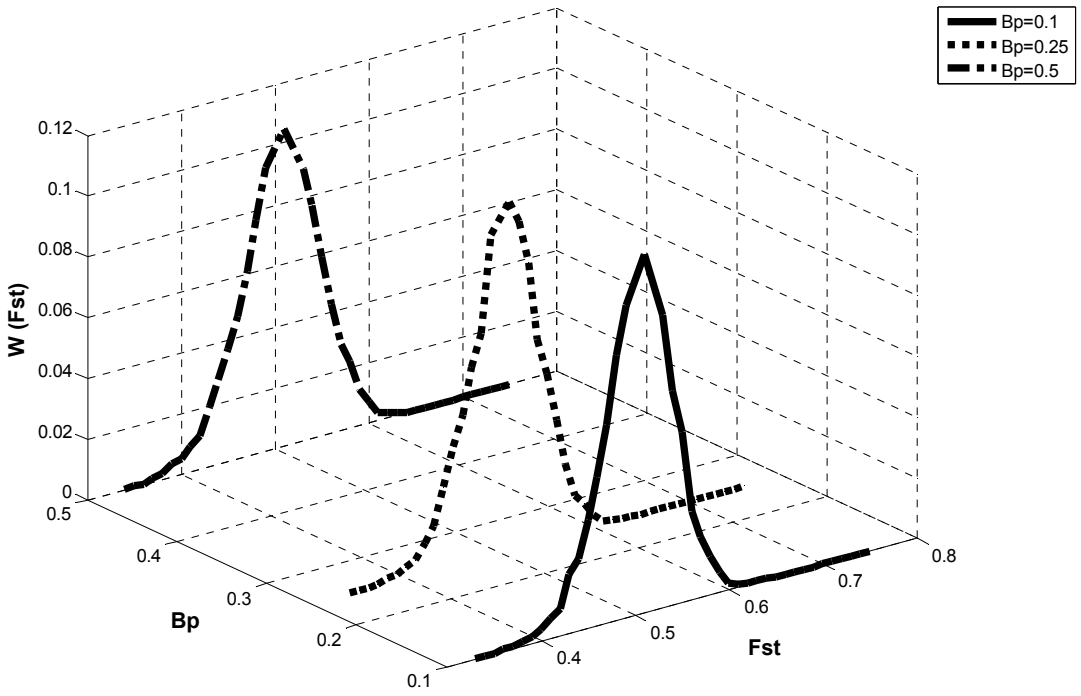

Figure 5.4 Monte Carlo Simulation results for the copolymerization of St-MMA. Effect of diffusion limitation on the propagation rate constant on: (a) monomer conversion as a function of time, (b) number Average M.Wt (Mn) as a function of time, (c) PDI as a function of time (d) molecular weight distribution, (e) chemical composition distribution. The initial comonomer molar fractions in the reactor were $f_{0,St} = 0.5$, $f_{0,MMA} = 0.5$. The equilibrium constant *(Keq)* is 6.87×10^{-10}. ***(Bt=0.1, Bb=0.05)***

Table 5.2: Standard deviation (σ) of the molar fractions for St-MMA

Dimensionless adjustable parameter	Σ
$Bt = 0$	0.037
$Bt = 0.5$	0.037
$Bt = 1.0$	0.039
$Bd = 0$	0.035
$Bd = 0.15$	0.035
$Bd = 0.25$	0.027
$Bp = 0.10$	0.036
$Bp = 0.25$	0.033
$Bp = 0.5$	0.024

5.5 Conclusion

A kinetic model using free volume theory was developed for St-MMA atom transfer radical copolymerization. The model accounts for diffusion controlled termination, deactivation and propagations reactions in ATRcP. The expected trends observed in the previous study carried out by Al-harthi et al. [28] (homopolymerization)

were basically the same for conversion, PDI and Mn. However in our present study, MWD and CCD predictions have also been illustrated, giving a much more detailed analysis of the microstructural properties. The important results were that the bimolecular termination was not much affected by diffusion for a system with a lower equilibrium constant (PDI was the same for all values of B_t). Diffusion controlled termination reactions play a bigger role when the equilibrium constant is on the higher scale. Thus the literature does not take a clear stance on whether or not diffusion plays a role in ATRP. Our simulations clearly show the deviations in the trends for a higher and lower equilibrium constant for diffusion controlled termination. The diffusion controlled deactivation and propagation kill the living behavior, and they increase the PDI and broaden the MWD. Our predictions also showed that diffusion does have an influence on CCD. At higher values of B_t, B_d and B_p a lower weight fraction of styrene is obtained. A narrower CCD is obtained when deactivation and propagation reactions are diffusion controlled, while a much broader distribution is obtained when termination reactions are diffusion controlled. This very important result which could also clarify whether diffusion plays a role while examining experimental data. Hence a comprehensive analysis of diffusion controlled reactions has been illustrated.

More importantly, we have shown, for the first time, how dynamic Monte Carlo simulation can be used to describe the effect of diffusion controlled reactions in ATRcP. MWD and CCD predictions are also a new addition in understanding the effect of diffusion on a novel process such as ATRcP.

5.6 References:

[1] M. Kamigato, T. Ando, M. Sawamoto, Chem Rev 2001:101:3689

[2] K. Matyjaszewski, J. Xia, Chem Rev 2001:101:2921

[3] A.S. Mohammad, A. Mahdi, Polymer 2008; 49:3060

[4] Y. Guillaneuf, D. Gigmes, S.R.A. Marque, P. Astolfi, L. Greci, P.Tordo, Macromolecules 2007; 40:3108

[5] W.A. Braunecker, K. Matyjaszewski, Prog Polym Sci 2007; 32:93

[6] F. Yao, F.Cunningham, R.A. Hutchinson, Macromolecular symposia (2007).

[7] D.C. Sherrington, M. Bouhier, P. Cornack, G. Susan, Polymer preprints 2008; 49: 105

[8] N.V. Tsarevsky, S. Traian, G.B. Bernd, K. Matyjaszewski, Macromolecules 2002; 35: 6142

[9] M. Al-Harthi, J..P. Soares, L.C. Simon, Macromolecular Reaction Engineering 2007; 1:468

[10] F. Luis, M. Garcia, M.Fernandes, E. Madruga, Macromolecular Communications 2001; 22: 1415.

[11] R.G. Norrish, R.R. Smith, Nature (London) 1942; 150: 336.

[12] G.V. Schulz, G. Harborth, Makromol. Chem. 1947; 1: 106.

[13] E. Trommsdorff, H. Kohle, P. Lagally, Makromol. Chem. 1948; 1:169.

[14] A. M. North, ‘‘Progress in high polymers’’, Vol. 2, J. C. Robb,F. W. Peaker, Eds., CRC Press, Cleveland, OH 1968.

[15] I. Mita, K. Horie, J. Macrom. Sci., Rev. Macromol. Chem. Phys.1987; C27: 91.

[16] K.F. O'Driscoll, ''Comprehensive Polymer Science'', Vol. 3, G.C. Eastmond, A. Ledwith, S. Russo, P. Sigwalt, Eds., PergamonPress, London 1989; Chap. 12.

[17] G.I. Litvinenko, V.A. Kaminsky, Prog. Reaction Kinetics 1994;19: 139.

[18] M. Dube, J.P. Soares, A. Penlidis, A.E. Hamielec, Ind. Eng.Chem. Res. 1997; 36: 966.

[19] A. Keramopoulos, C. Kiparissides, Macromolecules 2002; 35: 4155

[20] D.S. Achilias, Macromol. Theory Simul. 2007; 16: 319

[21] M.J. Scoraha, R. Dhibb, A. Penlidisa, Chemical Engineering Science 2006;61: 4827

[22] K. Matyjaszewski, ACS Symp. Ser. 2002; 854: 2.

[23] S. Zhu, J. Polym. Sci., Part B: Polym. Phys. 1999;37: 2692.

[24] M. Zhang, H. Ray, J. Appl. Polym. Sci. 2002; 86: 1047.

[25] H. Fischer, Macromolecules 1997; 30: 5666.

[26] H. Fischer, J. Polym. Sci., Part A: Polym. Chem. 1999; 37:1885.

[27] M. Villalobos, A. Hamielec, P. Wood, J. Appl. Polym. Sci.1991; 42: 629.

[28] M. Al-Harthi, J.P. Soares, C. Leonardo, S Macromol. Chem. Phys. 2006; 207: 469

[29] O. Delgadillo-Velazquez, E.Vivaldo-Lima, A. Irais, Quintero-Ortega, S. Zhu AICHE journal 2002;11:2597

[30] A. Gregory, M.T. John, Macromolecules 1999; 32:411

[31] G.A. O'Neil, M.B. Wisnudel, J. Torkelson, Macromolecules 1996; 29:7477

[32] W.Y. Chiu, G.M. Carratt, D.S. Soong, Macromolecules 1983; 16:348

[33] G.A. O'Neil, M.B. Wisnudel, J. Torkelson, Macromolecules 1998; 21:4537

[34] D. Gillespie, J. Phys. Chem. 1979, *81,* 2340.

[35] A. Keramopoulos, C. Kiparissides, Macromolecules 2002, *35,* 4155.

[36] G.M. Buback, R. Hutchinson, R. Klumperman, B. Kuchata, F. Manders, B. O'Driscoll, K. Russell, G. Schweer, J. Macromol. Chem. Phys. 1995, *196,* 3267.

[37] D.S. Achilias, C. Kiparissides, Macromolecules 1992, *25,* 3739.

[38] H. Suzuki, V.B. Mathot, Macromolecules 1989, *22,* 1380.

[39] A.W. Hui, A.E. Hamielec, J. Appl. Polym. Sci. 1976, *16,* 749.

[40] A. Keramopoulos, C. Kiparissides, Macromolecules 2002, *35,* 4155.

[41] Principles of Polymerization, George Odian

CHAPTER 6

MODELING OF ATOM TRANSFER RADICAL COPOLYMERIZATION IN CONTINUOUS STIRRED TANK REACTORS.

In this Chapter, the modeling of free radical polymerization in continuous reactors is introduced in section 6.1, which also reviews the literature on the modeling efforts carried out in free radical polymerization. Section 6.2 deals with our current work in line with our objectives on ATRcP. The methodology and results are detailed in sections 6.3 and 6.4.

6.1 Review of Modeling of Free Radical Polymerization in continuous reactors

Free radical polymerization is one of the most common methods for producing polymers on a large industrial scale. It is used to make polymers from vinyl monomers, that is, from small molecules containing carbon-carbon double bonds. Due to its industrial importance, it has attracted immense interest among researchers and industrialists. A common area of interest is in modeling and performance improvement of continuous production of polymers.

The continuous production of polymers presents several advantages relative to batch operation, particularly in free radical polymerizations, as the operation in continuous stirred tank reactors (CSTR) offers the possibility of decreasing composition in homogeneity. Therefore, many commercially important polymers are produced in CSTR. Styrene, ethylene, vinylidene chloride, acrylate, methacrylate esters and vinyl acetate are some examples of monomers often polymerized by using continuous processes. Unstirred tubular reactors, roughly equivalent to a cascade of CSTR with re-circulation, are also frequently used in these polymerization systems. A review of modeling and experimental work done in this field is considered in the following section.

High-temperature polymerization is a class of commercially important processes characterized by their high rates of productivity. Applications of these processes abound as attested by the large number of patents. [1-5] The high polymerization temperatures involved in these processes (>180 °C and often >250 °C) lead to fast reaction kinetics, resulting in high monomer conversion (typically greater than 85%), at relatively short residence times.

The first attempts to understand the kinetics of this polymerization at temperatures above 180 °C were made by Hui and Hamielec. [6] They studied the bulk thermal polymerization of styrene in ampule reactors between 100 and 200 °C. They confirmed that the thermal initiation kinetics was third order in monomer, in agreement with the initiation mechanism first proposed by Mayo.

Hussain and Hamielec [7] extended this work to 230 °C and confirmed the initiation and monomer depletion kinetics. Continuous high-temperature thermal polymerization of styrene in a CSTR was first reported by Hamielec et al.,[8] who studied experimentally the relationships between molecular weight and both temperature and reactor residence time. They found that the molecular weight was inversely proportional to the reaction temperature as well as the CSTR residence time.

Kirchner et al. [9] also studied the polymerization of styrene in a CSTR, although at lower temperatures than either work by Hamielec et al. In addition, Spychaj [10] studied the polymerization of styrene-acrylic acid copolymers in a CSTR at high temperatures in an attempt to identify the volatile oligomer production mechanisms. J.D.Cambell et al. [11] studied the continuous high temperature polymerization of styrene between 250 and 350 °C. They concluded that under these reaction conditions, backbiting followed by β-scission not only occurs to a significant extent, but its rate with respect to that of propagation controls the average molecular weight development and oligomer formation.

Low-density polyethylene (LDPE) constituting a large tonnage of plastics is commercially manufactured in high-pressure processes. The technique requires a highly purified ethylene in the feed, and the process must be operated at an elevated pressure in the range 1000–3000 atmospheres and a temperature range of 120–300°C. Temperatures exceeding 300°C cause ethylene to decompose and are not recommended in practice. The high-pressure process is usually a bulk polymerization initiated by organic peroxide used as an initiator.

Monofunctional initiators has been used in the production of LDPE[12,13]. However, the setback of obtaining only limited low conversion of ethylene in high-pressure polymerization has been persistently an unpleasant and discouraging reality in spite of the classical approach to enhance the conversion upon recycling the product. Hence, in order to increase the effectiveness of the conversion process, bifunctional organic peroxide initiators were analyzed. For relatively low temperature polymerization processes such as methyl methacrylates, a number of difunctional peroxides were tested and analyzed, and they were proven to be effective in increasing polymerization rates [14-16].

Luft et al [17-21] conducted extensive research on using bifunctional organic peroxides and focused on the chemistry and kinetics of specific organic peroxides. In comparison with monofunctional peroxides, difunctional initiators accelerate the polymerization rate and produce polymers of higher molecular weight at high temperature. Besides, they can produce special polymers like star and description of free radical polymerization of ethylene catalyzed by difunctional initiators.

It is important to note that experimental data on polyethylene are limited. Nevertheless, enough data were collected from the literature for testing the model performance.

6.2 Modeling of ATRcP in continuous stirred tank reactors .

We have already mentioned in detail the advantages of ATRcP in the previous chapters. One of the drawbacks of ATRcP is that the product is relatively expensive,

although it is to be expected that it may be less costly than the currently available well-defined polymers made by anionic or cationic polymerization. One way to reduce costs is through production in continuous processes, such as in continuous stirred-tank reactors (CSTRs) and tube reactors. Another advantage of continuous processes is that they yield a consistent product over time, once the process is running at steady state. The most important advantage is the use of multiple CSTRs in series or parallel or any configuration which suits the requirement. In technical terms, the livingness of the copolymer made in a CSTR is enhanced by using multiple CSTRs while a compromise is made in the PDI, i.e the control over the polymerization. The PDI can reach around 1.4 when using 8 CSTR's in series. [22] Thus it is difficult to get PDI of around 1.1 which has been reported while using batch and semibatch reactors. While PDI might be high when using a CSTR, the living growth of the polymer chain is enhanced when a series of CSTR is used. This practice of using series of CSTR also produces tailor-made polymers. An example is the use of styrene and MMA as monomers in the first reactor while using styrene exclusively in the second reactor. This produces a copolymer in the first reactor followed by a completely dominated styrene tail. So far, the reports in the literature about ATRcP concern primarily batch and semi-batch processes, and little has been reported on living ATRcP in a continuous process. Hence the modeling of CSTRs would make the thesis complete as we have looked into the important reactors used in the area of ATRcP.

In fact, most of the experiments about LFRP were carried out in batch reactors under isothermal conditions. Only a few papers treating continuous reactors have been published. [22-27] Zhang and Ray [22] proposed a model for the RAFT polymerization scheme, corroborating their results with experimental data obtained for methyl

methacrylate RAFT polymerization. Their paper was of special interest, being the first one studying the effect of the reactor type in LFRP processes. Their work analyzed the behavior of variables such as molecular weight and polydispersity in a single CSTR, a series of CSTR's and semibatch reactor schemes. Zhang and Ray [23] also modeled living polymerization by using batch, semibatch and CSTR. They validated their data against experimental data obtained for nitroxide-mediated styrene polymerization and atom transfer radical copolymerization of styrene and n-butyl acrylate.

Zhu et al [24] studied the continuous ATRP (both homo-and co-) polymerization of methyl methacrylate employing a novel approach in which the catalyst was supported on silica gel. They demonstrated the potential for molecular weight control through adjustment of the reactant feed rate, along with the feasibility of easily preparing block copolymers in a continuous reactor system.

Schork and Smulder [25] discussed the theoretical aspects of CRP in continuous reactors. They predicted that PDI approaches two for a homogeneous continuously stirred tank reactor. This led them to use a train of CSTRs for the production of styrene by using RAFT. [26] Their study proved that using a combination of CSTRs decreases the polydispersity index. It is well known that polymerization reactors exhibit exotic behavior due to the high exothermicity associated with them due to the phenomenon called the gel effect. Hence this effect is also taken into consideration while modeling with CSTR in a few papers. Mariano Asteasuain [27] modeled NMP in tubular reactors. The paper emphasized the importance of obtaining complete Molecular weight Distribution. MWD was obtained by using the Probability Generating Function (PGF) transformation.

Even though some research has been done on modeling NMP and RAFT by using CSTRs, very little work has been done on modeling Atom Transfer Radical Copolymerization (ATRcP) in CSTRs. Modeling has been done mostly employing the method of moments and hence dealing only with conversion and average molecular weight. But the prediction of the complete MWD plays an important role in determining the material characteristics. The commercial software PREDICI, which uses the h-p Galerkin method to compute the MWD, has also been employed to model RAFT processes. [28, 29] The major drawback is the high cost of the package and as far as we know this, method has not been applied in ATRcP. A newer method called the PGF transformation method has been used to predict the MWD in free radical polymerization[30,31] and has also been applied to NMP process.[27] The PGF transformation requires the computation of a large number of differential equation. Commercial software such as gPROMS and FORTRAN are needed for implementing the program. Access to special DAE software, and integration of FORTRAN into gPROMS modules are necessary for obtaining the MWD. Hence again the cost and accessibility provides a drawback to this method. The method has not yet been used to describe ATRcP or modeling in CSTR, but we have shown in Chapter 3, 4 and 5 that Monte carlo simulation have emerged as a powerful tool to describe ATRcP.

6.3 Methodology

The methodology has been explained in detail in Chapter 2. Modeling CSTR needs special coding in addition to following the methodology mentioned in Chapter 2. The concept of predicting the exact residence time of individual polymer chains is a

major criterion in order to model by Monte Carlo. Once the time of the individual chains that have been in the reactor is known, it becomes easy to remove them. The kinetic rate constants used for modeling ATRcP in CSTR are enumerated in Table 1.

Table 6.1. Kinetic rate constants and physical properties for styrene (1) -methyl methacrylate (2) copolymerization at 383K.

Parameter	**Value**	**Reference**
$k_{p\mathrm{AA}}$	$4.266\times10^{7}\exp(-7769/RT)$ (L/mol s)	30
$k_{p\mathrm{BB}}$	$2.95\times10^{7}\exp(-4353/RT)/60$ (L/mol s)	39
r_A	0.52	32
r_B	0.46	32
$k_{tc\mathrm{AA}}$	$(k_{\mathrm{pAA}})^2\times1.1\times10^{-5}\exp(12452.2/RT)$ (L/mol s)	33
$k_{td\mathrm{BB}}$	$9.80\times10^{7}\exp(-701/RT)$ (L/mol s)	31
$k_{td\mathrm{AA}}$	0	29
$k_{tc\mathrm{BB}}$	0	29
$k_{tr\mathrm{A}}$	$(k_{\mathrm{pAA}})\times2.198\times10^{-1}\exp(-2820/\mathrm{R}T)$ (L/mol s)	33
$k_{tr\mathrm{B}}$	$(k_{\mathrm{pBB}})\times((9.48\times10^{3}\times\exp(-13880/(RT)))/60)$ (L/mol s)	29

$k_{a\mathrm{A}}$	0.45 (L/mol s)	34
$k_{d\mathrm{A}}$	1.15×10^{6} (L/mol s)	35
$k_{a\mathrm{B}}$	0.55 (L/mol s)	34
$k_{d\mathrm{B}}$	1×10^{5} (L/mol s)	35
Initial Catalyst Concentration	0.087 mol/L	
Initial Initiator Concentration	0.027 mol/L	
Total Monomer Concentration	8.7 mol/L	
MW_{A}	104.14 (g/mol)	
MW_{B}	100.13 (g/mol)	

6.4 Results and Discussion

In the present study, a dynamic Monte Carlo model has been developed to study ATRcP using CSTRs. The model has been developed to study the effect of residence time distribution on the MWD, CCD along with the other usual predictions. A comparison with batch and semibatch reactors is illustrated to understand the importance

of using different reactors in terms of the requirement. To our knowledge, this is the first time that a Monte Carlo model has been used to describe ATRcP copolymerization using CSTRs.

Figure 6.1 shows the influence of residence time on the PDI of the copolymer simulated in a CSTR. The PDI is much higher than that simulated by using a batch or semibatch reactor. The PDI is close to a value of two for a residence time of 5000 seconds. Our predictions are in agreement with the work of Schork and Smulder[25]. In a batch or semibatch reactor, each chain starts almost at the same time and hence has a very low PDI whereas in a CSTR this is not the case. Hence a higher PDI is obtained as clearly inferred from figure 6.1.

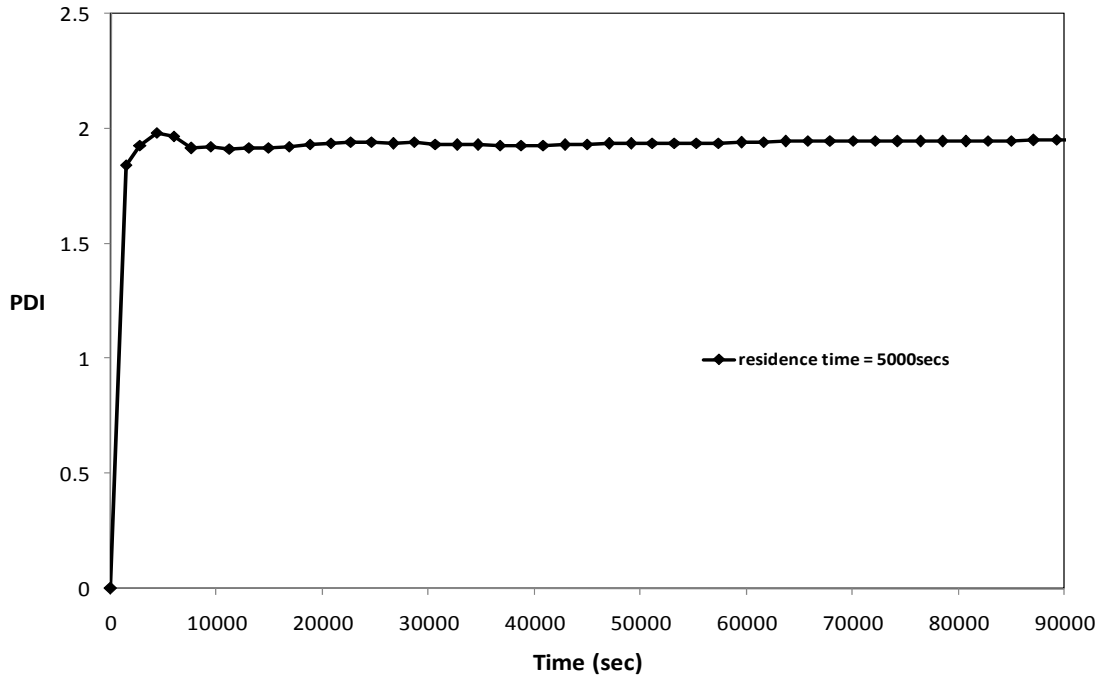

Figure 6.1: PDI as a function of time for the copolymerization of St-MMA in a CSTR for varying residence times. The initial comonomer molar fractions are $f_{0,MMA} = 0.50$ and $f_{0,St} = 0.50$.

Figure 6.2 shows the MWD of the simulated copolymers for a residence time of 5000 seconds. A broad distribution is obtained in agreement with our PDI results. While figure 6.3 shows the instantaneous molar fraction of styrene for the different values of residence time. It is evident, that due to continuous flow of the comonomers, a constant value of the molar fraction is obtained. Since an equimolar concentration is used, the instantaneous molar fraction of styrene is maintained at a value of 0.51. Figure 6.4 shows the CCD predictions for St-MMA copolymer. A narrow distribution with the weight fraction between 0.3 and 0.6 is obtained.

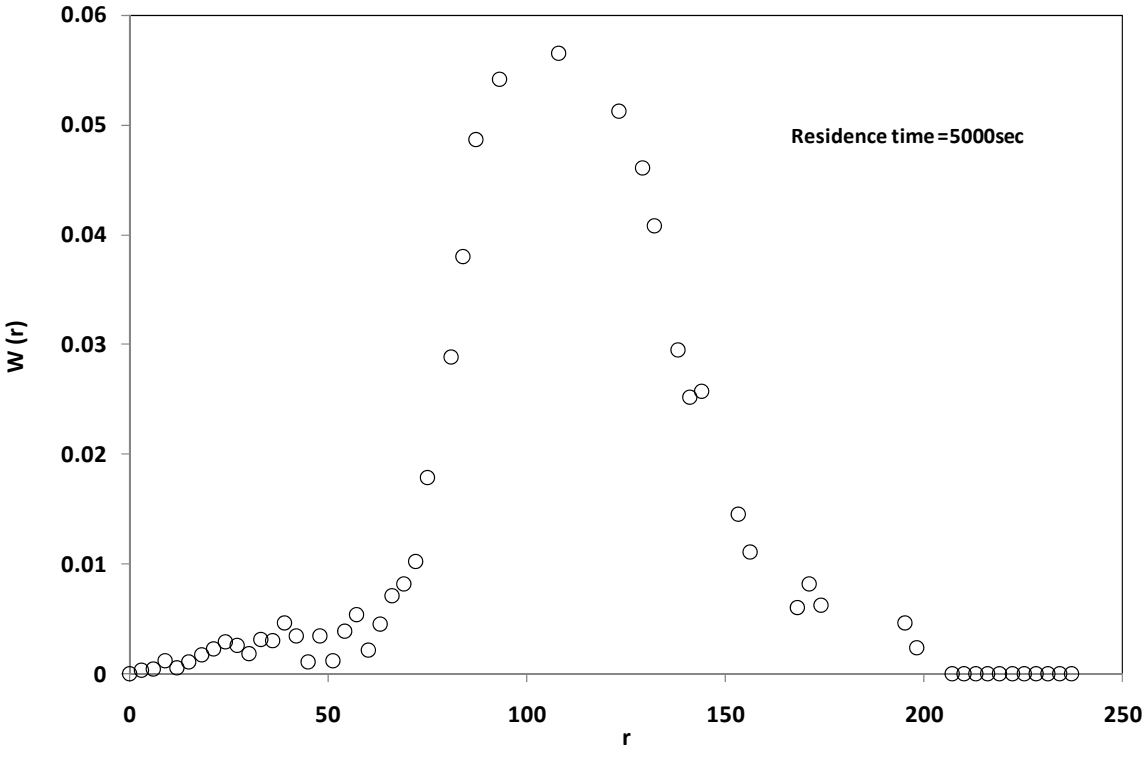

Figure 6.2: Chain length distribution for St-MMA made in a CSTR. Polymerization time = 1600 minutes. The initial comonomer molar fractions are $f_{0,MMA} = 0.50$ and $f_{0,St} = 0.50$.

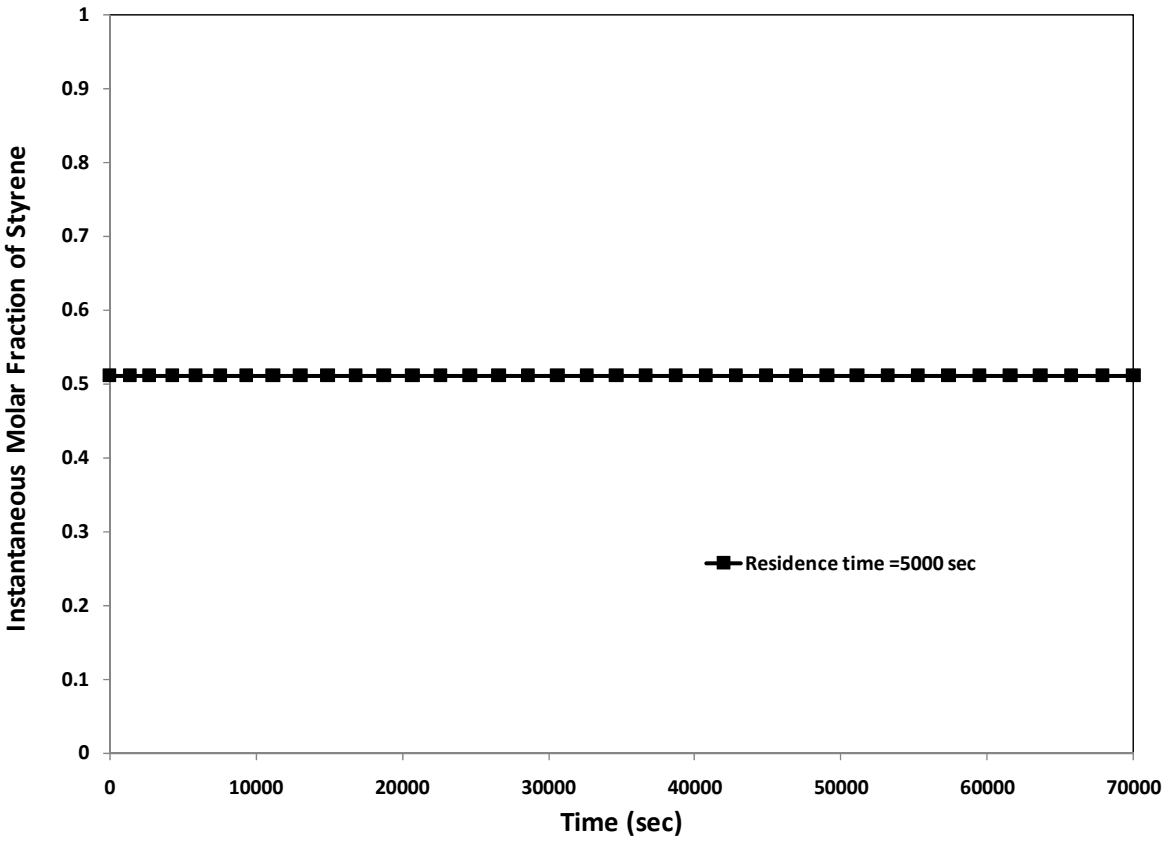

Figure 6.3: Instantaneous molar fraction of St in St-MMA copolymers as a function of polymerization time. The initial comonomer molar fractions are $f_{0,MMA} = 0.50$ and $f_{0,St} = 0.50$.

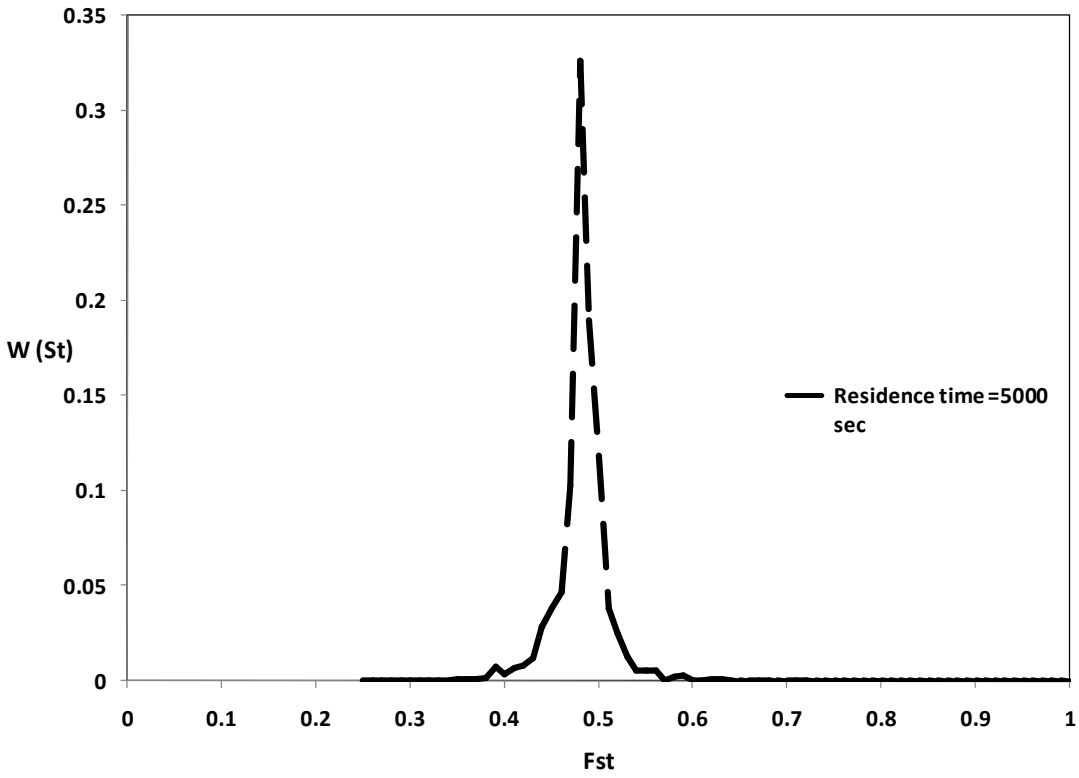

Figure 6.4 Chemical composition distributions of St-MMA copolymers made in a CSTR. The initial comonomer molar fractions are $f_{0,MMA} = 0.50$ and $f_{0,St} = 0.50$. Polymerization time = 1600 minutes

Figures 6.5 show the diad predictions of St-MMA copolymers for the residence time of 5000 seconds. The previous chapters focused on the production of gradient copolymers which were evident from the simulations. But in CSTRs production of gradient copolymers by using a single CSTR is not a viable option, as shown from figures 6.3 and 6.5. Block copolymers are formed in a higher proportion while using a CSTR. The diads clearly shows that the fraction of homodiads is considerably smaller while the fraction of the block copolymer is very high.

Figures 6.6 illustrates the triad predictions for St-MMA copolymers. The predictions are coherent with the diad predictions. Homotriads are formed with a lesser

fraction while the dominating triads are the triblock copolymers as evident from the figures.

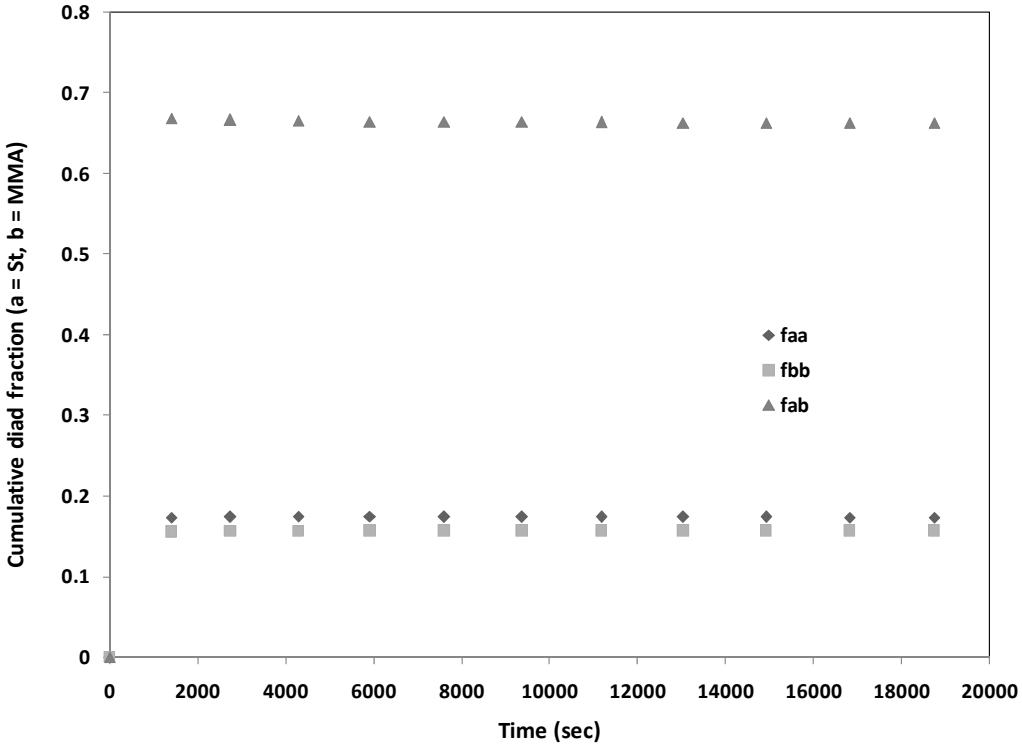

Figure 6.5: Cumulative diad fraction as a function of total comonomer conversion for St-MMA system. The initial comonomer molar fractions are $f_{0,MMA} = 0.50$ and $f_{0,St} = 0.50$. The residence time for the reactor is 5000 seconds.

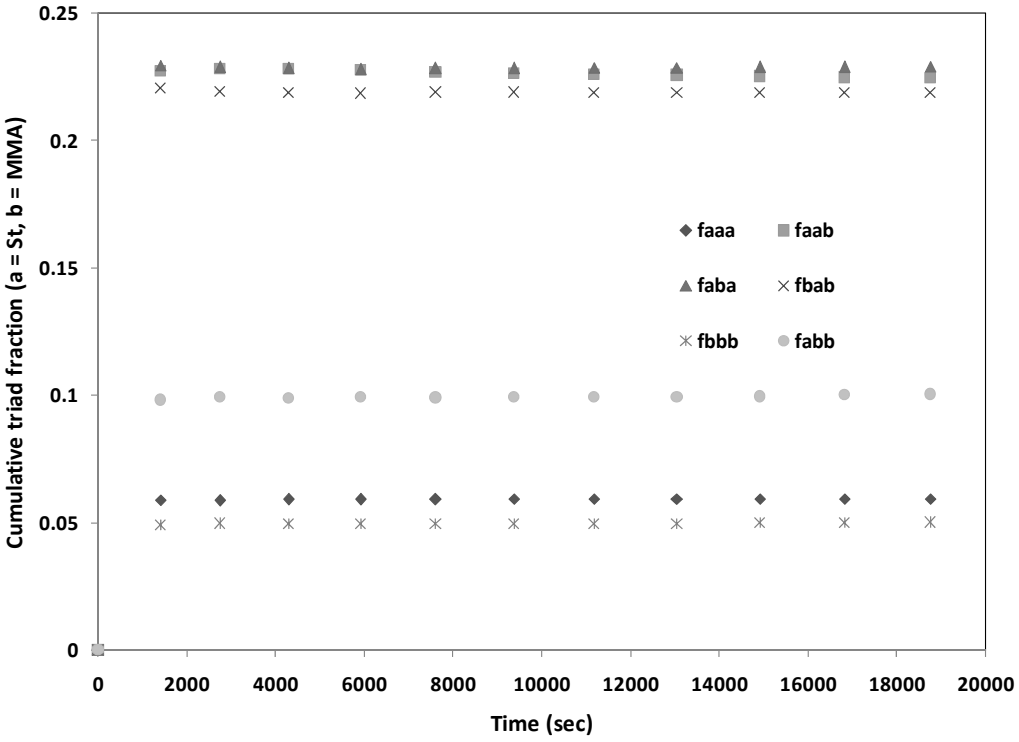

Figure 6.6: Cumulative triad fraction as a function of total comonomer conversion for St-MMA system. The initial comonomer molar fractions are $f_{0,MMA} = 0.50$ and $f_{0,St} = 0.50$. The residence time for the reactor is 5000 seconds.

A comparison is made between batch, semibatch and CSTRs in terms of PDI, instantaneous molar fraction and the NMR results (homodiads and homotriads). A polymerization time of 12 hrs was maintained for all the three reactors. Figure 6.7 shows the PDI obtained in the three different reactors. The PDI is high for the CSTR with a value of 2 while the PDI as low as 1.1 in both the batch and semibatch reactors. Hence a single CSTR is not option to produce polymers with a low PDI. A series of CSTRs imparts the living character to the chains and hence reduces the PDI considerably. Figure 6.8 shows a comparison of the instantaneous molar fraction of styrene obtained in batch, semibatch and a CSTR. Clearly we see the gradient copolymer formation in semibatch

while a transition to gradient copolymer is seen in the batch reactor. Increasing the polymerization time will produce a gradient copolymer in a batch reactor. But clearly no gradient copolymers are formed in a CSTR with the same initial molar fraction. An increase in the molar fraction will also not create a gradient when a single CSTR is used. But gradient copolymers may be formed by using a series of CSTR depending on the intelligent use of comonomers in each CSTR.

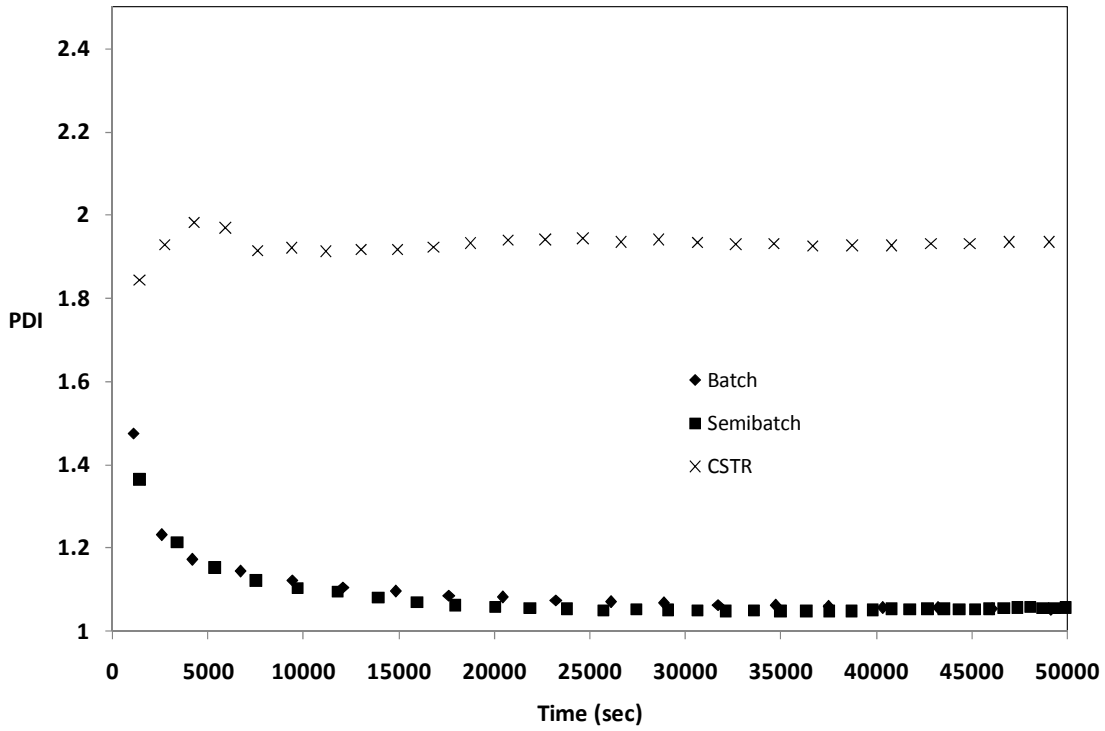

Figure 6.7: PDI of St-MMA copolymers as a function of polymerization time in batch, semibatch and CSTR. The initial comonomer molar fractions are $f_{0,MMA} = 0.50$ and $f_{0,St} = 0.50$.

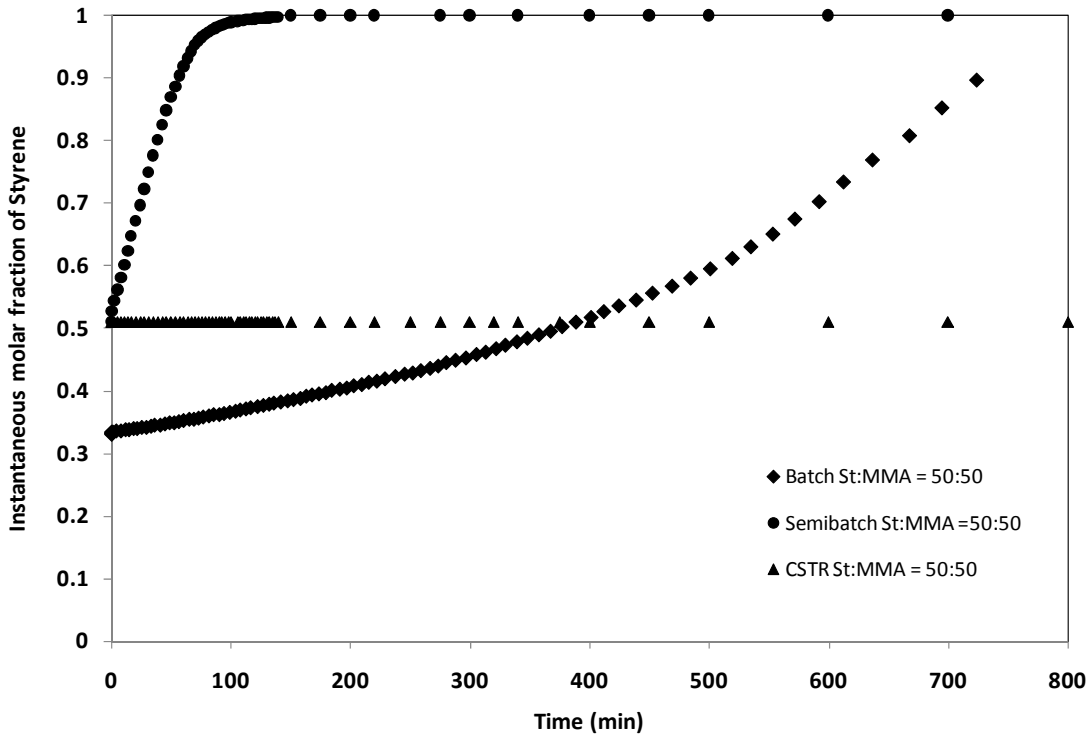

Figure 6.8: Instantaneous molar fraction of St in St-MMA copolymers as a function of polymerization time in batch, semibatch and CSTR. The initial comonomer molar fractions are $f_{0,MMA} = 0.50$ and $f_{0,St} = 0.50$.

Figure 6.9 shows the comparison between batch, semibatch and a CSTR for the fraction of homodiads of St in St-MMA copolymer. The semibatch reactor clearly shows the increase in the fraction of homodiads. The batch reactor shows an increasing trend at the end of the polymerization. The CSTR clearly shows no increase in the homodiads. Thus the semibatch reactor shows the formation of gradient copolymers, while the batch reactor will produce a gradient if the polymerization time is increased.

Figure 6.10 shows the homotriads of MMA simulated in batch, semibatch and a CSTR. A decrease or an increase in the fraction of MMA indicates the formation of gradient copolymer. As seen, only the semibatch system shows a decrease in the fraction of

homodiads of MMA. The batch reactor shows a slight decrease in the formation of MMA while the CSTR has no change in the fraction of homodiads of MMA. Thus the comparison shows that a single CSTR cannot produce a gradient copolymer.

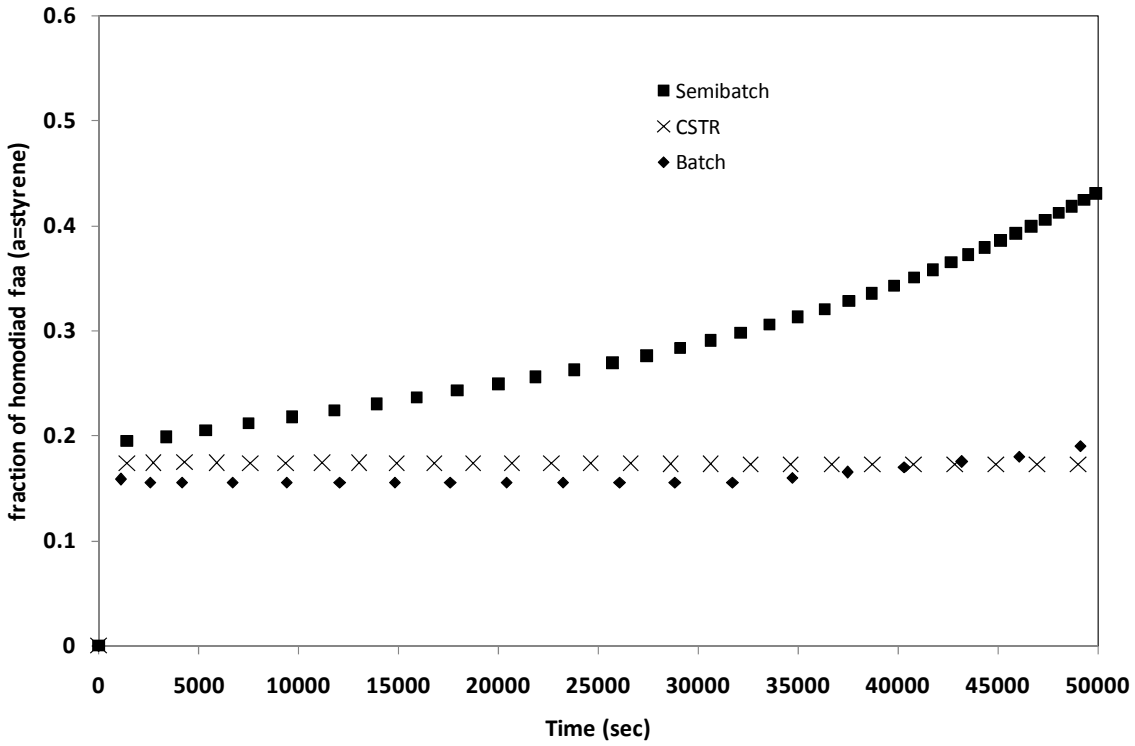

Figure 6.9: fraction of homodiads of St in St-MMA copolymers as a function of polymerization time in batch, semibatch and CSTR. The initial comonomer molar fractions are $f_{0,MMA} = 0.50$ and $f_{0,St} = 0.50$.

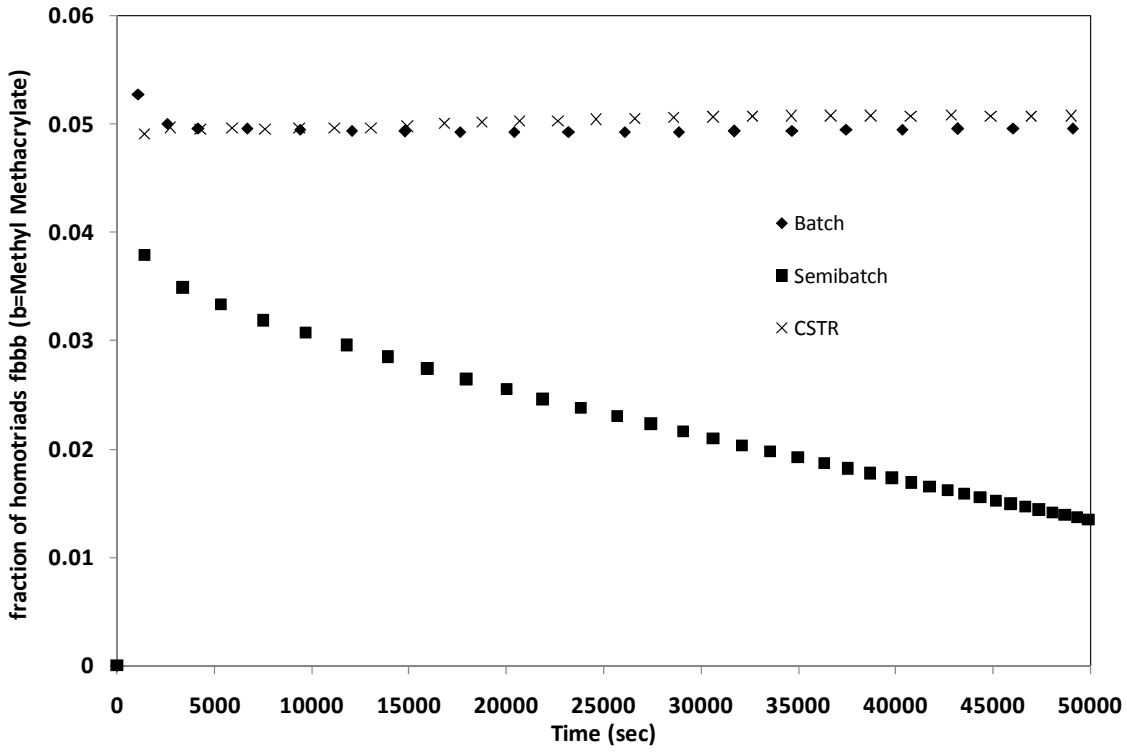

Figure 6.10: fraction of homotriads of MMA in St-MMA copolymers as a function of polymerization time in batch, semibatch and CSTR. The initial comonomer molar fractions are $f_{0,MMA} = 0.50$ and $f_{0,St} = 0.50$.

6.5 Conclusion

Thus a continuous reactor model was developed for ATRcP. The effect of residence time on the PDI, MWD, CCD and other properties have been discussed. It is inferred that the PDI approaches a value of two for a single CSTR. There is no formation of gradient copolymers as seen in the batch and semibatch reactors. Block copolymers are formed in a higher proportion while a CSTR is utilized. Future recommendations include modeling ATRcP by using CSTRs in series and parallel, since the inclusion of CSTRs in series in this thesis would make it too laborious for a M.S thesis. High performance computers are a necessity to model CSTRs in series. The use of CSTRs in living radical polymerization may very well be a topic for a separate M.S thesis.

6.6 References:

[1] A.E. Hamielec, G.P. Lawless, H.H.Schultz, US Patent 4,414,370, **1983**.

[2] R.E. Schmidt, H.H. Schultz, D.M. Wilson, US Patent 4,- 529,787, **1985**.

[3] J.A. Brand, L.W. Morgen, US Patent 4,546,160, **1985**.

[4] F. Brandstetter, H.Gausepohl, R. Thiele, DE Patent 4, 236,-058 A1, **1994**.

[5] J. Hambrecht, M. Volker, H.H Bankowsky, E. Wistuba, EPO Patent 0100444 B2, **1993**.

[6] A. Hui, A.E. Hamielec, *J. Appl. Polym. Sci*. **1972**, *16*,749.

[7] A. Hussain, A.E. Hamielec, *J. Appl. Polym. Sci*. **1978**, *22*,1207.

[8] A.E Hamielec, J.E MacGregor, S. Webb, T. Spychaj, in Polymer Reaction Engineering; Reichert, K. H., Geisler, Eds: Huthig and Wepf New York, **1986**; p 185

[9] K. Kirchner, T. Katzenmayer In Polymer Reaction Engineering, Reichert, K. H., Geisler, Eds: Huthig and Wepf: New York, **1986**; p 287.

[10] T. Spychaj, A.E.Hamielec, *J. Appl. Polym. Sci*. **1991**, *42*, 2111.

[11] J. D. Campbell, F. Teymour, M. Morbidelli, *Macromolecules* 2003, 36, 5491

[12] T.Y.Ham, H.K. Rhee, **1996**, *6*, 241

[13] J.Villermaux, L.Blavier, *Chemical Engineering Science*, **1984**, *39*, 87.

[14] K.J.Kim, K. Choi, *Chemical Engineering Science*, **1989**, *44*, 297.

[15] M.A.Villalobos, A.E. Hamielec, P.E.Wood, Journal of Applied Polymer Science, **1991**, *42*, 629.

[16] R.Dhib, J. Gao, A.Penlidis, *Polymer Reaction Engineering*, **2000**, *8*, 299.

[17] G. Luft, H. Bitsch, H. Seidl, *Journal of Macromolecular Science-Chemistry*, **1977**, *A11*, 1089.

[18] H.Seidl, G. Luft, *Journal of Macromolecular Science-Chemistry*, **1981**, *A15* , 1.

[19] G.Luft, P. Lim, S. Pavlaskis, H. Seidl, *Journal of Macromolecular Science-Chemistry*, 1985, *A22*, 1183.

[20] G.Luft, H. Seidl, *Die Angewandte Makromolekulare Chemie*, **1985**, *129*, 60.

[21] G. Luft, M. Dorn, *Journal of Macromolecular Science-Chemistry*,**1988**, *A25*, 987.

[22] M. Zhang, W.H.Ray, *Ind. Eng. Chem. Res*. **2001**, *40*, 4336.

[23] M. Zhang, W.H. Ray, *Journal of Applied Polymer Science*, **2002**, *86*, 1630.

[24] Y. Shen, S.Zhu, *A.I.Ch.E. Journal*, **2002**, *48* ,2609.

[25] F. J. Schork, W. Smulders, *J. Appl. Polym. Sci*., **2004**, *92*,539.

[26] W. Smulders, C. Jones, and F. J. Schork *AIChE Journal,* **2005**, *51*, 3.

[27] M. Asteasuain, M. Soares, M.K. Lenzi, M.Cunningham, Claudia Sarmoria,Jose´ Carlos Pinto, A. Brandolin *Macromol. React. Eng*., 2007, *1*, 622.

[28] H. Chaffey-Millar, M. Busch, T. P. Davis, M. H. Stenzel,C. Barner-Kowollik, *Macromol. Theory Simul.*, **2005**, *14*,143.

[29] P. Vana, T. P. Davis, C. Barner-Kowollik, *Macromol. Theory Simul*., **2002**, *11*, 823.

[30] M. Asteasuain, C. Sarmoria, A. Brandolin, *Polymer*, **2002**, *43*, 2513.

[31] M. Asteasuain, A. Brandolin, C. Sarmoria, *Polymer,* **2002**, 43, 2529.

CHAPTER 7

CONCLUSIONS AND RECOMMENDATIONS

7.1 Introduction

The main objective of this research was to develop kinetic models for ATRcP in batch, semibatch and CSTRs by the Monte Carlo method. The influence of diffusion limitation on this process was also studied. The apparent disadvantage relative to other techniques such as method of moments and PREDICI, motivated us to find an appropriate technique. Hence the Monte Carlo method was chosen in order to better understand the formation of the MWDs, CCD and other parameters. The thesis has contributed to two journal papers and two conference presentations.

7.2 Conclusions

Monte Carlo simulations have been modeled for the first time for ATRcP. The model has been developed for ATRcP in batch, semibatch and continuous reactors. The models can predict monomer conversion, average molecular weight, polydispersity index, and copolymer composition as a function of polymerization time in batch reactors. Two copolymers, poly(styrene-co-methyl methacrylate) and poly(acrylonitrile-co-methyl methacrylate), were chosen to demonstrate the effect of reactivity ratios and initial

comonomer molar ratios on the copolymer composition as a function of time or monomer conversion in batch and semibatch reactors. The effect of residence time in a CSTR was illustrated, and the performances of the three different reactors were compared. The formation of gradient copolymers have been analyzed in all the three reactors, clearly inferring that semibatch reactors are ideal for producing gradient copolymers with controlled architecture. The phenomena of residence time increased the PDI to a value of two but the literature suggests a train of CSTRs may lower the PDI. The effect of diffusion on ATRcP had also been examined for the first time. A quantitative approach has been made to better understand the effect of diffusion on bimolecular termination, deactivation and propagation reactions. The diffusion controlled deactivation and propagation killed the living behavior and increased the PDI and broadened the MWD. The use of two different catalyst systems (different equilibrium constants) was also analyzed, clearly showing the impact of equilibrium constant on ATRcP. We have modeled the effect of diffusion MWDs and CCD for ATRcP, which has not been reported before. Thus we conclude that this thesis has given a comprehensive analysis of the polymer microstructure and the feasibility of large-scale production of this class of polymers.

7.3 Recommendations for Further Research

The kinetic models obtained are comprehensive, and we may additionally synthesize and characterize these specific comonomers in our labs. Based on our findings (modeling), we can easily produce tailor-made polymers with more control in the lab

environment. As a result, we may be on the verge of achieving a new class of copolymers specific to solving real-time engineering problems.

Another area of further research is in the modeling of series or combination of CSTRs to achieve a lower PDI. The intelligent use of a train of CSTRs could be of great interest as it is a more potent tool to produce tailor-made polymers on a larger scale.

VITA

Masihullah J.Khan was born in Chennai, India. After graduating from secondary school he enrolled for Bachelor of Technology at the **University of Madras**, Chennai, India. In June 2003, he graduated with **distinction as a Bachelor of Technology in Polymer Technology.** In May 2009, he secured the **M.S. degree in Chemical Engineering**, from King Fahd University of Petroleum & Minerals, Dhahran, Saudi Arabia.

The author can be contacted at: jmasihullah@gmail.com